BEHAVIOR OF A SANDY CLAY UNDER VERTICAL IMPACT OF GEOMETRIC SHAPES

By Arthur R. Poor, William R. Cox and Lymon C. Reese

Department of Civil Engineering

The University of Texas

Austin, Texas

a report to

National Aeronautics and Space Administration

Langley Research Center

Hampton, Virginia

May 1965

ABSTRACT

33501

An experimental investigation was performed to define the soil response on three geometric shapes during impact. Two sizes of vehicles were utilized having plate, sphere and cone configurations with constant ratios of diameter, available surface contact area, and weight being maintained between each size. Impact velocity and mass were varied for each series of test vehicles.

The acceleration-time history of the reactive soil forces on the impacting vehicle was recorded on an oscilloscope utilizing accelerometers as the sensing devices. Analysis was accomplished by computer program to obtain the magnitude of reactive force as a function of deformation. A modulus of deformation was determined as a constant for each geometric configuration. The magnitude of reactive force was a function of vehicle mass and impact velocity. Equations for the modulus of deformation and maximum reactive force were defined to permit prediction by extrapolation of the phenomenological behavior of larger vehicles.

Author

TABLE OF CONTENTS

BEHAVIOR OF A SANDY CLAY

UNDER VERTICAL IMPACT OF GEOMETRIC SHAPES

by

Arthur R. Poor
William R. Cox
Lymon C. Reese

Prepared for

NATIONAL AERONAUTICS AND SPACE ADMINISTRATION

Langley Research Center
Hampton, Virginia

Contract NsG-604

THE UNIVERSITY OF TEXAS

DEPARTMENT OF CIVIL ENGINEERING

Austin, Texas

May 1965

SYMBOLS AND NOTATIONS

A	Area in $in.^2$ or ft^2
a	Acceleration in ft/sec^2 or $in./sec^2$
c	Unit cohesion of soil in lb/ft^2
C1	0.355 microfarad capacitor
C2	0.750 microfarad capacitor
C3	0.355 microfarad capacitor
CH	Clay soil of high plasticity
CL	Clay soil of low plasticity
cm	Centimeter
D	Spherical diameter of test vehicle in ft or in.
d	Test vehicle diameter in ft or in.
E	Bulk modulus in lb/ft^2 or $lb/in.^2$
E_d	Modulus of deformation in lb/in.
E_{dp}	Modulus of deformation, plate test vehicle in lb/in.
E_{ds}	Modulus of deformation, sphere test vehicle in lb/in.
f	Soil reactive force in lb
f_s	Soil reactive force for sphere vehicle in lb
F	Calibration factor of transducer in mv/v-g
g	Acceleration of gravity in ft/sec^2 or $in./sec^2$
l	Length in ft or in.
LL	Liquid limit in %
M	Test vehicle mass in slugs
MC	Moisture content in % of dry weight

msec	Millisecond
mv	Millivolt
N	Calibration constant of accelerometer in g's
PI	Plasticity index in %
PL	Plastic limit in %
Q	Soil resistance force in lbs
R	Spherical radius of test vehicle in ft or in.
r	Test vehicle radius in ft or in.
R1	33,000 ohm resistor
R2	150,000 ohm precision shunt resistor
R3	1,000 ohm helipot
R4	175 ohm resistor
R5	175 ohm resistor
R6	87 ohm resistor
R7	5 ohm Nichrome wire resistor
R8	10,000 ohm resistor
R9	1,000 ohm helipot
R10	8 ohm/ft Karma wire
s	Drop height in ft or in.
SRF	Strain rate factor
S1	Toggle switch
t	Time in seconds
v	Volt
v_i	Impact velocity in ft/sec or in./sec
v_o	Initial velocity in ft/sec or in./sec

V1	5 volts regulated direct current voltage
V2	12 volts direct current
V3	102 - 180 volts direct current
W	Weight of test vehicle in lb
W_s	Weight of soil mass in lbs
x	Definition of soil particle size
γ	Soil density in lb/ft^3
δ	Deformation in in.
η	Viscosity of the soil in $ft\text{-}sec^2/in.^2$
ρ	Mass density of soil in $lb\text{-}sec^2/ft^2$
σ	Normal stress in lb/ft^2 or $lb/in.^2$
σ_1	Major principle stress in lb/ft^2 or $lb/in.^2$
σ_3	Minor principle stress in lb/ft^2 or $lb/in.^2$
τ	Shear stress in lb/ft^2 or $lb/in.^2$
τ_f	Maximum static shear strength in $lb/in.^2$ or lb/ft^2
τ_{fd}	Maximum dynamic shear strength in $lb/in.^2$ or lb/ft^2
ϕ	Angle of internal friction
Ω	ohm

LIST OF TABLES

LIST OF FIGURES

CHAPTER ONE

INTRODUCTION

1.1 General

The manned spacecraft flights which have been conducted by the United States thus far have all been terminated in water. However, at some future time it may be necessary, or highly desirable, to terminate a flight on a land mass. At present there is no reliable procedure for predicting the interaction processes which will occur between a soil system and a spacecraft landing head. While the in-flight behavior of the spacecraft can be predicted with an optimum degree of precision, the same cannot be said for the phenomenological behavior which takes place at impact. This is due primarily to the lack of knowledge and to the complexity of the soil behavior to allow a reliable prediction of reactive forces against various geometries of the impact head when subjected to a dynamic loading situation.

The functional relationships and behavioral characteristics of soils are much more complex than for other common engineering materials, thus making generalized behavior conditions extremely difficult to determine with reliable accuracy. However, information can be obtained which will serve as a prediction basis within a given soil classification.

Increased emphasis is being directed towards research on the dynamic response of soils. This is evidenced by the ever increasing number of publications in the engineering literature on the subject. Considerable attention has been given to the interaction processes which occur between a structural foundation and a soil system when the structure has been sub-

jected to dynamic loading conditions generated by earthquake shock or blast effects. Research has also been directed towards the effects of repeated dynamic loadings on foundation elements and the soil system. However, in the specific area of interest considered, published information is practically nonexistent. Previous research conducted at The University of Texas[5] has provided certain information having a relationship to this investigation.

A test program utilizing a full-scale prototype would provide the reliable data for development of theoretical relationships required between spacecraft heads and a soil system. Such a program, unfortunately, is not practical or feasible due to the size of the prototype and the expense. As a compromise, a test program utilizing model test vehicles will serve as the basis for predicting prototype behavior. While a model test vehicle will not represent the prototype vehicle, a test program under field and controlled laboratory conditions will provide much useful data and essential information to form the basis for the development of theoretical considerations for the prototype vehicle.

1.2 Objective

The primary objective of this investigation is the determination of the force-deformation behavior of geometric shapes impacted into a soil system.

In this investigation, models in the shapes of several possible landing heads of spacecraft were studied experimentally. Models of different size, mass, and geometry were impacted into a soil system at varying velocities to determine reaction of the soil medium from the instant of impact

until the test vehicle came to rest.

Due to the complexities of the gross behavior of a spacecraft at impact, this investigation was limited in an attempt to provide a degree of understanding of the interaction conditions resulting from a vertical component of motion.

From the experimental investigation, expressions were determined which would allow extrapolation to predict vehicle response based on phenomenological behavior.

1.3 Scope of Investigation

The scope of this investigation was limited to vertical motion, impact loading tests on three types of foundation elements: namely, plates, spheres, and cones. Originally it was believed that a complete laboratory procedure would be possible to provide a dynamic test program that would parallel the static program of the overall project. It was determined, however, that larger test vehicles would be mandatory to provide a stable platform for the instrumentation required to provide the desired data from the drop tests. The use of larger test vehicles made the use of laboratory soil test beds impractical due to the size required to eliminate undesirable side and bottom effects. Further the labor required to duplicate the conditions of the soil bed for each test drop proved unrealistic. A number of impact tests were conducted in the laboratory, however, in the same sand bed utilized for the static series. These tests, while conducted under adverse conditions, fulfilled a definite requirement within the overall program and are discussed more fully in Chapter IV.

The principal test program conducted in this investigation consisted of a series of drop tests performed under field conditions. The impact tests were conducted on a soil system of sufficient surface area to contain soil classification throughout.

1.4 Test Vehicles

The test vehicles selected for this investigation were circular, conical, and spherical in shape. For convenience the available surface contact area of the circular plates was used to develop the dimensions of each size series.

Plate test vehicles of 10 and 20 in. diameters were chosen with surface areas of 78.6 and 314.2 in.^{2} respectively. These same available contact surface areas were used in developing the dimensions for both the spherical and conical test vehicles. The basic weights of the 10 and 20 in. plates were 8 and 64 lb respectively; the cones and spheres had these same weights. For each series of tests, additional weights were provided to permit doubling the weight of each model. This provided the capability of having two different diameter test vehicles for the plates, spheres, and cones, with weights of 8, 16, 64, and 128 lb.

The test vehicles are discussed in more detail in Chapter II, Art. 2.2.

1.5 Foundation Media

The soil used for the series of impact tests performed in the laboratory was clean, dry sand kept at room conditions. The same sand was utilized in the static test investigation,[8] which is part of the overall project.

The sand was Colorado River sand obtained locally in Austin, Texas, quite rich in silica, and was comprised of smooth round grains. The material utilized in the test program was that portion which passed a No. 30 and was retained on a No. 200 U. S. Standard Sieve.

The foundation material utilized for the field test series was a clay of low plasticity (CL). Classification test results indicated that the soil within the test area was uniform (refer to Art. 3.3B, Chap. III). The assumption that the area was comprised of a uniform soil both homogeneous and isotropic was considered appropriate.

The development and selection of the field test site is discussed fully in Chap. III.

CHAPTER TWO

DEVELOPMENT OF TEST APPARATUS

2.1 General

The decision to conduct the impact drop tests under field conditions was necessitated by a number of factors. Ceiling height in the Soil Mechanics laboratory precluded a drop in excess of four feet when the container size of the soil bed was considered. Further, preparing the soil bed for each test drop would be quite difficult for a cohesive soil. It was believed that the test vehicle should be of such size that the instrumentation would not appreciably influence the test results or impart undesirable components of motion during the test drop. Finally, consideration was given to the desirable situation wherein a field test site could be located that was fairly uniform to a depth of approximately fifteen feet. This would provide a test area of sufficient size that each drop test could be performed on a soil mass which could be considered undisturbed.

The drop test program under field conditions required preparation of the test vehicles, the test platform, and associated instrumentation.

2.2 Test Vehicles

The test vehicles utilized in this research had configurations of plates, spheres, and cones. Selected ratios were maintained between the sizes and weights of vehicles for the different geometries in order that correlation of drop test data could be made.

It was convenient to use the circular plate configuration as having the governing available surface contact area. This area would be the basis for establishing the dimensions of the sphere and cone vehicles.

The maximum diameter for the plate test vehicles was arbitrarily established at 20 in. This size was for convenience as 20 in. was the largest diameter which could be effectively accommodated in the machine shop lathe. In order to obtain the most effective range of vehicle sizes, a ratio of 2 to 1 was established between diameters. This ratio determined the next smaller size of plate vehicle to have a 10 in. diameter. There remained the capability to provide a still smaller vehicle with a 5-in. diameter if required.

Doubling the diameter between vehicle sizes increased the available surface contact area by a factor of four. The weight was increased by a factor of eight. Due to the rapid increase in vehicle weight and to maintain a capability to utilize the smallest vehicle if required, the weight for this vehicle was established at one pound. This also established the weight of the 10-in. plate at 8.0 lb, and the 20.0-in. plate at 64.0 lb.

Based on the available contact surface area of the 10 and 20 in. circular plates of 78.6 and 314.2 $in.^2$, respectively, the diameters of the cone vehicles were established at 7.08 and 14.16 in. The diameters for the sphere test vehicles having the same available contact surface area as the plates, and with spherical radii of 5 and 10 in., were 8.66 and 17.32 in.

It was convenient to manufacture the test vehicles from aluminum for ease in handling, in working the models to the same weight for each series,

and provide a test vehicle considered to be a rigid body. The use of aluminum was also desirable due to the rapid increase in model weight by doubling the diameter.

Since much additional information could be obtained by varying the mass of the basic test vehicles, auxiliary weights were provided so that the weight of each basic diameter vehicle could be doubled. Twelve test vehicles were utilized for the field test series. Table 1 shows the dimensions and weights for all test vehicles utilized in the research program.

TABLE 1

TEST VEHICLE INFORMATION

Item	Plate Series		Cone Series		Sphere Series	
	1	2	1	2	1	2
Diameter (in.)	10.00	20.00	7.08	14.16	8.66	17.32
Surface Area ($in.^2$)	78.60	314.20	78.60	314.20	78.60	314.20
Height from Maximum Diameter to Vehicle tip (in.)	-	-	6.13	12.26	2.50	5.00
Weight (lb) Model A	8.00	64.00	8.00	64.00	8.00	64.00
Model B	16.00	128.00	16.00	128.00	16.00	128.00

Manufacturing the test vehicles by conventional machine shop processes was found to be impractical. It was not possible to obtain aluminum billets in the sizes desired to allow the test vehicles to be machined from one piece of stock. Nor was it feasible to manufacture the models in sec-

tions and subsequently join the sections to form an acceptable test vehicle. Casting the vehicles seemed to be the most practical solution. After a number of discussions with officials of a local foundry, and after their assurances of meeting the tolerances desired, a contract was initiated with the Hall Level Manufacturing Company, Austin, Texas, to cast the test vehicles.

The models utilized a wall thickness of 3/8 in. and crossribs of 3/8 in. for the smaller series, and a wall thickness of 1/2 in. and crossribs of 1/2 in. for the larger series. Hollow castings were specified to preclude the possibility of any shrinkage during the cooling process. It was believed that an attempt to cast the vehicles as solid units would result in geometric deformities rendering the castings useless for the intended purpose. Hollow castings would still provide a test vehicle which could be considered as a rigid body, and additional weight could be furnished without any significant difficulty.

The surface of each casting was smoothed by hand in the laboratory. The hand work did not result in a surface perfectly smooth, but it did produce a surface which was reasonably uniform and free from surface irregularities.

The castings were drilled and tapped to permit attachement of slide wire guides. Weighting plates were prepared for all models at each basic weight configuration. The weighting plates were then drilled and tapped to hold the release and primary sensor bracket.

Additional weights were provided for each test vehicle for the second weight configuration. These weighed either 8 lb or 64 lb.

The final step in the test vehicle preparation process was that of bringing each model to the desired weight for each series. This was accomplished by fitting each vehicle with all attachments and instrumentation that would be utilized in the actual drop test, and adjusting to the final desired weight by the use of plastic aluminum and lead shot.

Figures 1, 2, 3, 4, 5 and 6 show sketches of the test vehicles utilized in this investigation.

2.3 Test Platform

A drop tower was necessary for conducting the field test program. An effective drop height of 15 ft was established for convenience as the upper limit for the field test series. This distance would require the over-all effective height for the drop tower to approximate 17 ft due to the size of the largest cone vehicle plus other required attachments.

Certain other requirements were essential in developing a drop tower which could be utilized efficiently in the field investigation. The tower must provide a stable work platform and be completely transportable with each individual section weighing no more than could be easily handled by one person. The components must allow simple erection in the field. The assembled structure should permit rapid leveling adjustments, and be easily moved from one test location to another. A requirement was also established that all components to be attached to the tower would be provided in a manner to facilitate mounting and removal.

After much consideration, the most effective solution to all of the above requirements was to utilize ladder sections of Safway steel scaffolding in developing the basic drop tower. The tower was prepared in three indi-

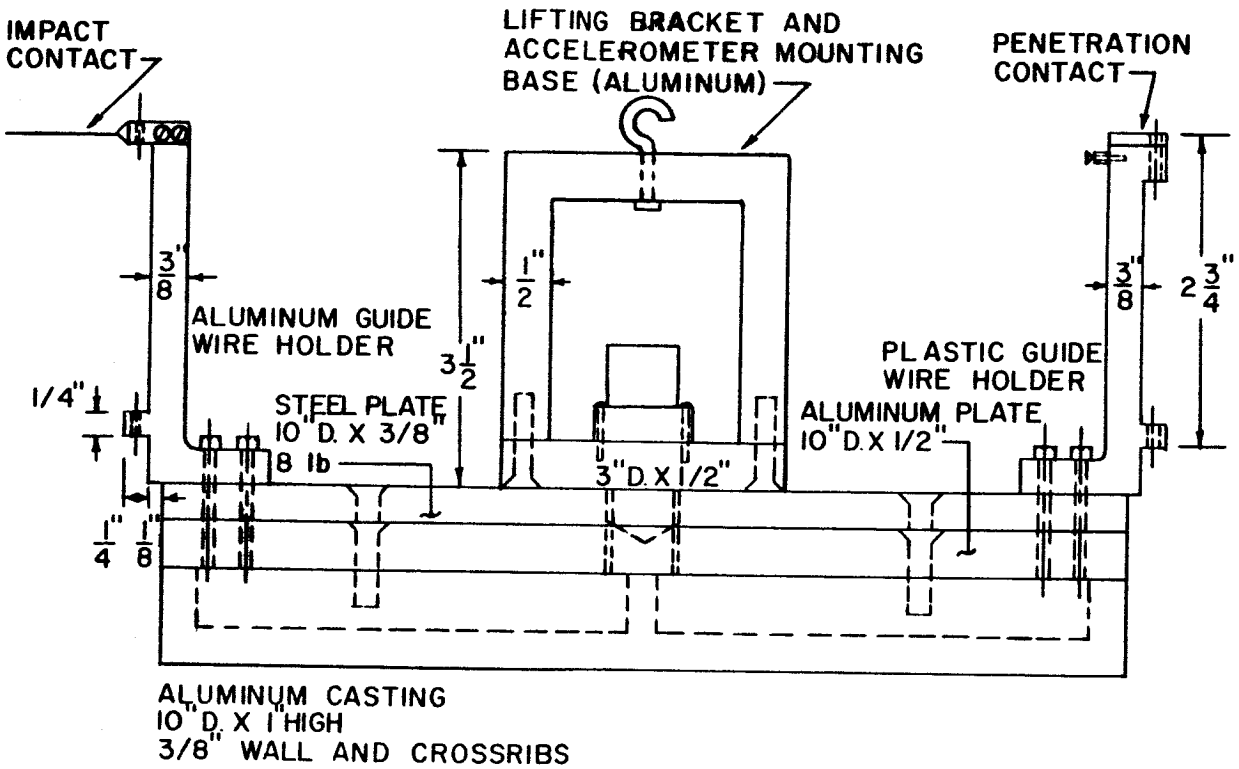

MODEL A 8 lb WITHOUT STEEL WEIGHT
MODEL B 16 lb AS SHOWN

FIG. 1 PLATE TEST VEHICLE – 10.0 in DIAMETER

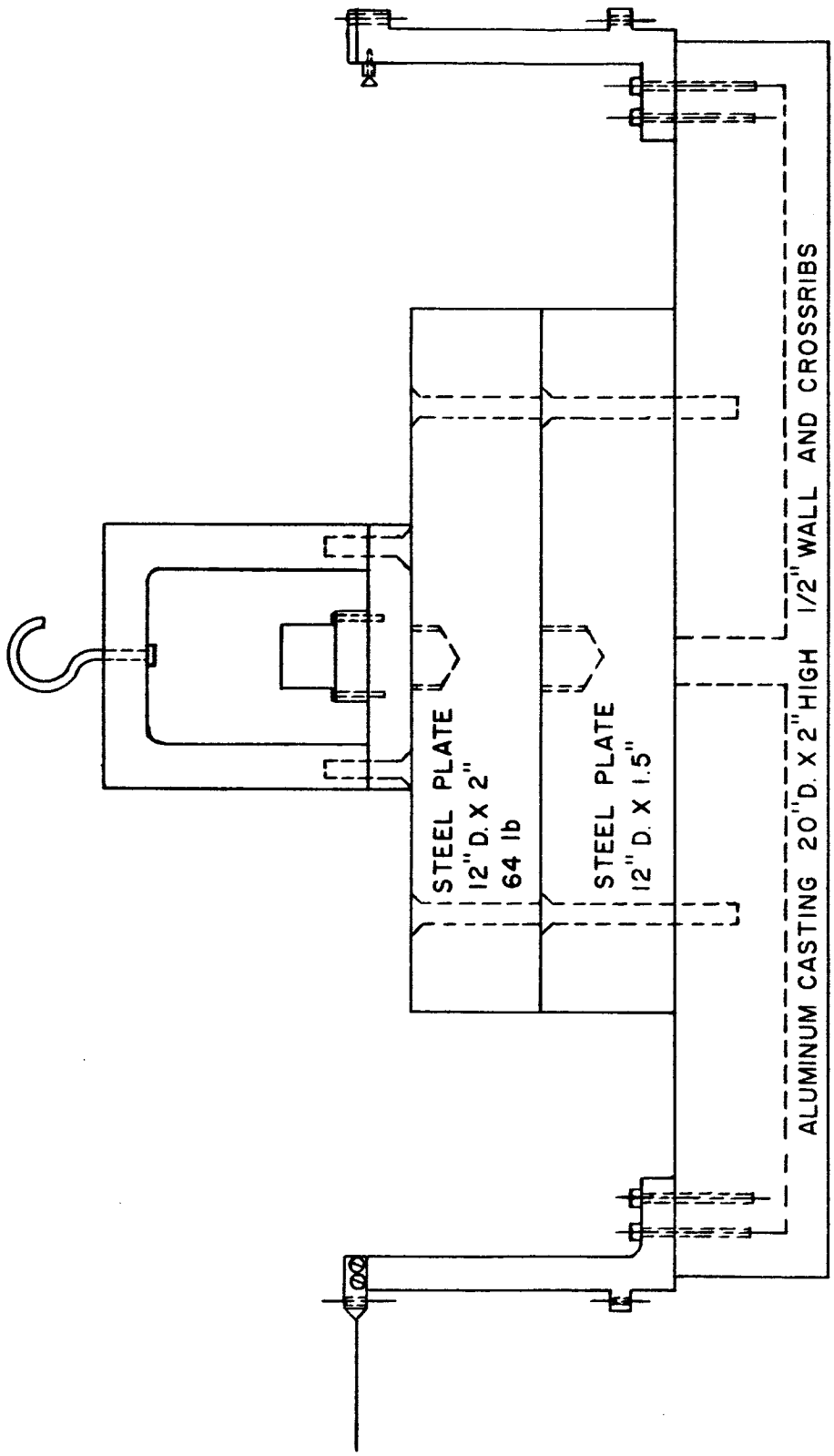

FIG. 2 PLATE TEST VEHICLE – 20.0 in DIAMETER

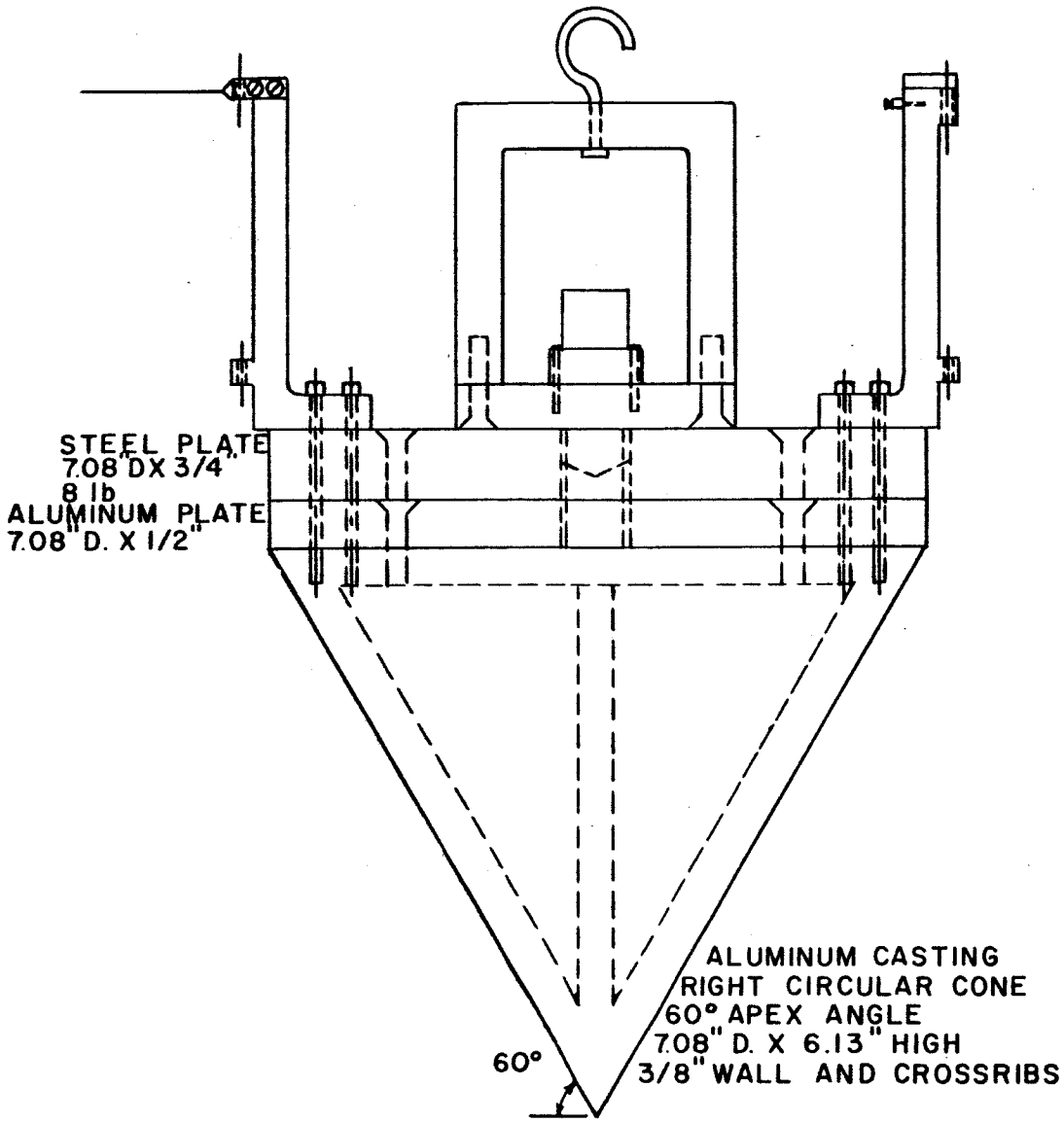

MODEL A 8 lb WITHOUT STEEL WEIGHT
MODEL B 16 lb AS SHOWN

FIG. 3 CONE TEST VEHICLE – 7.08 in DIAMETER

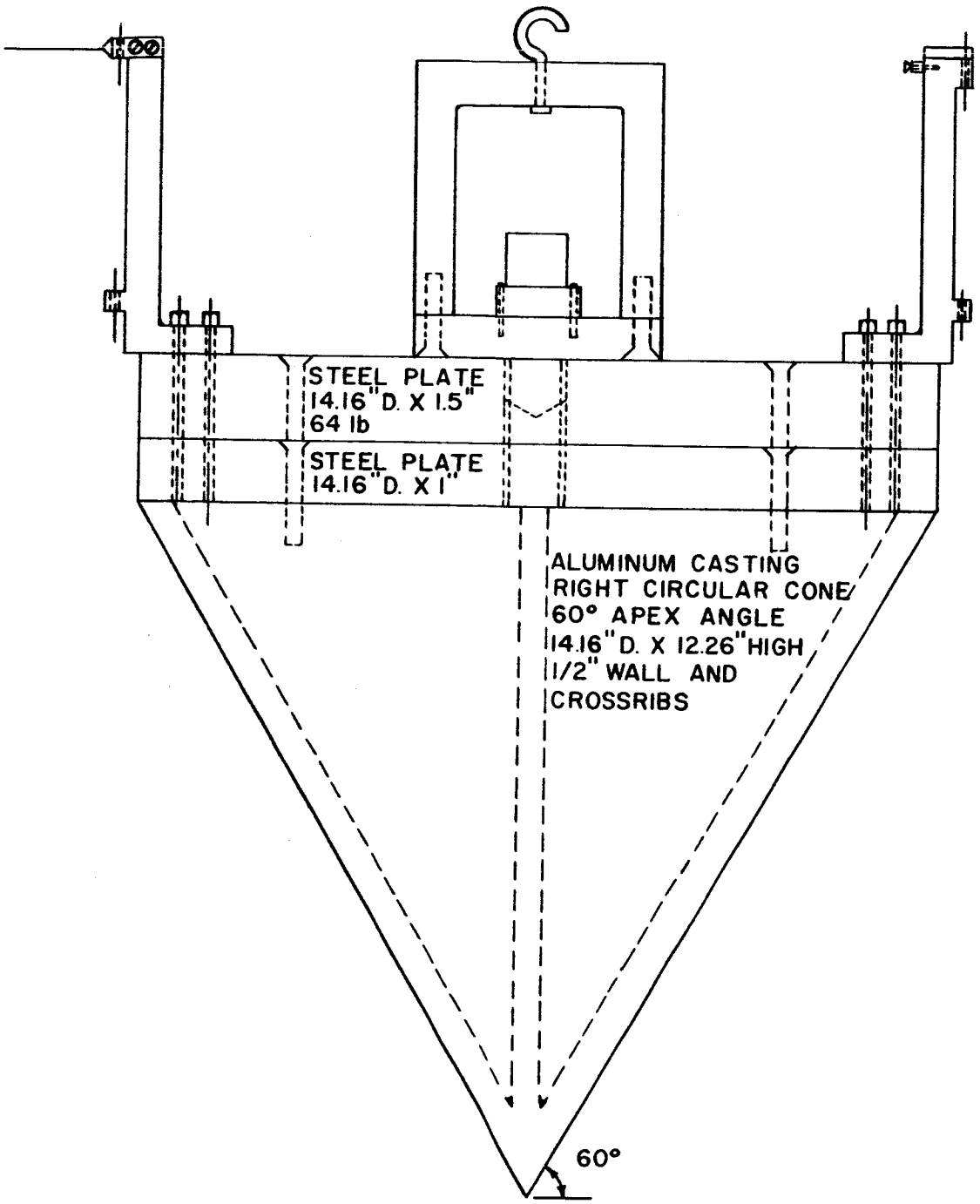

MODEL A 64 lb WITHOUT STEEL WEIGHT
MODEL B 128 lb AS SHOWN

FIG. 4 CONE TEST VEHICLE – 14.16 in DIAMETER

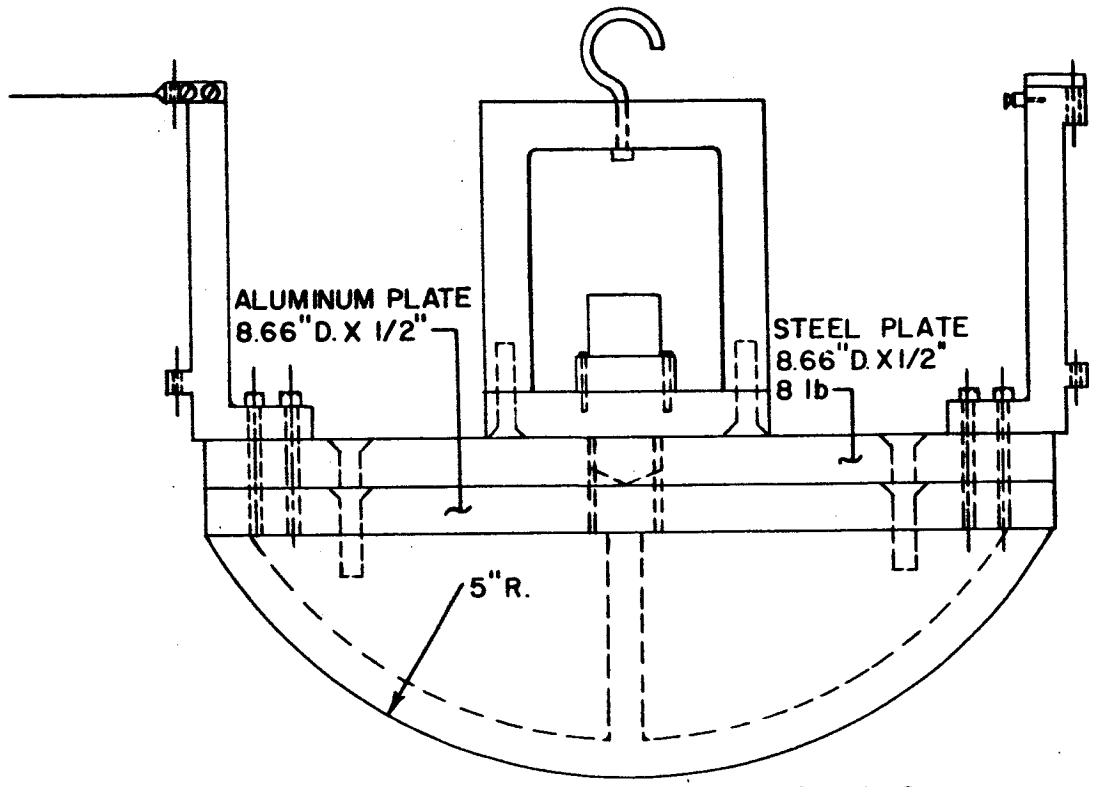

MODEL A 8 lb WITHOUT STEEL WEIGHT
MODEL B 16 lb AS SHOWN

FIG. 5 SPHERE TEST VEHICLE – 8.66 in DIAMETER

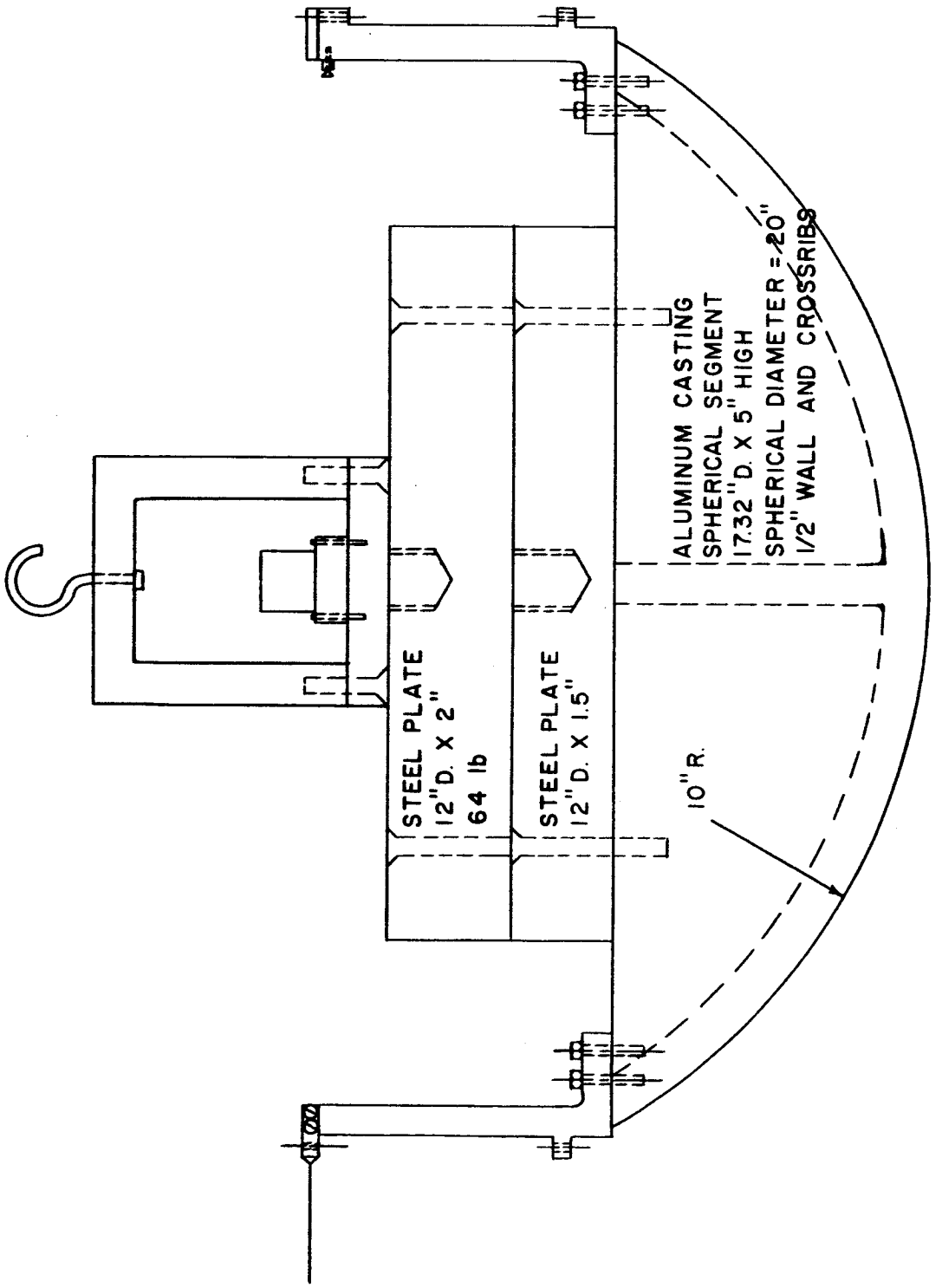

MODEL A 64 lb WITHOUT STEEL WEIGHT
MODEL B 128 lb AS SHOWN

FIG. 6 SPHERE TEST VEHICLE – 17.32 in DIAMETER

vidual sections. The upper two units were fabricated with ladder sections 6 ft long by 2 ft wide, with the cross braces providing a separation between sections of 3 ft. Ladder base sections were obtained which would interconnect with the upper sections while providing a base width of 4 ft for increased stability of the structure. The effective height of the base sections was 4 ft. The base sections were fitted with individual screw jacks to permit rapid leveling of the entire structure, and equipped with locking rollers to permit movement of the tower from one location to another. Assembly of the structure provided a drop tower 2 ft by 3 ft and an over-all height of approximately 17 ft.

Angles were welded to the bottom cross members to provide a rigid base to mount the adjustable lower guide-wire holders. These holders were prepared in the laboratory and facilitated adjusting the guide wires to accommodate the diameter of the test vehicle. The holders were also adjustable up and down to permit tensioning the guidewires, account for irregularities in the ground surface, and allow for raising the holder when moving the tower to a new drop location.

The top of the tower was fitted with a 1/2 in. thick aluminum plate. This plate added rigidity to the top of the drop tower and served as the top holder for the guide wires and raising point for the test vehicles. The aluminum plate was drilled at the appropriate distances and eye bolts provided to hold the guide wires at the top of the tower.

A winch was attached to one side of the drop tower for raising the test vehicles to the appropriate drop height. This winch had a capacity of 1,200 lb with a gear ratio of 4.1 to 1. The winch drum was equipped

with a nylon rope which ran through a pulley attached to the midpoint of the top aluminum plate and attached to the single point lifting and release mechanism.

A steel tape was attached between the top aluminum plate and the lower guide wire holder. This provided a convenient, rapid means for determining the test drop height.

Figure 7 provides a schematic representation of the test platform developed for and utilized in this investigation.

2.4 Instrumentation

A. Oscilloscope

In order to obtain an acceleration-time history of the test vehicle during contact with the soil, an oscilloscope recording system was essential. Because of the very small period from the instant of impact until the vehicle is at rest, a permanent record of the occuring phenomenological behavior was mandatory to permit analysis of the interaction process resulting between the test vehicle and the soil medium.

A dual-beam oscilloscope was utilized throughout this test program. This oscilloscope was manufactured by Tektronix Incorporated, Beaverton, Oregon, and is identified as Type 502A. This oscilloscope provided these extremely useful features: 100 microvolt per centimeter sensitivity, single-sweep operation, variable sensitivity and sweep time controls, intensity balance, and beam finders.

Included as part of this system was the Tektronix Type C-12 Camera to provide a permanent record of the acceleration-time information appearing on the oscilloscope screen. This camera was fitted with a Polaroid

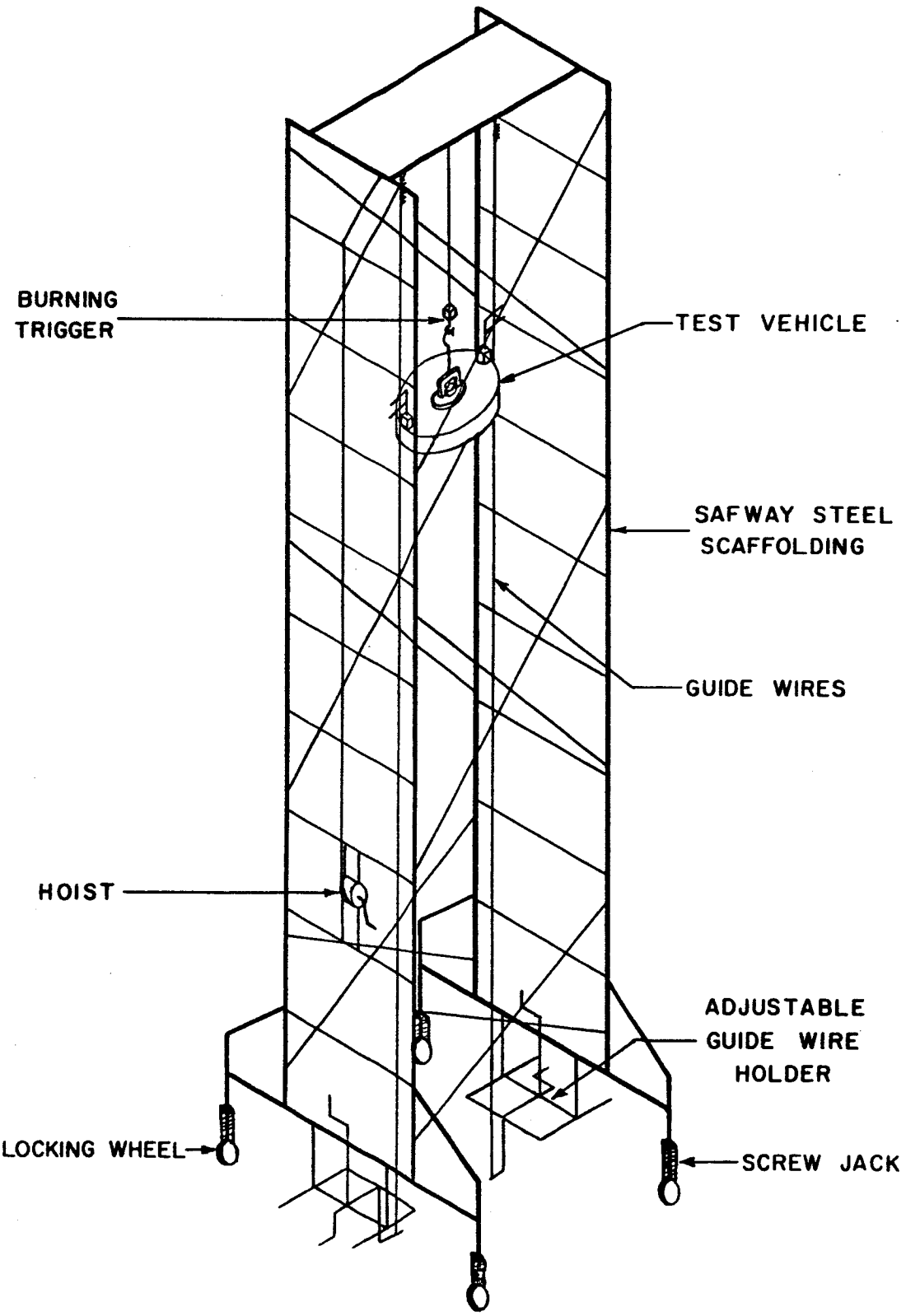

FIG. 7 DROP TEST TOWER

film pack back to permit immediate observation of the drop test record and validity of the test results.

B. Accelerometers

Accelerometers were utilized in this testing program as the primary sensors for determining the acceleration-time history of the test vehicle from the moment of impact to an at-rest condition. The use of this instrument was desirable as double integration could be performed on the acceleration-time pulse, thus determining the soil deformation as a function of time. Further, since the impact force or the resultant soil reactive force was a function of the vehicle mass and the magnitude of the acceleration pulse at any particular instant of time, a force-deformation relationship could be established throughout the pulse interval.

The accelerometers utilized were of the strain-gage type, with the sensitive axis perpendicular to the mounting plane, and temperature compensated. Two accelerometers were used: one ± 500 g. and one ± 250 g. The accelerometers were manufactured by Consolidated Electrodynamics, Transducer Division, Monrovia, California.

Before effective performance could be obtained from the accelerometers, certain modifications were essential to obtain a reliable and useable oscilloscope record. The natural frequency of the accelerometer caused the acceleration pulse to appear on the oscilloscope as a jagged curve. It was desirable to filter out this frequency, however, calibration of the sensor would then be essential. The calibration of each accelerometer would provide a constant representing a known number of

g's, which would provide a scaling factor to determine the magnitude of the acceleration pulse at any particular time. It was considered desirable to portray the calibration constant of known magnitude as part of the permanent oscilloscope record to provide the vertical scale in the data reduction process.

Figure 8 shows the wiring diagram for the accelerometers which is discussed as part of the calibration procedure. The bridge network configuration of the accelerometer produces a direct current output proportional to the applied acceleration. A constant regulated input of 5 volts dc is applied to terminals 1 and 4, and an output from 0 to 42 millivolts dc is taken off terminals 2 and 3. Normally, the four legs of the bridge are not of equal resistance. Consequently an output may be read without an applied acceleration. R1 is a current limiter to preclude any possibility of ruining the accelerometer. R2 is the calibration shunt resistor. The resistor R3 is a balancing device and varies the potential of terminal 3 with respect to 2 so that they may be made equal under static conditions.

When the switch, S1 is closed, R2 is placed in parallel with the bridge leg between terminals 1 and 2. This, in effect, applies an acceleration by unbalancing the bridge and since R2 is known and is a precision resistor, the effective acceleration may be determined.

The network shown in Fig. 8, consisting of R4, R5, R6, C1, C2 and C3 is the natural frequency filter. This particular type of filter is referred to as the parallel "T" and has the property of eliminating a certain portion of the frequency spectrum. Its use is to eliminate the approximately 2,500 cycles per second natural frequency of the accelero-

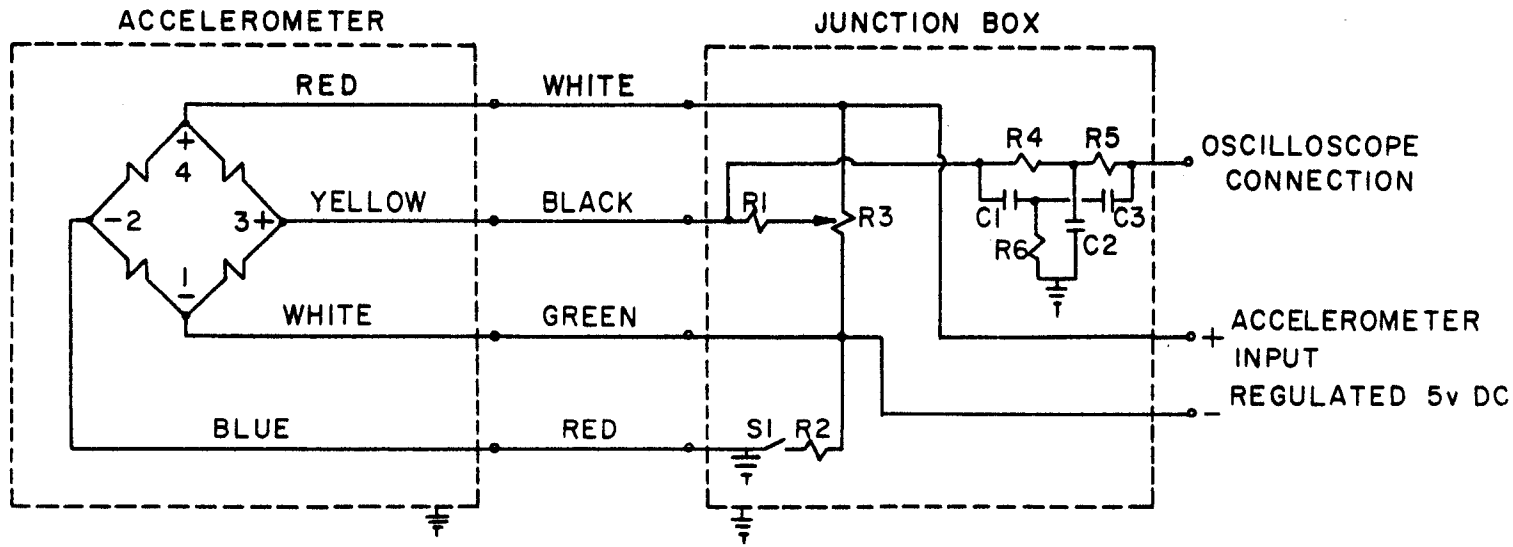

LEGEND:
R1 = 33,000 OHM RESISTOR
R2= 150,000 OHM RESISTOR
R3= 1,000 OHM HELIPOT
R4=R5=175 OHM RESISTOR
R6= 87 OHM RESISTOR

C1=C3= 0.355 MICROFARAD CAPACITOR
C2 = 0.750 MICROFARAD CAPACITOR

S1 = TOGGLE SWITCH

FIG. 8 ACCELEROMETER WIRING DIAGRAM

meter from the oscilloscope record. It will also remove this frequency component from the desired pulse, but the pulse contains this particular component with a very small amplitude; therefore the result is negligible. Not only will the filter eliminate the approximately 2,500 cycles per second, but it acts as an attenuator for the other components of the pulse. The attenuation is the same at all frequencies except at approximately 2,500 cycles per second. For this reason, the output to the oscilloscope is not the same as the output of the accelerometer and some calibration is necessary. Hence, we use R2 to calibrate the accelerometer by placing a known number of g's on the oscilloscope record. A calibration constant (scaling factor) may then be determined equal to a known number of g's.

The computation of the accelerometer constants were determined from the following equations:

$$F = \frac{\text{Full range output of accelerometer in microvolts}}{(\text{Rated excitation in volts})\quad(\text{Accelerometer range in g's})} \tag{1}$$

$$R2 = \left[\frac{10^6}{4NF} - 0.5\right] R \tag{2}$$

$$N = \frac{10^6}{4F}\left[\frac{R}{R2 + 0.5\,R}\right] \tag{3}$$

where

F = Calibration factor of the transducer in micro volts/volt-g

R2 = Precision shunt resistance in ohms

R = Output resistance of the transducer in ohms

N = Calibration constant (scaling factor) of the accelerometer in g's.

The calibration factors of both accelerometers utilized in this investigation were determined from information furnished by the manufacturer. A constant (scaling factor) of a convenient magnitude was chosen to determine the approximate value of the precision shunt resistance (R2) required. From this approximate value, a precision shunt resistance was chosen and the appropriate accelerometer calibration constant (N) was recomputed from Eq. 3.

Table 2 summarizes the information for calibration of the accelerometers utilized in this investigation.

TABLE 2

ACCELEROMETER DATA

Item	Accelerometer No. 7460	Accelerometer No. 6803
Acceleration Range (g's)	± 250.000	± 500.000
Full Range Output (millivolts)	42.120	38.180
Rated Excitation (volts)	5.000	5.000
Calibration Factor (F) (microvolts/volt-g)	16.848	7.636
Precision Shunt Resistance (R2) (1,000 ohms)	150.000	150.000
Accelerometer Constant (N) (g's)	34.680	76.520

The appropriate accelerometer constant was made a part of the photographic record of each test drop. This was accomplished by photographing the trace line when the bridge was balanced and again photographing the trace line with the shunt resistance in the circuit. The vertical separation between these two lines was always equal to the accelerometer constant regardless of the sensitivity setting of the oscilloscope. This provided an accurate available scaling factor for setting the vertical ordinate of the acceleration-time curve during the data reduction process.

C. Impact Pulse Trigger

One of the most critical components of the entire test apparatus was to devise a simple and reliable trigger which would initiate the start of the oscilloscope trace at the exact instant when the test vehicle came into contact with the soil medium. All subsequent data analysis and data reduction were dependent upon this factor being correct. Therefore, a great many preliminary tests were performed in the laboratory to insure that a reliable trigger was provided for the test sequence. It can readily be seen, when considering the cone test vehicle, that significant penetration could be effected into the soil before the vehicle would decelerate appreciably.

Initially, the oscilloscope was triggered by allowing the vehicle to impact onto a strip of aluminum foil which was placed upon the contact surface. This method did not prove to be reliable in the laboratory where conditions could be more or less controlled. Any wrinkling of the foil would introduce an error into the record and a great deal of difficulty was experienced in placing the foil. It was believed that the difficulties

experienced in the laboratory would be magnified many times when the field test series was initiated. The wind factor alone could result in a great number of test drops being wasted due to movement of the foil strip. Therefore, this method was abandoned.

A trigger was then developed which was placed on one of the guide wires. A sliding contact was insulated from the guide wire, and the trigger was adjusted with the test vehicle just touching the ground surface. The model was then raised and dropped, with the guide wire slide pushing the contact of the trigger into making contact with the guide wire, thus triggering the oscilloscope. This method also resulted in a great deal of difficulty. The friction between the guide wire and the insulation must be sufficient to insure that the contact would be pushed off of the insulation and make contact with the slide wire. However, the friction could not be excessive so as to hinder the impact of the model into the soil. This method resulted in a number of tests being useless due to the insulation moving along the slide wire and the trigger not firing, or firing after the model had impacted with the soil surface. This triggering method was also abandoned.

A positive action trigger was then devised and which is shown in Fig. 9. This trigger could be rigidly attached to the lower guide wire holder and was fully adjustable. Many drop tests were performed with this trigger and it proved fully reliable. This trigger also had the capability to fire the oscilloscope with the model at the contact surface, or in the vicinity of the contact surface if early triggering was desired. Providing the trigger was set precisely, and providing the instant the

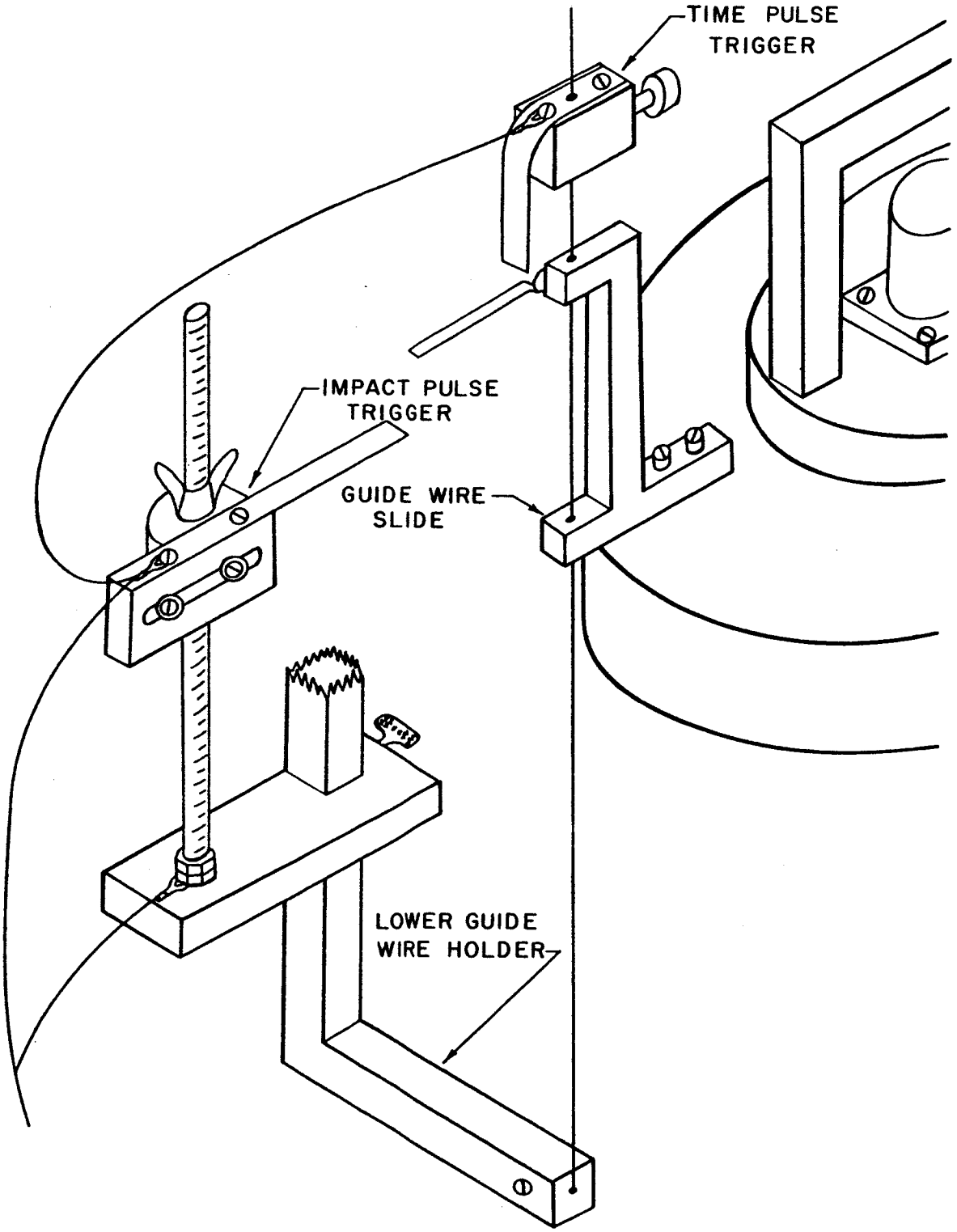

FIG. 9 IMPACT AND TIME PULSE TRIGGER SYSTEM

trace appeared on the oscilloscope could be considered zero time, it could reasonably be assumed that this trigger was completely reliable. Another possibility existed to insure that the scope picture was providing a record indicating the exact instant of zero time or contact with the soil surface. This method was incorporated into the test sequence and utilized along with the positive action trigger. This method is discussed in part D. below.

The impulse trigger was activated using a 12 volt DC battery source. The circuit consisted of an input into the oscilloscope external trigger connection along with connections to the impact pulse trigger. A contact mounted on the guide wire slide served to close the circuit and initiate the impact trace on the oscilloscope.

D. Penetration Pulse

A critical evaluation of the test instrumentation and procedures appeared to be dependent on the assumed zero time instant. That is, was the point of impact of the test vehicle with the soil surface as indicated by the beginning of the trace on the oscilloscope indeed factual. It was decided to use the second trace of the oscilloscope as a check on the actual penetration of the test vehicle into the soil, and to provide a definite point on the ground reference line of the oscilloscope for the zero time instant.

One of the guide wires on the test tower was replaced with a Karma (Nickel Alloy) wire having a resistance of approximately 8 ohms per foot of length. The wire was insulated on both ends and provided with electrical connections. Direct current voltage was supplied to this wire at

approximately one-half volt per inch of length. A new guide wire slide was prepared from plastic, fitted with electrical connections, a platinum alloy contact, and attached to the test vehicle. As the test vehicle moved down the guide wire, a change in voltage occurred causing the second trace on the oscilloscope to move across the screen in relation to the voltage change in the wire and the sensitivity setting of the oscilloscope. By superimposing both traces on a ground reference line with the test vehicle just at ground contact, and by triggering the oscilloscope early by means of the positive action trigger, a complete record could be photographed as the test vehicle penetrated the ground surface.

The amount of penetration of the test vehicle could be obtained directly from the photograph by calibrating with a dial gage the inches of travel along the slide wire corresponding to one centimeter of travel on the oscilloscope screen. This served as a positive check on the amount of penetration calculated from the data reduction process. While this method worked reasonably well in the laboratory, it was determined in the field that a more expedient procedure resulted by measuring the voltage per foot of wire and equating this directly to the sensitivity settings on the oscilloscope. Details of the penetration pulse system are shown in Fig. 10.

E. Time Pulse

In addition to obtaining the point when the test vehicle made contact with the soil surface, or zero time, it was essential in analyzing the acceleration-time record to determine the impact velocity of the test vehicle at the zero time instant.

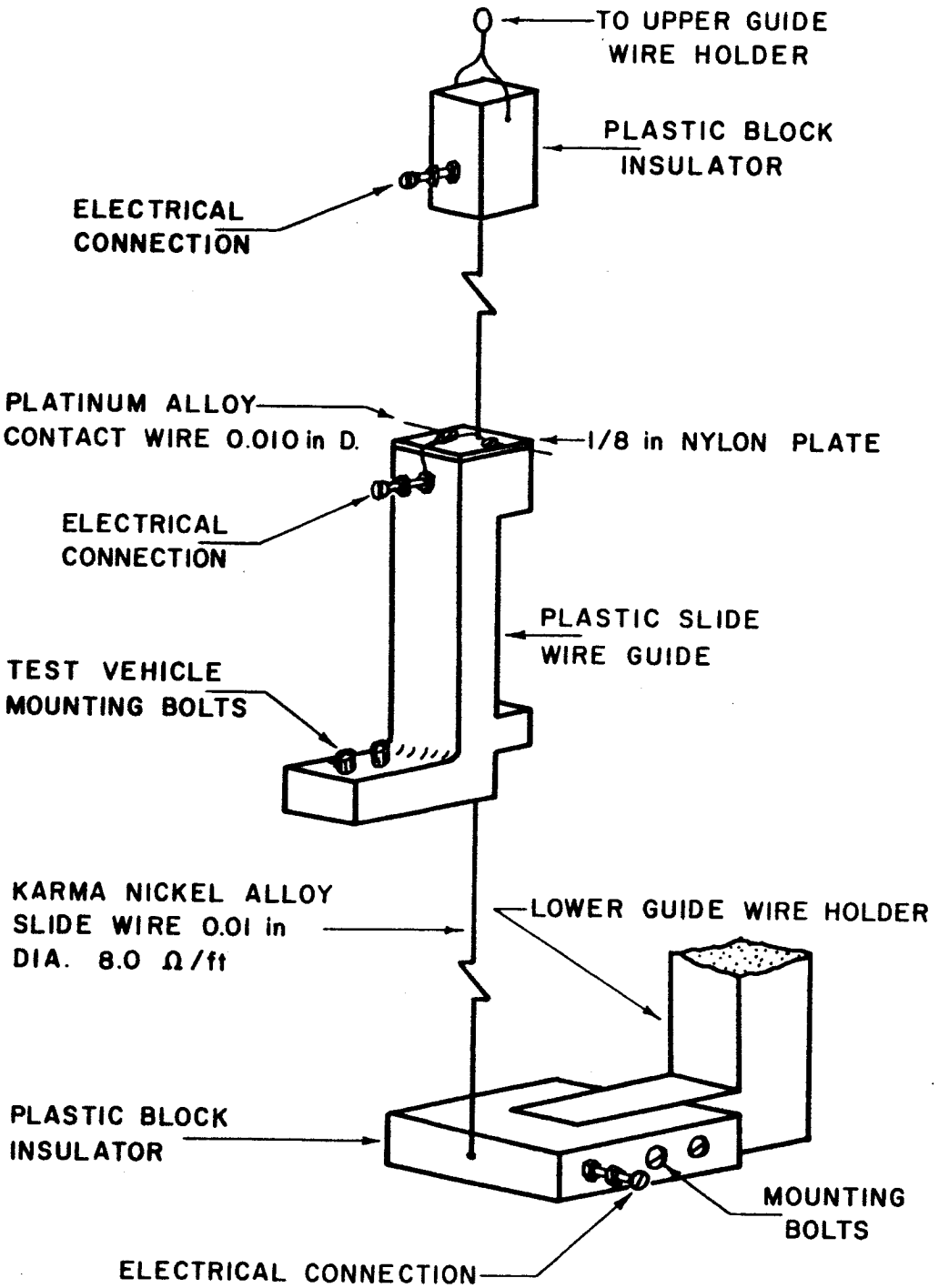

FIG. 10 PENETRATION PULSE SYSTEM

The necessity of utilizing guide wires to inhibit lateral oscillations of the test vehicle when at the appropriate drop height was required to insure that the path of drop would be vertical. As the test vehicle was raised and released from a single point support, the guide wires served as a damping influence limiting any oscillations caused by raising the model to the appropriate height. These guide wires also served an equally important purpose in being utilized within the overall instrumentation of the test setup.

Because the test drop could not be considered as free fall, it was necessary to determine what effect the guide wires would have on the velocity of the test vehicle during the drop phase. A procedure was devised and a series of test drops accomplished to determine if the guide wires contributed an appreciable frictional resistance opposing the velocity of the test vehicle when considered in a free fall condition.

A fully adjustable trigger was prepared and placed on the same slide wire as the impulse trigger, and wired into the impulse trigger circuit. The complete system is as shown in Fig. 9. This trigger was made out of plastic and equipped with a brass contact which would complete the circuit with the contact of the impulse trigger mounted on the test vehicle. The impulse trigger was adjusted with the test vehicle at ground zero, the model raised to the appropriate drop height and the time pulse trigger adjusted to make contact. As the test vehicle was released, contact was broken and a trace line initiated across the oscilloscope. As the test vehicle impacted with the soil surface, the impulse trigger circuit was closed causing a "blip" to occur on the trace line moving

across the oscilloscope screen. The amount of time from the beginning of the trace to the point of the "blip" could be taken from the oscilloscope record and utilized to determine the amount of frictional force contributed by the slide wires and impeding the acceleration of the test vehicle due to gravity.

The test vehicle may be considered falling with uniformly accelerated rectilinear motion or straight-line motion with constant acceleration. By knowing the height of the drop and the time interval from release to impact, the acceleration may be computed from the formula:

$$a = \frac{2\,s - 2\,v_o\,t}{t^2} \qquad (4)$$

where:

a = acceleration in ft/sec^2

s = height of drop in ft

v_o = initial velocity in ft/sec

t = time in seconds.

The initial velocity, v_o, is zero as the model starts from an at-rest condition, therefore equation (4) reduces to:

$$a = \frac{2\,s}{t^2}\,. \qquad (5)$$

In all tests, the acceleration computed from the test drop data corresponded to the value of gravitational acceleration, therefore, it was concluded that opposing friction from the guide wires was not significant. It was further concluded that no practical benefit would be served by con-

tinuing the time pulse as part of the oscilloscope record and it could be eliminated from the testing procedural sequence without any inaccuracy in the data reduction process. The value of the velocity of the test vehicle at impact could be computed directly from the equation:

$$v_i = \sqrt{2\,g\,s} \qquad (6)$$

where:

v_i = impact velocity in ft/sec

g = acceleration due to gravity in ft/sec^2

s = height of test drop in ft.

F. Burning Trigger

A release mechanism was essential for the test vehicles which would insure a vertical drop. It was especially desirable to preclude lateral oscillations at the initiation of the drop phase, which would be magnified when the vehicle reached the impact point. The guide wires were not intended to be utilized for this purpose, but only to damp test vehicle movement prior to release.

Various mechanical release mechanisms were considered and discarded due to the inability of controlling lateral movement. An electro-magnet was considered and also discarded due to the possibility of the electro-magnet field triggering the oscilloscope prematurely.

The final consideration, which has proven to perform extremely satisfactorily, was for a burning trigger arrangement. Figure 11 shows the configuration adopted. A small transformer was included in the single

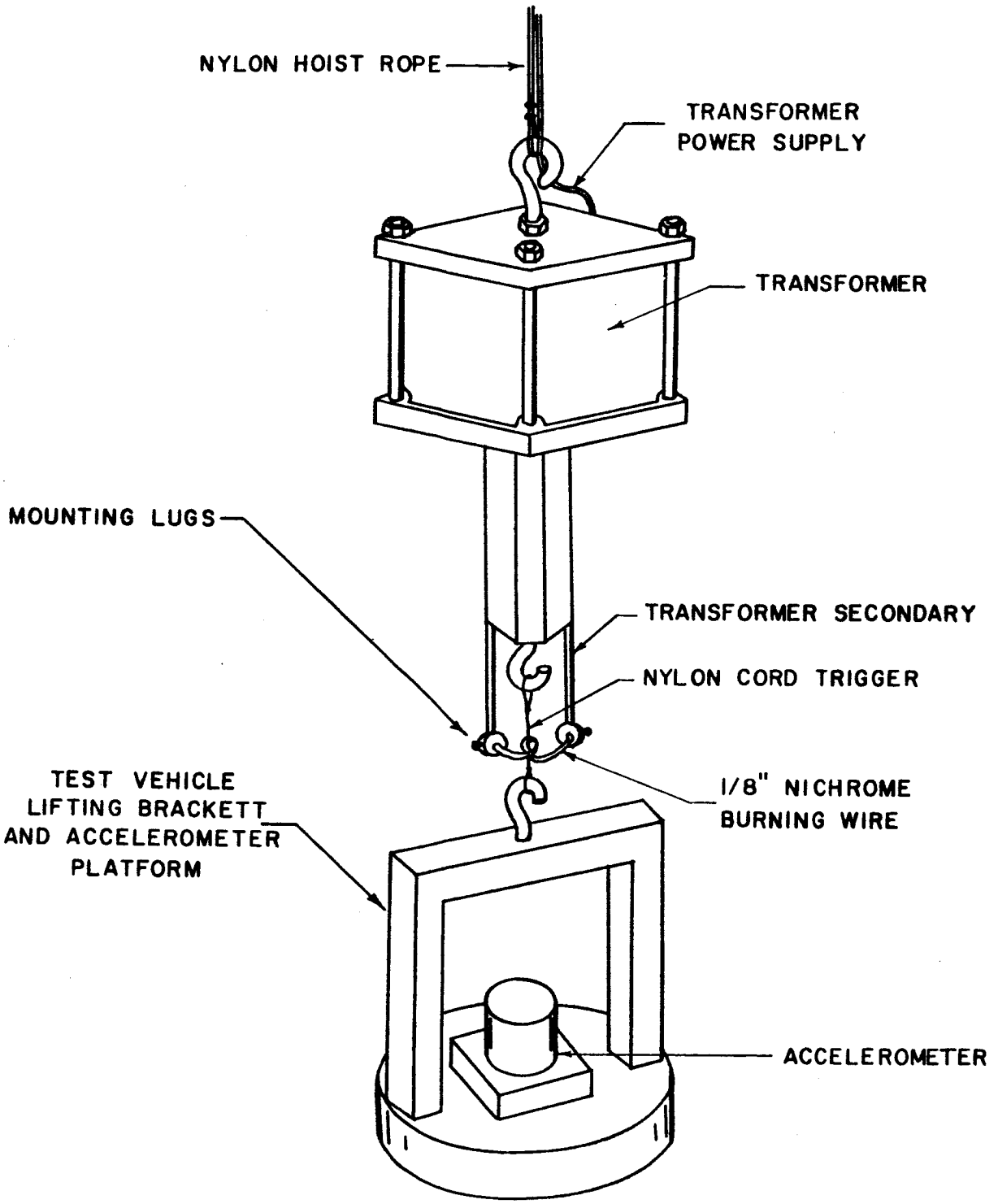

FIG. 11 BURNING TRIGGER

point lifting mechanism to serve as the power source to burn the trigger. This transformer was manufactured by the Merit Coil and Transformer Corporation and had the following characteristics: The primary side was for 117 volts at 60 cycles, and the secondary side was 6.3 volts at 10.3 ampheres. The transformer was enclosed in a metal framework to which lifting eye-bolts were attached. The secondary wires were fitted with small mounting lugs containing set screws. These lugs permitted the attachement of a strip of 1/8 in. Nichrome wire, which served as the burning element. As this wire required frequent replacement, the mounting lugs facilitated this accomplishment. Between the eye-bolts attached to the transformer and the test vehicle lifting bracket was placed a nylon cord trigger which passed through the loop in the Nichrome wire. The size of the nylon cord and its tensile strength depended on the weight of the test vehicle being utilized. When the transformer was activated, the heat from the Nichrome wire would melt the nylon trigger and the model would pull free in a vertical motion.

This trigger proved to be very reliable both in the laboratory and in the field. The increase in size of the nylon cord for the larger series of test vehicles did not decrease the effectiveness of the system. As the nylon cord melted, the weight of the test vehicle caused a vertical separation of the trigger.

G. Wiring

All wiring of the circuits from the oscilloscope to the drop tower was accomplished utilizing shielded cable. This was required to eliminate the pickup of extraneous wave forms on the oscilloscope, and to

permit grounding of the system. A console was manufactured to house the controls of all but the battery circuits. This permitted the oscilloscope operator to conduct all phases of the drop test.

Figure 12 indicates a complete wiring diagram for the test apparatus as utilized, and consists essentially of four individual circuits. The first of these is the circuit to activate the horizontal sweep on the oscilloscope. The circuit interconnects the impulse trigger on the test tower with the external trigger connection on the oscilloscope. Voltage, V2, consists of a 12 volt dc battery which furnishes the excitation required.

The second circuit is for the strain-gage accelerometer which produces the acceleration pulse. Excitation to the accelerometer is provided by a 5 volt dc regulated power supply through resistors R1 and R3 which provide the required balancing of the accelerometer bridge. Resistor R1, is a current limiter to protect the accelerometer. Resistor, R2, in conjunction with switch, S1, simulates a known number of "g's" for calibration of the accelerometer. The network consisting of R4, R5, R6, C1, C2, and C3 is a parallel "T" filter which removes the approximately 2,500 cycles per second natural frequency of the accelerometer.

The third circuit is utilized to provide the information required for the penetration pulse. Excitation, V3, is provided to the slide wire, R10, by batteries ranging from 102 to 180 volts dc, dependent upon the vehicle being tested. Resistors, R9 and R8, in conjunction with the differential input on the upper beam of the oscilloscope allows the upper beam to be placed in the ground position when the test vehicle is adjusted

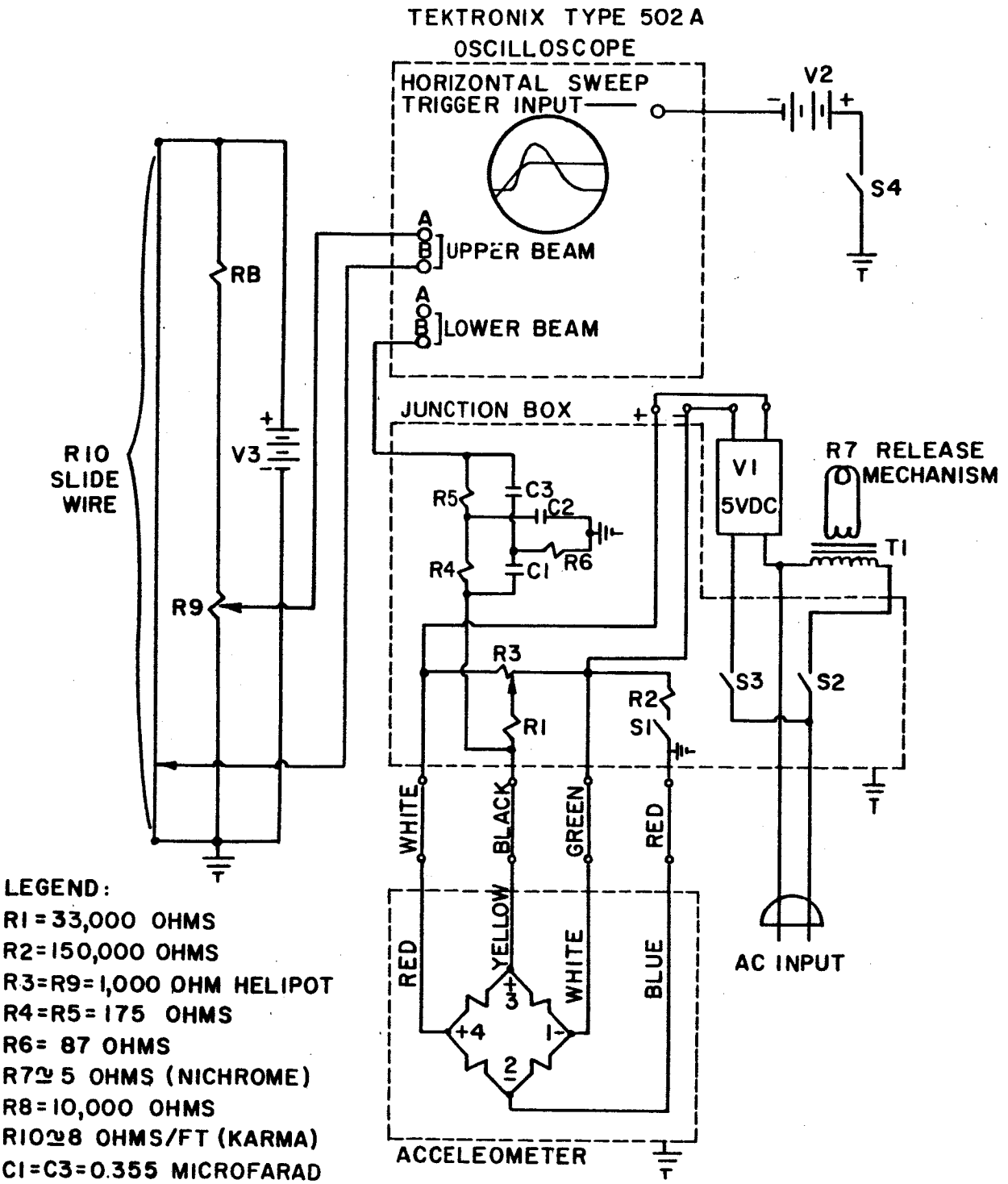

LEGEND:
R1 = 33,000 OHMS
R2 = 150,000 OHMS
R3 = R9 = 1,000 OHM HELIPOT
R4 = R5 = 175 OHMS
R6 = 87 OHMS
R7 ≅ 5 OHMS (NICHROME)
R8 = 10,000 OHMS
R10 ≅ 8 OHMS/FT (KARMA)
C1 = C3 = 0.355 MICROFARAD
C2 = 5.25 MICROFARAD
V1 = 5VDC REGULATED
V2 = 12VDC
V3 = 102 – 180 VDC
NOTE : ALL EXTERNAL WIRES ARE SHIELDED

FIG. 12 TEST APPARATUS WIRING DIAGRAM

to the point of impact.

The fourth circuit serves the test vehicle release mechanism. Transformer T1, is a 6.3 volt, 10.3 amphere device providing the required power to R7. R7 is an approximately 5 ohm, Nichrome wire which melts the nylon trigger supporting the test vehicle.

2.5 Idealized Record

The objective in the development of the test apparatus and procedures was to obtain reliable drop test information. This must be information which could be effectively utilized to analyze the interaction relationship between a geometric shape and a soil system when dynamic impact occurs.

Figure 13 portrays an idealized photographic record of a drop test. The information contained provides the acceleration-time history of the test vehicle and the soil from the instant of impact to an at-rest condition. A reference point is provided for the instant of impact or zero time. A computable value is indicated for the maximum penetration of the test vehicle into the soil medium. Calibration lines for the accelerometer are provided, a known value apart, to establish the vertical ordinate of the acceleration-time curve.

All of the information portrayed is considered essential to the test record in the data reduction process.

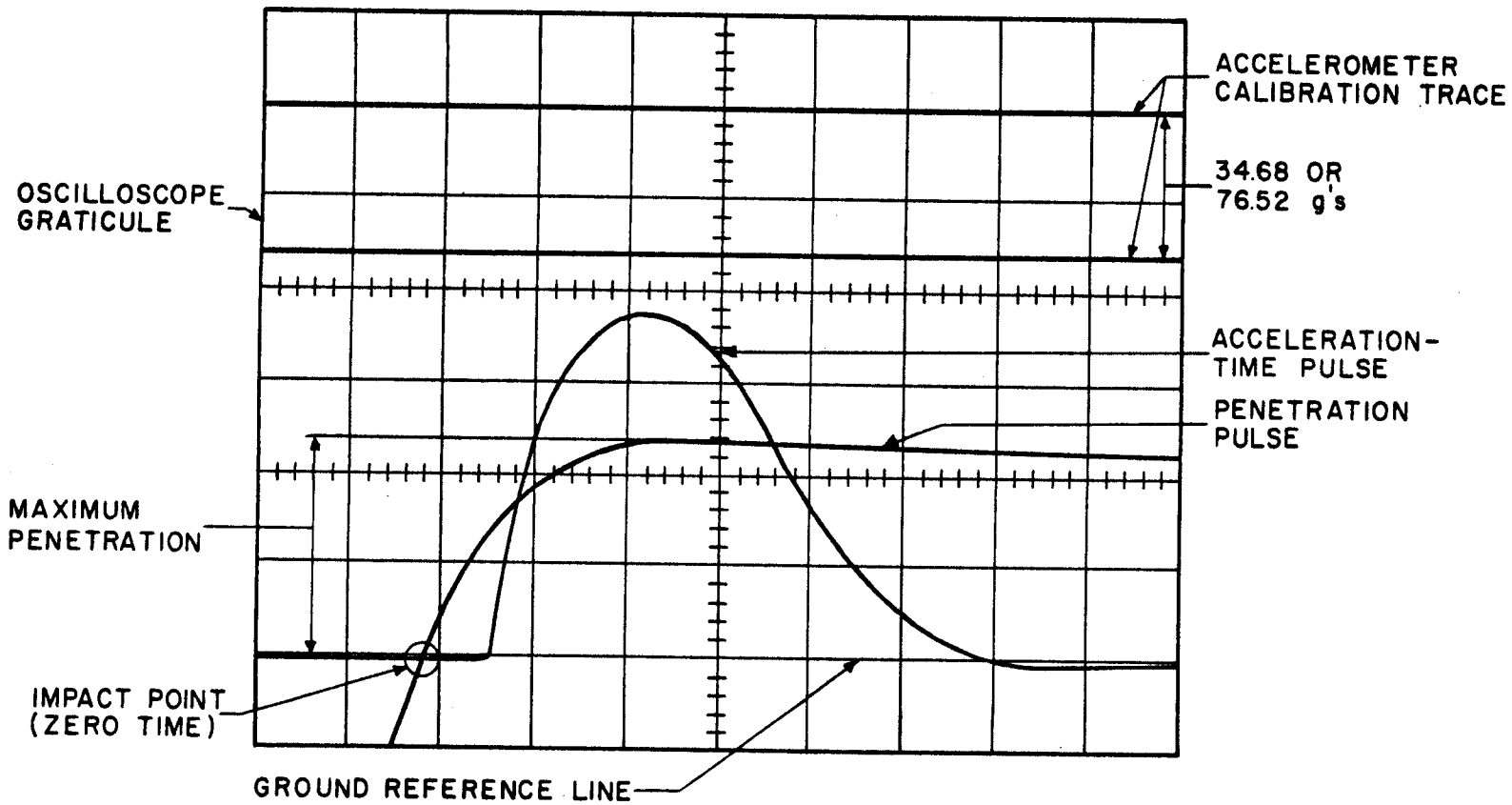

FIG. 13 IDEALIZED RECORD

CHAPTER THREE

TEST SITE

3.1 General Requirements

A series of field drop tests required the location of a soil deposit which would fulfill specific requirements. While it is realized that if a requirement was forthcoming at a future date for a spacecraft to impact on a land mass, it may or may not be expedient to provide a landing area with the same soil classification as utilized in this program. However, it is to be considered that a clayey type soil would be evident in most of the areas where such a landing would be attempted.

In order to obtain results from the test program that could be realistically analyzed, a test area had to be located that would provide uniform soil conditions. The area should also be of sufficient area that the entire testing program could be accomplished within the boundaries. Further, the soil strata must be of sufficient thickness to preclude any effects of sub-surface rock layers reacting with the drop test vehicles. Specifically, it was extremely desirable to locate a soil test area which could realistically be considered homogeneous and isotropic throughout the confines of the test area, and to a depth of approximately fifteen feet.

3.2 Test Borings

A field survey was conducted within the vicinity of Austin, Texas, to determine if a suitable area could be located which would fulfill the

necessary requirements. In addition to the specific stipulations for the test area, certain highly desirable features were considered which, while not mandatory, would facilitate the entire field test program. These were the availability of both a power and water supply source.

Test borings were accomplished at four areas at The University of Texas, Balcones Research Center. These borings were made with a standard, hand earth auger. In all cases, it was found that the soil depth was insufficient before encountering a limestone formation known locally as Austin Chalk. This area was determined to be unsuitable and was eliminated from further consideration.

Test borings were performed on the south bank of the Colorado River on property owned by the City of Austin. Here it was found that very coarse sand was encountered at a depth of approximately three feet and auger borings could not be accomplished to the desired depth. Other areas in this general vicinity were inspected visually and were considered unsuitable due to the complete unavailability of a power and water source.

Three areas were then tested within the confines of the Austin Country Club. All of these borings indicated that the depth of soil was sufficient to permit development of a drop test area. Two of these areas indicated some variation of soil type with depth. Visual classification ranged from a very lean clay (CL) at the surface to an extremely plastic clay (CH) at depths ranging from 8 to 12 feet. The third area indicated a relatively uniform soil from the surface down to 15 feet. Four borings were then taken in this area and were located to encompass sufficient area to accomplish the field series of drop tests. All borings indicated

the soil to be extremely uniform and suitable for the intended test program. Visual classification indicated the soil to be a lean clay (CL) with some fine sand and organic material depending on the depth. Pending further testing, this area was believed to be suitable for the testing program. In addition, a source of power and water was available within the immediate vicinity.

3.3 Site Selection and Preparation.

A. Borings

Four additional auger borings were performed encompassing the general test area. Samples for moisture content determination were taken in the field at each foot of depth. The sample cans were sealed with tape in the field to preclude any moisture loss before weighing could be accomplished. In addition, disturbed auger samples were taken at each foot of depth. These samples were placed in quart jars to provide a sample of sufficient size to perform standard classification tests.

B. Classification

From the samples obtained from the auger borings, tests were performed in the laboratory to determine the Atterberg Limits of the material at each foot of depth. Having determined the Liquid Limit (LL) and the Plastic Limit (PL), the Plasticity Index (PI) for each sample could be determined and the material classified on a plasticity chart. The moisture content for each foot of depth was determined directly from the samples taken in the field. Table 3 provides a summary of the index properties utilized in classifying the soil structure.

TABLE 3.

SOIL CLASSIFICATION

	BORING 1					BORING 2					BORING 3					BORING 4				
	LL	PL	PI	MC	CLASS	LL	PL	PI	MC	CLASS	LL	PL	PI	MC	CLASS	LL	PL	PI	MC	CLASS
0				14.64	CL				15.38	CL				13.40	CL				11.09	CL
1	29.41	19.22	10.02	8.26	CL	30.80	19.06	11.74	6.78	CL	29.99	20.00	9.99	8.96	CL	28.14	18.44	9.70	5.88	CL
2	29.30	18.84	10.46	6.81	CL	27.90	17.76	10.14	6.30	CL	29.08	18.12	10.96	6.07	CL	27.55	18.70	8.85	5.76	CL
3	31.30	16.74	14.56	9.44	CL	28.52	20.10	8.42	7.31	CL	30.12	18.87	11.25	6.54	CL	28.80	19.63	9.17	5.89	CL
4	30.88	17.71	13.17	11.08	CL	27.53	19.42	8.11	8.44	CL	29.45	17.68	11.77	6.86	CL	28.85	19.30	9.55	6.49	CL
5	30.75	16.24	14.51	12.06	CL	28.74	18.57	10.17	9.70	CL	29.45	19.20	10.25	7.16	CL	27.90	15.70	12.20	6.86	CL
6	28.06	18.27	9.79	11.80	CL	27.36	17.32	10.04	10.07	CL	26.80	17.92	8.88	7.67	CL	25.15	17.43	7.72	6.81	CL
7	27.73	14.87	12.86	11.58	CL	26.48	17.64	8.84	9.79	CL	27.36	18.56	8.80	9.65	CL	24.85	14.92	9.93	8.19	CL
8	24.17	21.43	2.74	9.21	ML	23.73	17.42	6.31	9.70	CL-ML	25.93	17.40	8.53	8.68	CL	25.05	18.09	6.96	10.49	CL-ML
9	24.20	23.15	1.05	7.91	ML	22.88	20.77	2.11	9.48	CL	21.80	20.68	1.12	7.30	ML	26.40	16.20	10.20	10.73	CL
10	23.23	22.90	0.33	8.95	ML	23.85	18.23	5.62	10.51	CL-ML	25.35	17.28	8.07	10.36	CL	25.75	15.82	9.93	6.92	CL
11	25.92	19.76	6.16	13.26	CL-ML	29.94	20.75	9.19	16.83	CL	29.60	18.56	11.04	12.89	CL	26.45	18.33	8.12	--	CL
12	32.59	21.35	11.24	19.17	CL	28.10	34.80	13.30	15.67	CL	27.90	16.57	11.33	11.89	CL	47.80	19.63	8.17	17.16	ML
13	34.84	12.63	22.21	19.10	CL	26.27	16.20	10.07	16.64	CL	36.50	16.92	19.58	16.17	CL	49.60	19.04	30.50	17.34	CL
14	29.45	16.58	12.87	17.88	CL	36.86	18.65	18.21	17.88	CL	44.90	20.47	24.43	15.93	CL	44.70	18.23	26.47	16.28	CL
15	28.63	16.48	12.15	19.32	CL	45.70	16.72	28.97	17.89	CL	41.50	19.47	22.03	8.88	CL	36.05	18.23	17.82	14.27	CL

As an aid in properly visualizing the condition of the soil from the surface downward, it was convenient to portray certain soil properties as a function of depth in graphic form. These properties are the Moisture Content (MC), the Liquid Limit (LL), and the Plastic Limit (PL), and are shown in Figs. 14, 15, 16, and 17. These plots aid in the classification process and serve to provide an indication of the soil history.

From all available information, it was determined that the area chosen for field testing comprised a portion of an alluvial flood plain from the Colorado River. The area was considered to be preconsolidated from desiccation, and may be classified as a lean clay (CL) of low plasticity.

Figure 18 portrays the location of the test borings in relation to the field test area, and the boring logs. Inasmuch as the soil in the upper third of the media was of the primary interest, it was concluded that the test area consisted of soil which was considered to be homogeneous and isotropic.

C. Moisture Content Monitoring

Figure 19 indicates the moisture content fluctuation with depth for the four borings. It was considered desirable to reduce the rapid drop in moisture content within the first three feet of the soil. Samples were taken every four inches to a depth of three feet in the vicinity of each boring twice a week. This was accomplished to monitor how the moisture content was varying with the weather conditions. After three weeks of observations, it was determined the moisture content of the upper three feet of the test area would have to be increased and then

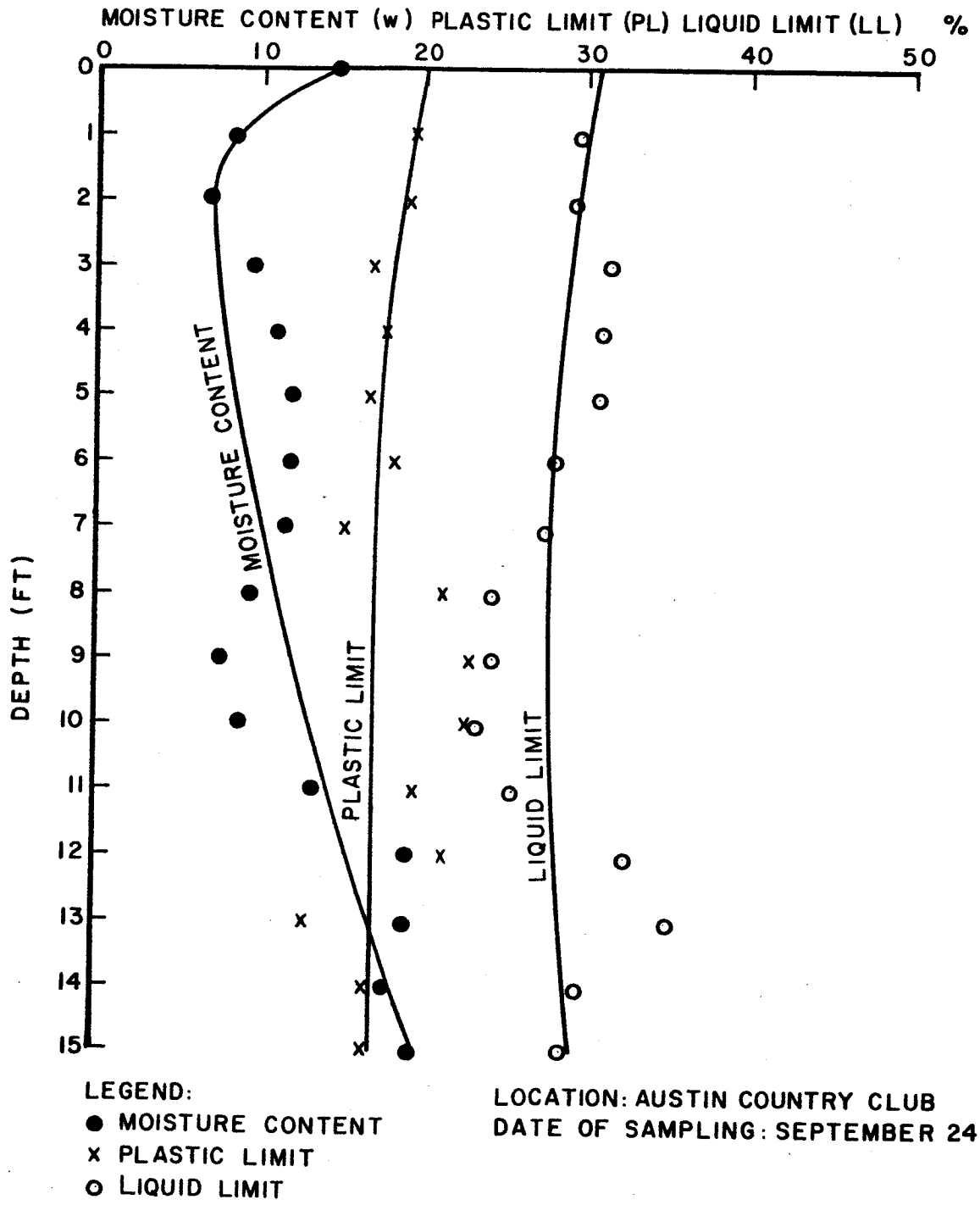

FIG. 14 ATTERBERG LIMITS & MOISTURE CONTENT vs DEPTH, BORING I

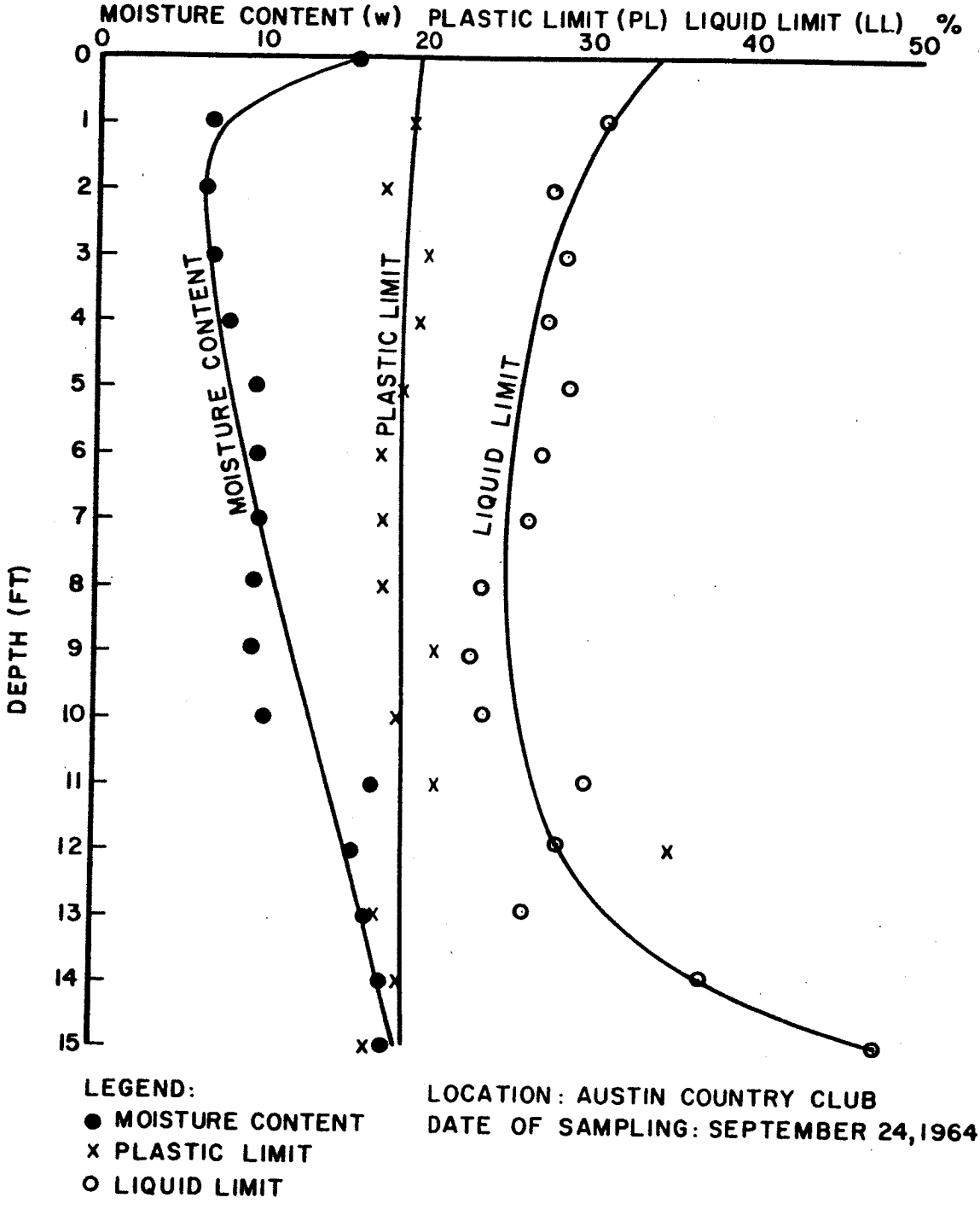

FIG. 15 ATTERBERG LIMITS & MOISTURE CONTENT vs DEPTH, BORING 2

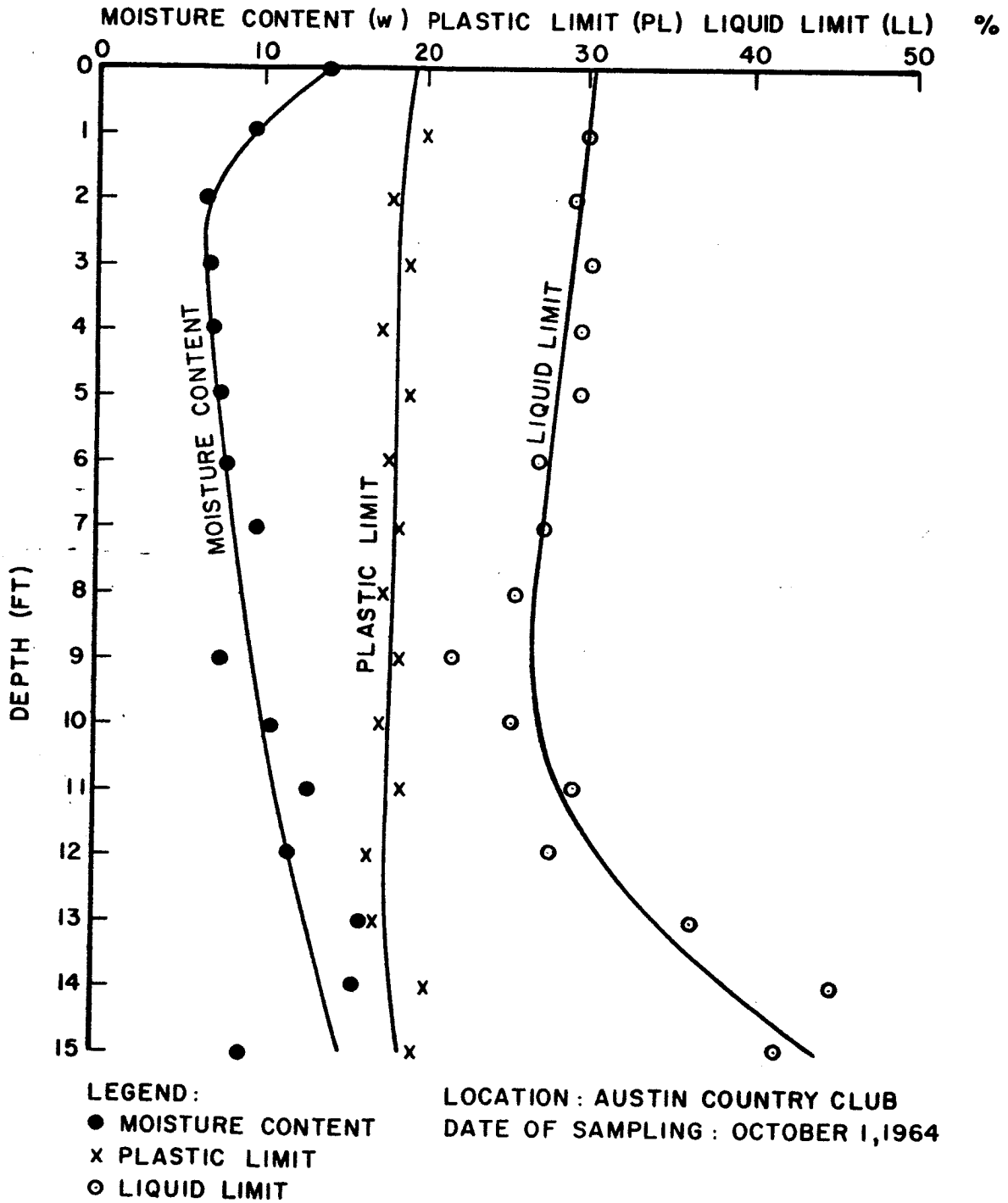

FIG. 16 ATTERBERG LIMITS & MOISTURE CONTENT vs DEPTH, BORING 3

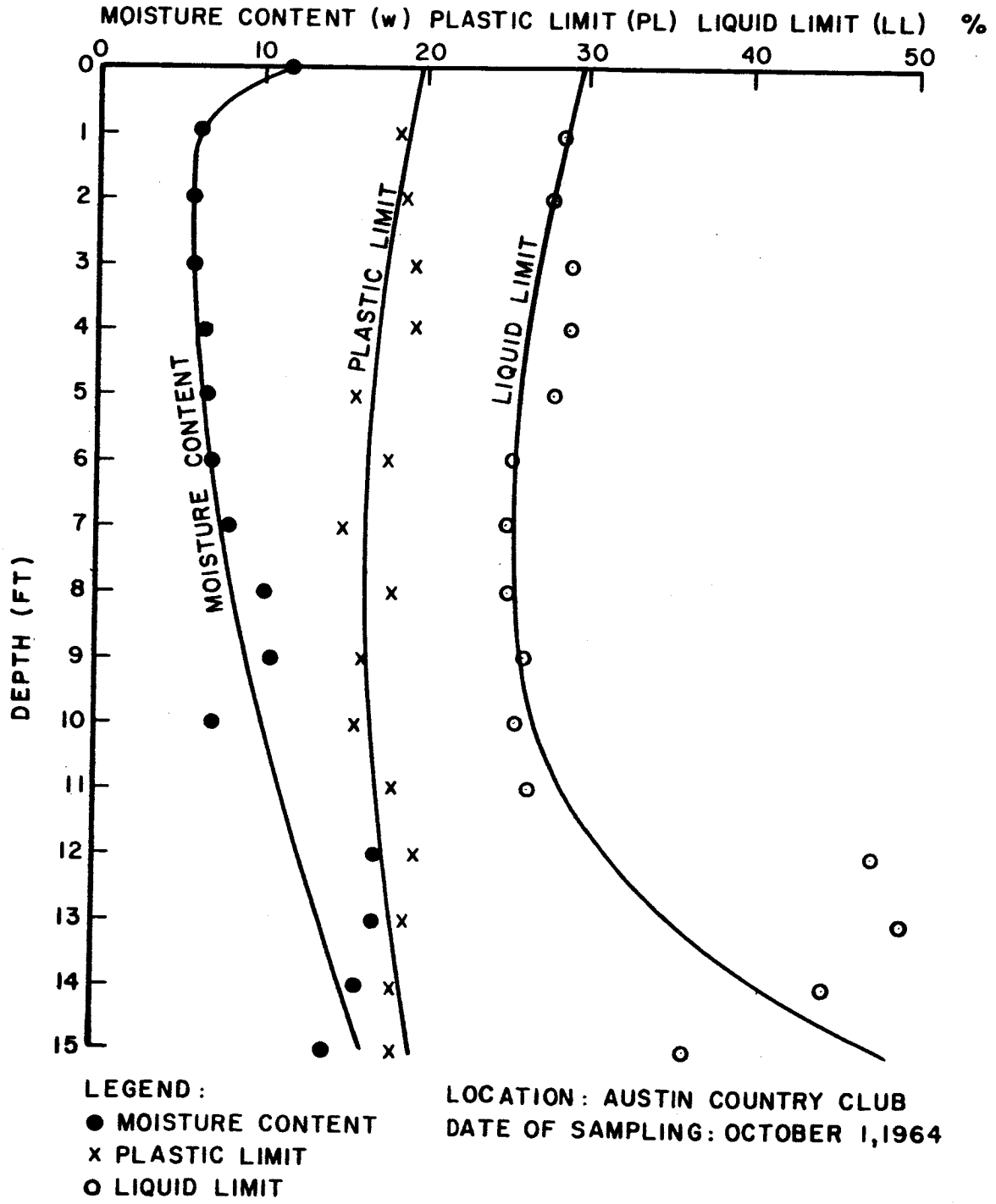

FIG. 17 ATTERBERG LIMITS & MOISTURE CONTENT vs DEPTH, BORING 4

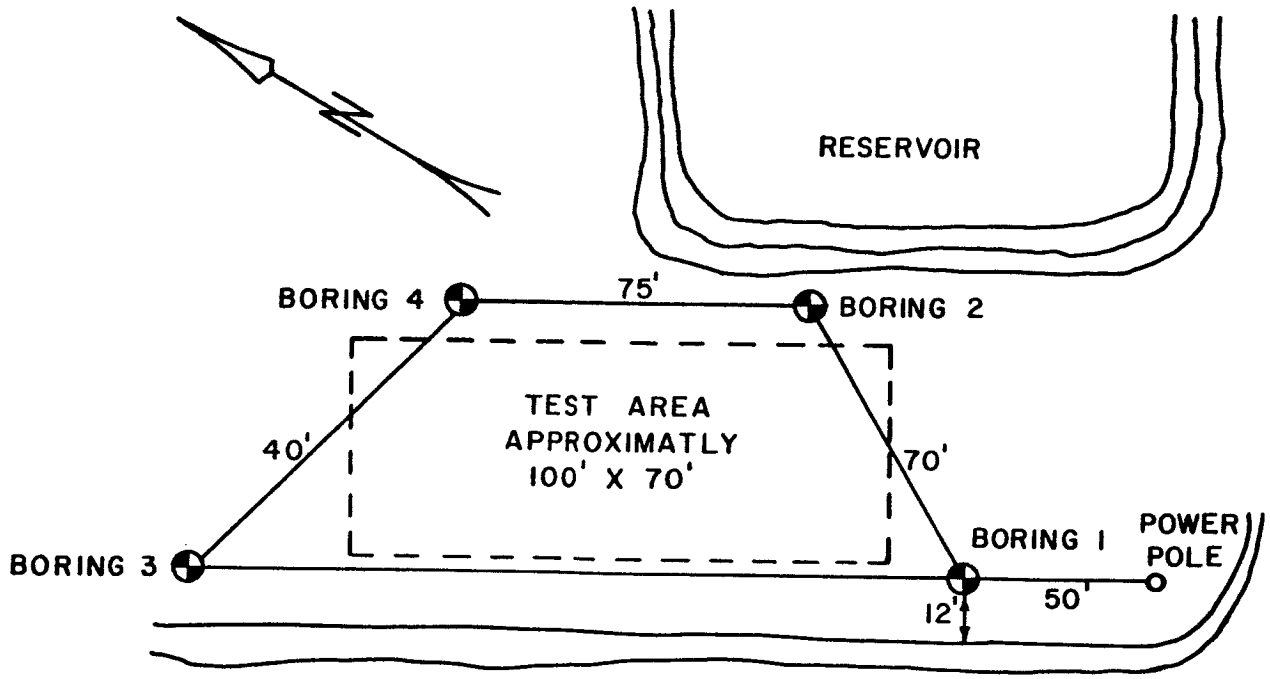

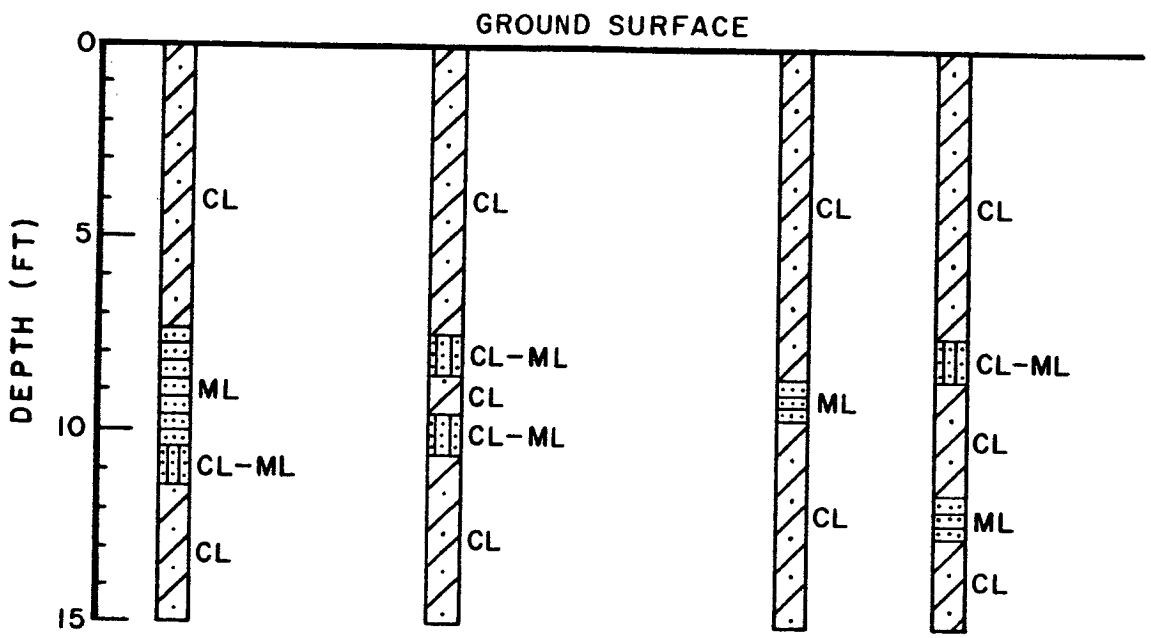

FIG. 18 SITE PLAN AND BORING LOG

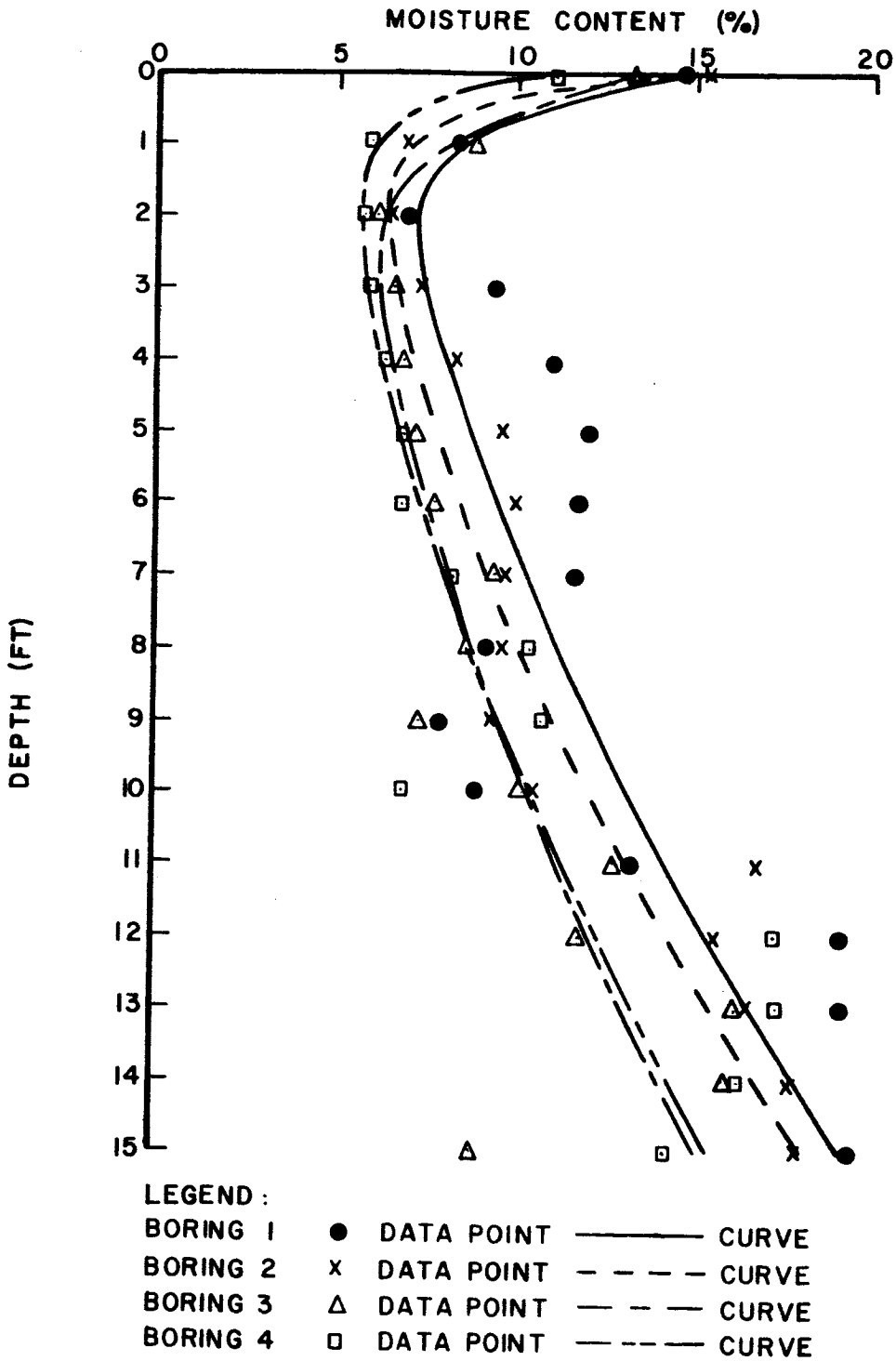

FIG. 19 MOISTURE CONTENT vs DEPTH, BORINGS 1,2,3, AND 4

allowed to stabilize.

D. Area Flooding

An area approximately 100 ft by 70 ft was chosen as the primary test site. This area was roughly graded utilizing a tractor equipped with a hydraulically controlled scraper. This was accomplished to remove the surface grass and weeds, but did not provide an absolutely smooth surface or eliminate elevation changes from one end of the area to the other. It was believed that gradual elevation changes could be accepted without any difficulty in the testing sequence. Further, it was considered desirable to avoid disturbing the surface area to any appreciable degree.

A small dike was built around the area and flooding was accomplished by pumping water from the reservoir located in the vicinity of the test area. The area was flooded on three different occasions and soil samples taken for moisture content determination between each flooding. When the moisture content to a depth of three feet was fairly uniform and in the vicinity of 18 per cent, flooding was stopped and the area prepared for stabilization prior to initiating the field test series.

E. Area Protection

In order to permit the moisture content to stabilize within the test area, and to preclude any appreciable loss of moisture due to evaporation, the entire test area was provided with a protective covering. Sufficient rolls of vinyl plastic were obtained in lengths of 100 ft and widths of 3 ft to cover the area and provide an overlap on adjacent strips of approximately four inches. Utilizing the strip method for

covering permitted separation at the overlap when a drop test was being accomplished and immediately resealing the plastic upon completion. It was necessary to continue with the area protection after completion of the drop tests in order to obtain undisturbed thin wall tube samples for shear strength determination. The undisturbed sampling was accomplished at this time as it was desired to obtain the cores with the soil medium at approximately the same condition as during the testing program.

3.4 Undisturbed Sampling

The soil properties within the upper three feet of the test area were of primary interest in analyzing the behavior characteristics occurring between the test vehicle and the soil system. The requirement to identify adequately these properties necessitated sampling the foundation medium in an undisturbed state. The shear strength, apparent cohesion, and apparent angle of internal friction of the soil were desired in order to establish the significant properties of the area more completely.

To accomplish the sampling process as expeditiously as possible, it was concluded that the apparatus required to obtain undisturbed cores could be fabricated within the laboratory. Figure 20 shows the configuration of the developed equipment. As the upper three feet of the soil layer were considered of primary interest, it was determined that the developed apparatus had sufficient driving capacity to obtain the undisturbed cores. The driving force was provided by a hydraulic jack of 3,000 lb capacity, and having a stroke of 20 in. The driving force was applied against a 6-in. channel held by chain to four earth anchors. The supporting

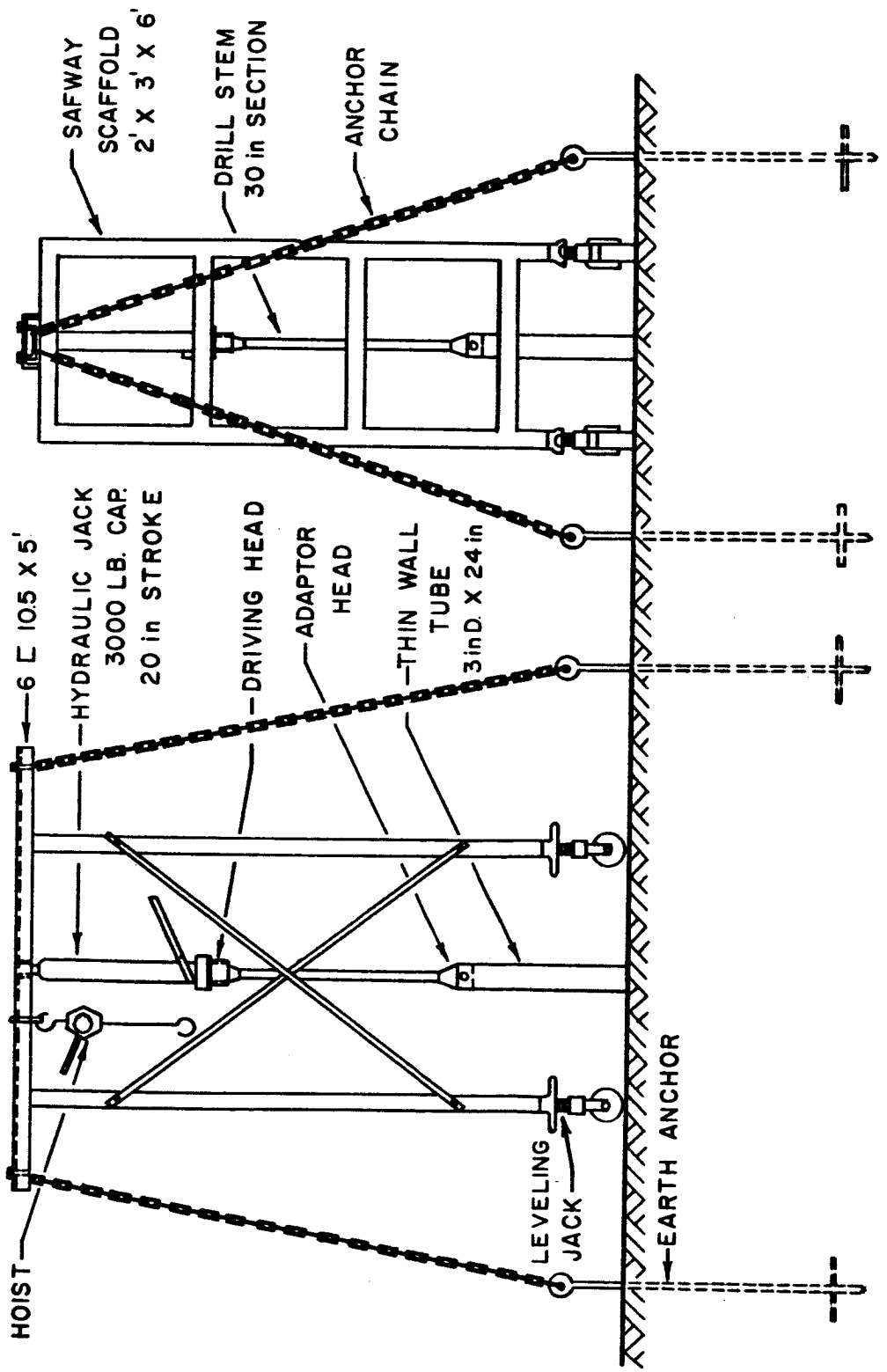

FIG. 20 UNDISTURBED CORE SAMPLING APPARATUS

structure for the apparatus consisted of a six-foot section of scaffolding utilized from the drop test tower. The ability to push hydraulically the 3-in., thin-wall tubing into the soil provided a core sample with a minimum of disturbance.

Two cores were obtained from each of four different locations within the center half of the test area from positions which were not disturbed during the impact testing program. The cores were immediately sealed after extraction to preclude any moisture loss from evaporation during transport to the Soil Mechanics laboratory. The undisturbed cores were extruded in the laboratory, wrapped in plastic, sealed in glass jars, and placed in the moisture room subsequent to testing.

Standard tests were performed on samples prepared from all four borings. These tests were unconfined compression tests, and triaxial compression tests at 2 and 3 $lb/in.^2$ confining pressure.

As it was assumed that the soil strata comprising the test area could be considered homogeneous and isotropic throughout, it was concluded for convenience, an average value of shear strength parameters could also be established. Figure 21 shows the Mohr Circle Diagram plotted to show the average values for the apparent cohesion, and the apparent angle of internal friction.

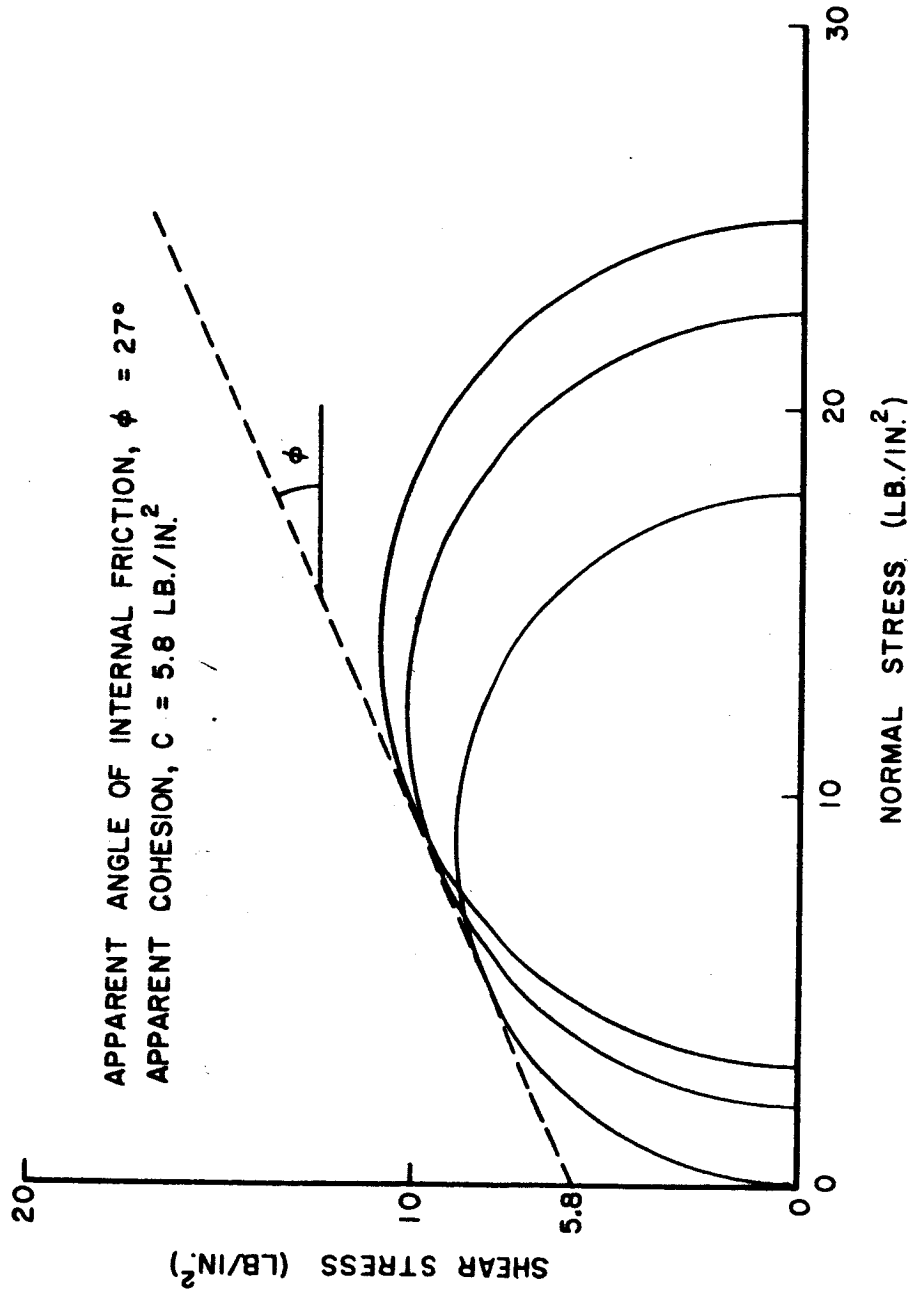

FIG. 21 MOHR CIRCLE OF TEST AREA SAMPLE

CHAPTER FOUR

LABORATORY TESTING PROCEDURES

4.1 General

The requirement was established to conduct a limited number of drop tests in the laboratory. The limitation on the number of tests was necessitated in part due to the sizes of the test vehicles, and also due to the physical limitations of the laboratory.

The overall height of the test tower precluded its erection in the Soil Mechanics laboratory, therefore, an alternate setup was required. A metal plate was fitted to one of the overhead structural loading points within the laboratory to hold the guide wires and pulley for raising the test vehicles. Metal holders were manufactured which could be attached to the soil container to provide the lower guide wire support and to position the impulse trigger mechanism.

The soil container utilized in these laboratory test drops was the largest size available from other phases of this overall project. The use of this soil container limited the depth and breadth ratio of the model to 3.6. However, a larger container could not be realistically provided and have sufficient vertical height to drop the vehicles. With the test setup as discussed, the maximum vertical drop height was limited to approximately 43 in.

One of the primary purposes of conducting laboratory test drops was to determine if the testing procedures were feasible, and the reliability of the equipment. It was essential to be able to obtain repeatable results.

in the laboratory where conditions could be controlled before attempting drop tests under field conditions.

The laboratory series was essential to determine the effect of the guide wires on the computed impact velocity of the test vehicle. This was found to be negligible in relation to the mass of the test vehicles.

The laboratory testing was also necessary in determining whether assumptions made during equipment development were factual or whether modifications would be required.

Finally, the laboratory test series served to provide repeatable oscilloscope records in order to determine the reliability of the data reduction process and computer program.

4.2 Foundation Medium

A. Container

The test bed utilized in the laboratory drop series was existing from other phases of this project. The container was constructed of 3/4-in. plywood and had a length of 36 in., a width of 36 in., and a depth of 37 in. The extra in. of depth was provided to permit placing sufficient sand to allow a 36-in. depth after the final vibration. The container was banded to prevent any pulling apart, and the box was mounted on a heavy duty cart to permit proper positioning in relation to the top guide wire support plate.

B. Soil Bed Preparation

Initially the soil bed was prepared by filling the container in 6-in. increments and vibrating each increment for 4 minutes. The vibration

process was accomplished with a standard concrete vibrator, placing it into the material at the four corners and at the midpoint of each side for a period of 30 seconds. After placing the final 6 in., but before vibration, the surface was leveled with a steel straight edge. At this time,the guide wire holders were positioned, with the alignment being determined with the aid of a transit. The material was then given the final vibration and remained undisturbed until the drop test was initiated. Upon completion of the drop test, the container was completely emptied and the entire process repeated.

Due to the amount of time and effort required to prepare the container after each drop, a revised procedure was implemented which still provided repeatable densities of the soil media. After the test drop, the top two layers or 12 in. of sand was removed from the container. The remaining material in the container was scarified or loosened and then vibrated by the same procedure for four minutes. The remaining two layers were then placed following the original procedure.

C. Material Data

The sand utilized for the laboratory test drops was the same material as was provided for the static load test phase of the overall project.[8] This material is a clean river sand obtained locally from the Colorado River. It is considered to be a uniform fine sand with well rounded grains. One hundred per cent of the material passes the No. 20

sieve, and seven per cent passes the No. 80 sieve. The average density of the material vibrated in place is 101 lb/ft^3 with a probable error of 0.8 lb/ft^3. The angle of internal friction of the sand at the average density is 38.7°.

4.3 Drop Test Procedure

The drop test procedure comprises a multitude of separate individual operations, each of which was essential in insuring that an accurate useable oscilloscope record was obtained. It is not intended to list each individual step for the entire testing sequence, but only to discuss the primary operations. It should be noted, however, that in order to insure useable results were obtained from the testing procedure, a step by step check list was mandatory to preclude any deviation from the desired sequence.

The photographic record obtained from the oscilloscope for each individual test was the acceleration-time history of the interaction relationship between the test vehicle and the soil system. A useable result from the testing sequence which could be analyzed in the data reduction process required portraying four separate photographs on one piece of film. The useable record must accurately indicate:

a. The complete acceleration-time history from zero time to the at-rest condition. This was provided by using an accelerometer as the primary sensor.

b. The point where the test vehicle contacted the soil surface. This is also known as the point of zero time and was provided by the intersection of the penetration

trace and the accelerometer trace with the referenced ground line. An additional benefit provided by the penetration pulse was that it gave an indication of the maximum penetration of the vehicle into the soil system and provided a check on values computed in the data reduction process.

c. Two horizontal lines whose distance apart was a known value. These lines were known as the calibration lines of the accelerometer and had been established to provide the vertical scale in the data reduction process. The distance between these lines always represented a known constant in "g's", depending upon the accelerometer used.

Briefly, the testing sequence proceded as follows after preparation of the soil bed.

a. The oscilloscope was balanced, the horizontal sweep rate was set, and the sensitivity of both traces established.

b. The test vehicle was positioned at the ground surface.

c. The impulse trigger was adjusted along with the oscilloscope external trigger.

d. Power supplies for the penetration pulse, impact pulse, and accelerometer were activated.

e. Both traces were superimposed on the ground reference line.

f. The test vehicle was raised to the appropriate drop height and the oscilloscope camera positioned.

g. The camera shutter was opened for a time exposure, and the burning trigger circuit activated allowing the model to drop. Impact of the model with the soil would provide the

accelerometer trace and the penetration trace on the photograph. The camera shutter was then closed.

h. The penetration trace was removed from the oscilloscope and the accelerometer trace moved to the top of the screen and photographed. The calibration circuit was then activated and another photograph taken.

i. The accelerometer trace was removed from the oscilloscope and the graticule of the screen photographed as the final step before the film was developed.

After each test drop, the model was removed and the soil bed reworked to the required density.

CHAPTER FIVE

FIELD TESTING

5.1 General

The primary test program of this research project was conducted in the field. All other laboratory testing, while essential and necessary to the successful completion of the project, served to support the field test program. This interpretation is intended to indicate that all preliminary testing was mandatory to insure the successful accomplishment of the field testing and provide the required validity of results.

The speed with which the entire field test series could be successfully accomplished was considered to be an important factor in obtaining results which would be meaningful. The rapid and accurate accomplishment of the series would insure that changes of the soil index properties would be at a minimum. Difficulties in adjusting the test equipment precluded testing during the hours of darkness, therefore, the program was established to run from first light until darkness. Approximately two hours was required to prepare and insure correct operation of the entire test facility. To obtain the maximum record test period, assembly and disassembly was accomplished during the hours of darkness.

To ascertain if the developed equipment would function as required under field conditions, a considerable number of non-record test drops were performed. These were essential to permit adjustments in the equipment, and to correct problem areas which developed in the field but were not apparent in the laboratory. The non-record drops were performed

adjacent to the prepared test area. This was done to avoid using up the test area while checkout of equipment was still being accomplished.

5.2 Test Area

The site of the area prepared for the field test series, as previously discussed in Chap. III, was located within the confines of the Austin Country Club. The area, approximately 100 ft by 70 ft was of sufficient size to contain the entire series of 48 test drops plus available space for tests which must be repeated due to unacceptable results. For the largest size series of test vehicles, drop tests were accomplished on 10-ft centers. For the smallest size series, the drop tests were performed utilizing 5 ft centers. Only one drop for record was permitted for any position. In the event that the results of a record drop were unuseable, the entire drop tower was moved to a new position. After each test drop, the exposed ground surface was covered to insure that the loss of surface moisture would not be significant.

5.3 Field Check of Equipment

A complete performance check of the entire test apparatus in the configuration to be utilized in the field was essential before initiating the field test series. The drop tower and supporting instrumentation could not be fully checked for performance in the laboratory due to physical ceiling height limitations. It is to be noted, however, that all portions and components of the complete system were checked to the maximum extent possible.

The field check consisted of a systematic step-by-step progression of the drop test sequence intended to be utilized. Deviations were not permitted in order to determine with assurance the degree of reliability of the system. The tower was erected, instrumented, and leveled. The guide wires for the test vehicles were positioned with the aid of a transit. The oscilloscope system was prepared, test vehicle positioned, and the drop test performed. Various size and shape models were utilized during this phase, with test drops being performed at the planned drop heights of 6, 9, 12 and 15 ft.

5.4 Problem Areas

The field check of the test apparatus disclosed a number of problem areas which were not apparent in the laboratory. Resolution of these difficulties was required during the field check phase in order to obtain reliable record data.

A. Sunlight

It was discovered that testing in bright sunlight would seriously effect the photographic record obtained from the oscilloscope. Sufficient light would pass to the oscilloscope screen through the case vents to overexpose or fog the polaroid film during the test sequence. It was necessary to manufacture a protective enclosure to fit around the oscilloscope and camera system to eliminate this problem. This hood was built utilizing screen mesh wire and black cloth, and was so prepared to facilitate simple installation and removal.

B. Wind

Wind was found to have an adverse effect on the vertical drop of the test vehicles. No serious problems were evidenced with velocities up to 10 miles per hour. However, at higher velocities, and in particular gusty conditions, oscillations would be imparted to the test vehicles which were undesirable. Under these conditions, test operations had to be suspended.

C. Oscilloscope Noise

Considerable difficulty was experienced in attempting to eliminate extraneous wave forms from the oscilloscope traces. In particular, the guide wire utilized for the measurement of the penetration of the test vehicle, which was charged with 102 to 180 volts of direct current, acted as an aerial into the oscilloscope. At sensitivity settings higher than 0.5 volts per centimeter, the oscilloscope trace would blossom so as to be unuseable. The wave form being picked up was isolated and found to be in the range of 1,500 kilocycles. Two radio stations exist in Austin, Texas, which broadcast within this approximate range. Numerous corrective measures were attempted to eliminate this problem. These ranged from all types of possible grounding techniques, to enclosing the entire tower in wire mesh. The latter method almost proved disastrous to the entire test program, for while this process was being tried a wind gust toppled the entire structure.

It was determined after considerable experimentation that the most acceptable solution to the problem was to operate the oscilloscope on lower sensitivity settings and increase the imput of direct current volt-

age into the guide wire for the penetration trace. This procedure was found to provide the most useful and desirable information on the oscilloscope record.

D. Penetration Pulse

Originally it was believed feasible to utilize a dial gage to measure the amount of movement of the test vehicle which would correspond to a movement of one centimeter of the penetration trace across the oscilloscope screen. While this method worked reasonably well in the laboratory, the adjustment of the dial gage under field conditions proved extremely difficult. This was particularly evidenced with the heavier test vehicles which could stretch the nylon hoist rope. In attempting to utilize this procedure under field conditions, it was found that repeatable readings could not be obtained with any degree of reliability. Because of this, the use of the dial gage was abandoned and a new procedure was developed.

A plastic bar with brass connections on each end was prepared. The overall length of the bar was established at 12 in. for convenience. The metal connections would slip across the penetration pulse guide wire, and voltage readings would be taken from the metal contacts. An electric volt meter was utilized to measure the voltage in the penetration guide wire across the 12 in. distance. The amount of voltage per inch of length along the penetration pulse guide wire would have a direct correlation to the voltage per centimeter sensitivity setting on the oscilloscope. This method proved very satisfactory and could be quickly accomplished in the field without difficulty.

E. Tower Leveling

The procedure followed to level the drop tower was to utilize a hand level along the four sides of the tower and adjusting as required with the individual leg jacks. This procedure was satisfactory for the cone and sphere test vehicles where clearance between the test vehicle and the bottom guide wire holders was not critical. It was found, however, that leveling of the tower to insure a vertical drop was extremely critical for the plate series where clearances were a minimum. It was also believed that even with the base section of the tower perfectly level, there was no positive assurance that the top sections could not have some deviation. To insure a high degree of accuracy, the 16 lb cone test vehicle was utilized as a plumb bob. Attachment was made to the single point lifting mechanism, and the weight of this model was sufficient to insure that a vertical reference line was in being between the top and bottom of the tower. The entire structure could then be leveled and adjusted with accuracy.

5.5 Test Procedure

The step-by-step sequence of events in conducting the actual drop test is the same as for the laboratory test procedure discussed in Chap. IV, Art. 4.3. The deviations in procedure for the two series occur prior and subsequent to each drop.

The drop tower is rolled into position, and the bottom guide wire holders are lowered and adjusted. The tower is then leveled and the supported test vehicle positioned. At this time the protective covering over the impact area is separated and the area examined for rocks or other

foreign material which could significantly influence the acceleration-time record. The area was lightly scraped with a steel straight edge to remove any loose material and eliminate undesirable ridges.

The test vehicle was then raised to the appropriate height and released following the standard sequence. All test vehicles for the field series were dropped from 6, 9, 12, and 15 ft.

Upon conclusion of the drop sequence, the test vehicle was raised and supported. The voltage per ft was measured on the penetration pulse guide wire and a physical measurement of penetration accomplished if feasible. A sample of the soil was taken from the center of the impact area for a moisture content determination.

The guide wire holders were then raised, the protective covering replaced, and the drop tower rolled to the next test position. In the event of a malfunction which eliminated the test from consideration, the same procedure was followed, as only one impact was allowed for any test position.

CHAPTER SIX

RESULTS

6.1 General

The amount of test data obtained necessitated a data reduction process of some magnitude. The methods employed in analyzing the information obtained from the acceleration-time photograph of the oscilloscope record were established to permit a maximum amount of useable information to be obtained, subject to a minimum of operator error. The data reduction procedure was initiated early in the research program. This was done to preclude any delay in analyzing data upon completion of the testing phase. The oscilloscope records of acceleration-time data were reduced to useable information by normal integration procedures. The first integration provided velocity-time data and the second integration provided displacement-time data. The oscilloscope records were digitized by use of a Universal Telereader, and the numerical computations were accomplished on a CDC 1604 digital computer.

6.2 Telereader Analysis

The photograph portraying the acceleration-time information from the oscilloscope record was placed in the Telereader and magnified approximately four times. The Y or vertical coordinates of the accelerometer calibration traces were first punched. The entire range (ten centimeters) of the X or horizontal coordinate was then punched. This initial procedure established data points to permit computation of the scaling

factors which was accomplished as part of the computer program. Information was then taken from the first zero coordinates of the acceleration-time curve until termination a number of data points later. The Telereader was nominally set for approximately 100 millivolts per centimeter on the photograph and coordinate data points were taken approximately 0.2 centimeters apart. Each acceleration-time record was thus broken down into 30 to 50 divisions by this procedure. Care was taken to insure that the range of the X-axis did not exceed +999 millivolts or the capacity of the Telereader would be exceeded and erroneous information output.

The output from the Telereader provided a punched paper tape in octal code. Each data point taken from the acceleration-time record was represented on the paper tape by 23 character frames which comprised a coordinate record. Each of the character frames, having six punch positions, must represent one alphanumeric or special symbol. It was essential to feed the tape back into a Teleprinter for a translation of the data points. This was necessary to insure the correctness of the data points, and to permit preparation of a new tape if errors existed. It was also found that physical detailed examination of each record on the tape was required to insure that punches essential to the proper operation of the tape were in being. These were special instruction punches and were not included as part of the Teleprinter output translation. Considerable care was mandatory in preparing the paper tape as it was input directly into the computer as part of the input data. There was no specific limitation on the number of individual tests which could be placed on a paper tape provided the additional input instructions to the computer were com-

patible. It was convenient in this research program to limit the number of tests per tape to a maximum of four. This corresponded to the number of drop tests accomplished on a particular configuration of test vehicle.

6.3 Computer Program

A computer program was developed to accomplish the numerical computations required in reducing the drop test data to useable information. In accomplishing the double integration of the acceleration-time record, the first integration of the curve was made assuming linear variation of acceleration between each data point, and utilizing the impact velocity for the initial condition. The second integration was performed by integrating the second degree velocity curve between each data point. At the instant of contact between the test vehicle and the soil surface, or zero time, the deformation was considered zero.

The computer program utilized a number of available library sub-routines to accomplish the numerical computations and provide more useable output information. A sub-routine was provided to permit feeding the paper tape directly as input data. A sub-routine was also included for the computer to furnish four plots for each individual test, in addition to the desired print-out of information. These plots were acceleration-time, velocity-time, deformation-time, and force-deformation. These plots proved to be an invaluable aid in immediately visualizing the test results and determining necessary corrections if appropriate.

The check-out of the computer program was accomplished by assuming a sine wave to represent the acceleration pulse. A wave generator was connected to the oscilloscope and a photographic record taken to permit

an accuracy determination of the data reduction process. In addition, a check was performed on the integration equations as written in the program to determine if a significant loss of accuracy existed. The program was modified to also perform the required integrations utilizing the Trapezoidal Rule and Simpson's Rule. Instructions were input to plot the results of all three methods on each of the four plots obtained. The output results from this procedure were so close that no benefit in accuracy would result from changing the established program.

Appendix A contains additional detailed information on the computer program utilized for the numerical computations in this research project.

6.4 Results from the Laboratory Test Series

One of the primary purposes of the laboratory test series was to determine the performance and reliability of the developed equipment and testing procedures. It was also desirable to ascertain if the equipment and procedures had the accuracy and capability to provide repeatable results. Tables 4, 5, and 6 list the results obtained from performing four drop tests into the prepared sand bed using the 8 lb sphere, cone, and plate. After each test, the sand foundation medium was reworked and vibrated back to the desired density. For the sphere and plate test vehicles, drops were accomplished from a height of 43 in. For the cone test vehicle, the drops were performed from a height of 41 in. due to height limitations.

It should be noted that the measured penetration values indicated for the cone and plate tests are the penetrations physically measured after the vehicle had reached an at-rest condition. This measurement was

TABLE 4

LABORATORY TEST SERIES

8.66 in. Dia. Sphere - 8.0 lb.

Test No.	Drop Height (in.)	Impact Velocity (ft/sec)	Maximum Acceler-ation (ft/sec^2)	Pulse Duration (ms)	Maximum Force (lb)	Maximum Stress (lb/ft^2)	Maximum Surface Area (ft^2)	Maximum Comp. (in.)	Maximum* Meas. (in.)	Final Comp. (in.)
50	43.0	15.19	3093	28.32	568.4	8,975	.3145	1.442	1.360	1.442
51	43.0	15.19	2314	27.66	575.0	8,745	.3378	1.548	1.500	1.548
52	43.0	15.19	2211	28.23	549.2	9,074	.3471	1.591	1.544	1.591
53	43.0	15.19	2276	28.09	565.4	7,013	.3579	1.640	1.575	1.640

*Measured displacement is related to the maximum computed displacement. Displacement measured with penetration pulse trace.

TABLE 5

LABORATORY TEST SERIES

7.08 in. Diam. Cone - 8.0 lb

Test No.	Drop Height (in.)	Impact Velocity (ft/sec)	Maximum Acceler-ation (ft/sec^2)	Pulse Duration (ms)	Maximum Force (lb)	Maximum Stress (lb/ft^2)	Maximum Surface Area (ft^2)	Maximum Comp. Disp. (in.)	Maximum* Meas. Disp. (in.)	Final Comp. Disp. (in.)
15	41.0	14.83	507.3	97.48	1260	2022	0.308	4.604	4.375	4.600
16	41.0	14.83	490.7	95.65	1219	2790	0.288	4.416	4.250	4.023
17	41.0	14.83	467.9	97.68	1190	5198	0.325	4.755	4.375	4.755
18	41.0	14.83	518.6	97.58	1288	2532	0.278	4.378	4.25	4.238

*Measured displacement is related to the final computed displacement. This is a physical measurement when vehicle is at a rest condition.

TABLE 6

LABORATORY TEST SERIES

10.0 in. Dia. Plate - 8.0 lb

Test No.	Drop Height (in.)	Impact Velocity (ft/sec)	Maximum Acceler-ation (ft/sec^2)	Pulse Duration (ms)	Maximum Force (lb)	Maximum Stress (lb/ft^2)	Maximum Surface Area (ft^2)	Maximum Comp. Disp. (in.)	Maximum* Meas. Disp. (in.)	Final Comp. Disp. (in.)
10	43.0	15.19	8,751**	9.550	1839	3370	0.546	.3277	0.25	.3277
11	43.0	15.19	7,785	7.964	1934	3550	0.546	.3000	0.25	.3000
13	43.0	15.19	8,435**	8.592	2096	3840	0.546	.3977	0.32	.3960
14	43.0	15.19	8,316**	9.385	2066	3785	0.546	.3600	0.32	.3490

*Measured displacement is related to the final computed displacement. This is a physical measurement when vehicle is at a rest condition.

**Drop tests 10, 13, and 14, exceeded linearity range of accelerometer.

accomplished prior to raising the test vehicle from the sand bed to preclude any displacement of the sand and permit a more accurate determination. It represents the final penetration of the vehicle, but not necessarily the maximum penetration which had occurred during the acceleration-time interval. Any elastic rebound of the soil would have taken place when the vehicle reached an at-rest condition. This value has a correlation to the final computed deformation given in the results.

The measured penetration values indicated for the sphere test vehicle are related to the maximum computed deformation. This more meaningful and accurate value was obtained when the penetration pulse was incorporated into the testing procedure. This value of penetration comprises both plastic and elastic deformation of the soil during the acceleration-time interval. It was measured from the oscilloscope record and provided a check of the computed deformation.

Figure 22 shows an oscilloscope record for the sphere test vehicle as obtained during the laboratory test series. This figure also indicates the testing equipment utilized in the laboratory.

Figures 23, 24, and 25 show the plots of the force-deformation curves of the four tests for each test vehicle. These figures indicate the capability of the testing procedure to provide both reliable and repeatable results. The results as shown are considered to be remarkably good. Especially so when working with a soil as complex as sand, and realizing that the foundation medium was reworked following each drop test.

The force-deformation curves have a primary significance. This relation indicates the force of the foundation medium reacting against the

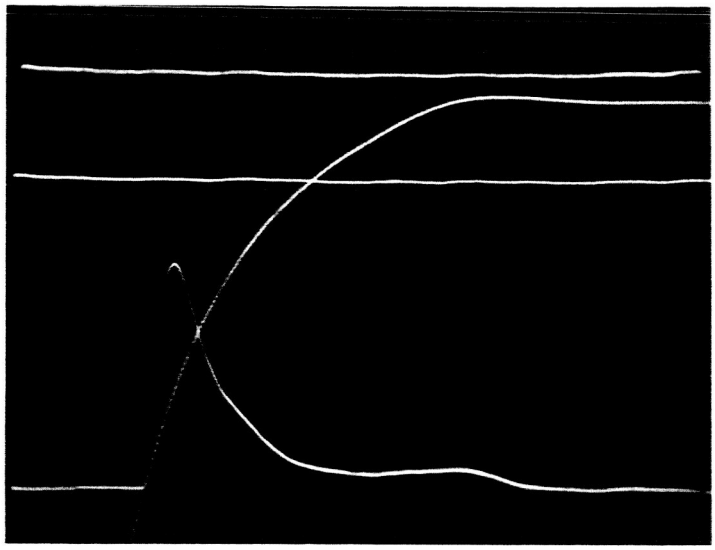

Laboratory Test 51 - 8.0 lb Sphere
Drop Height 43 in. Sweep Rate 5 msec/cm
Sensitivity: 0.1 v/cm Penetration Pulse
2 mv/cm Acceleration Pulse

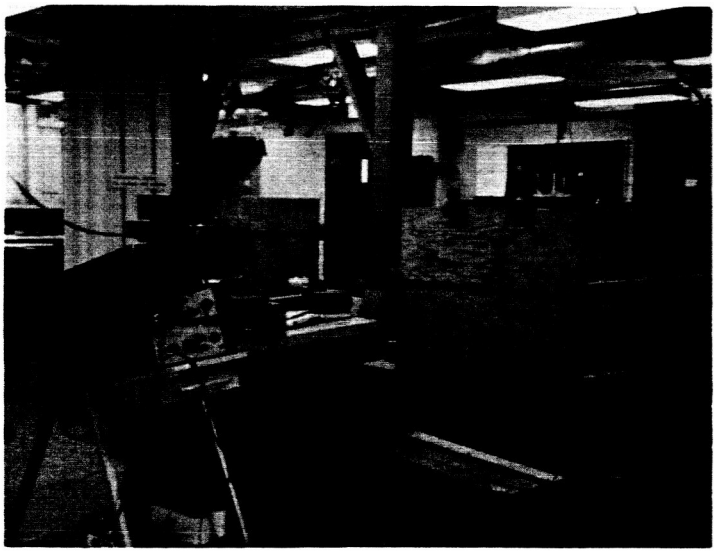

Laboratory Test Equipment

Fig. 22 Laboratory Test 51 Record and Test Equipment

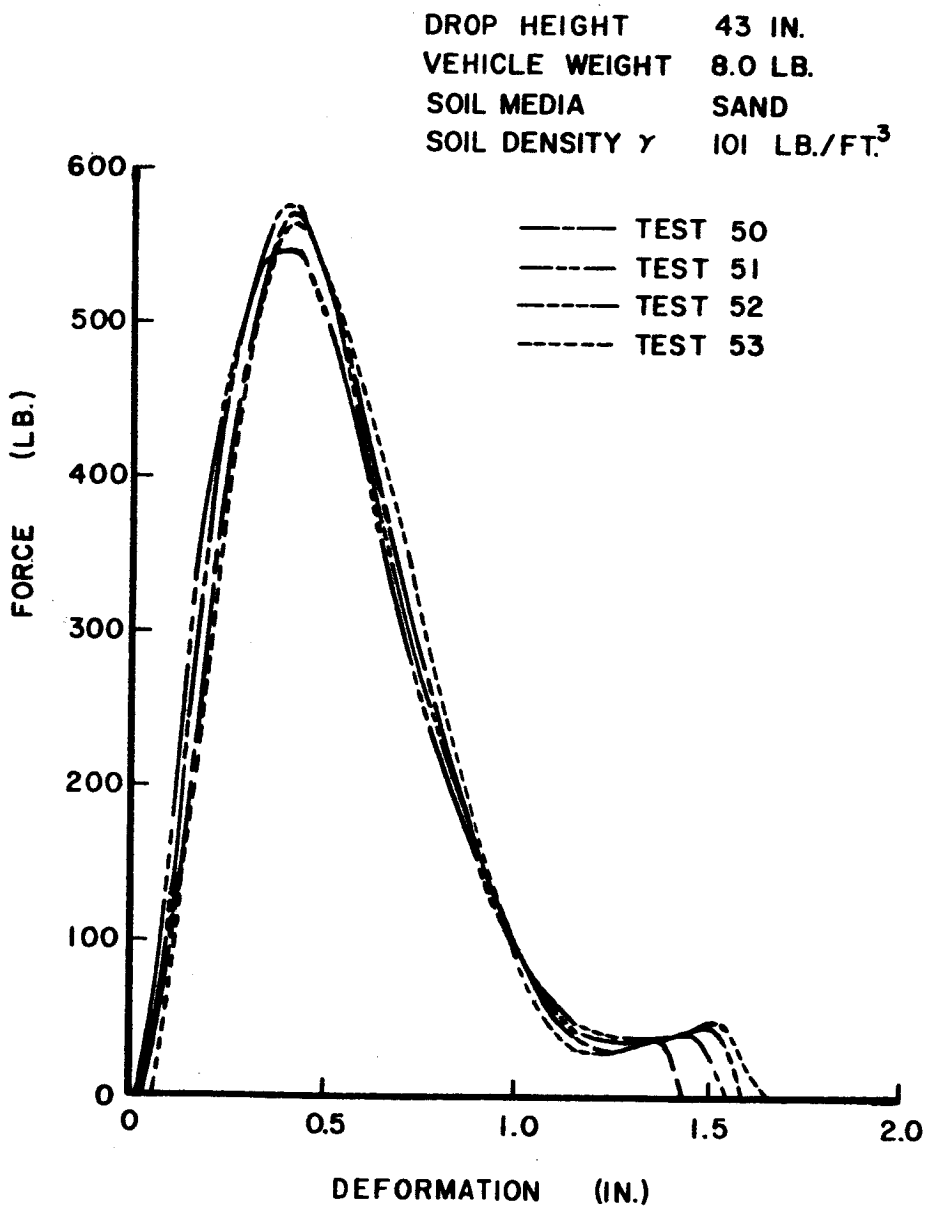

FIG. 23 FORCE – DEFORMATION CURVES
LABORATORY TEST SERIES – 8.66 IN. DIA. SPHERE

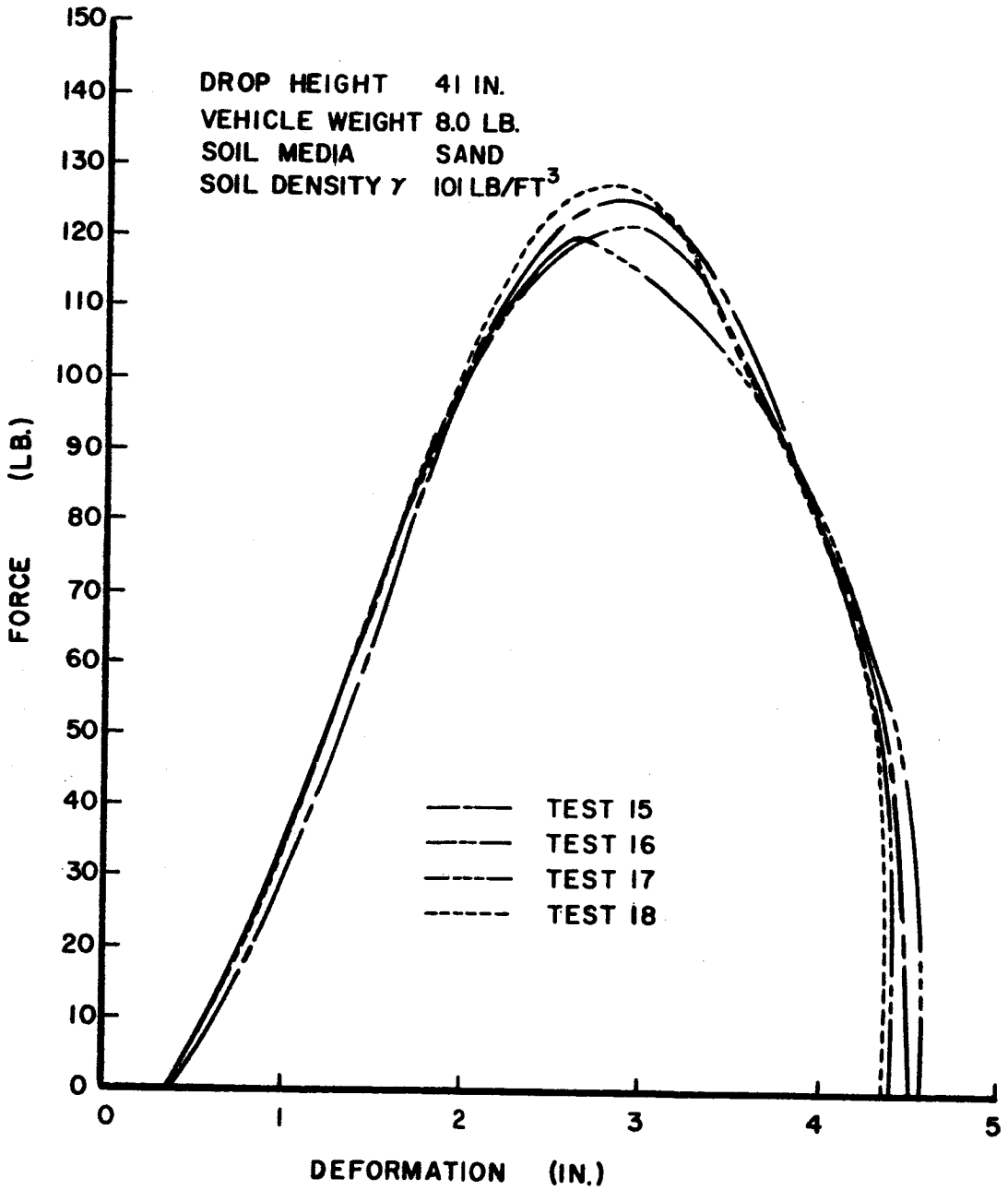

FIG. 24 FORCE-DEFORMATION CURVES
LABORATORY TEST SERIES - 7.08 IN. DIA. CONE

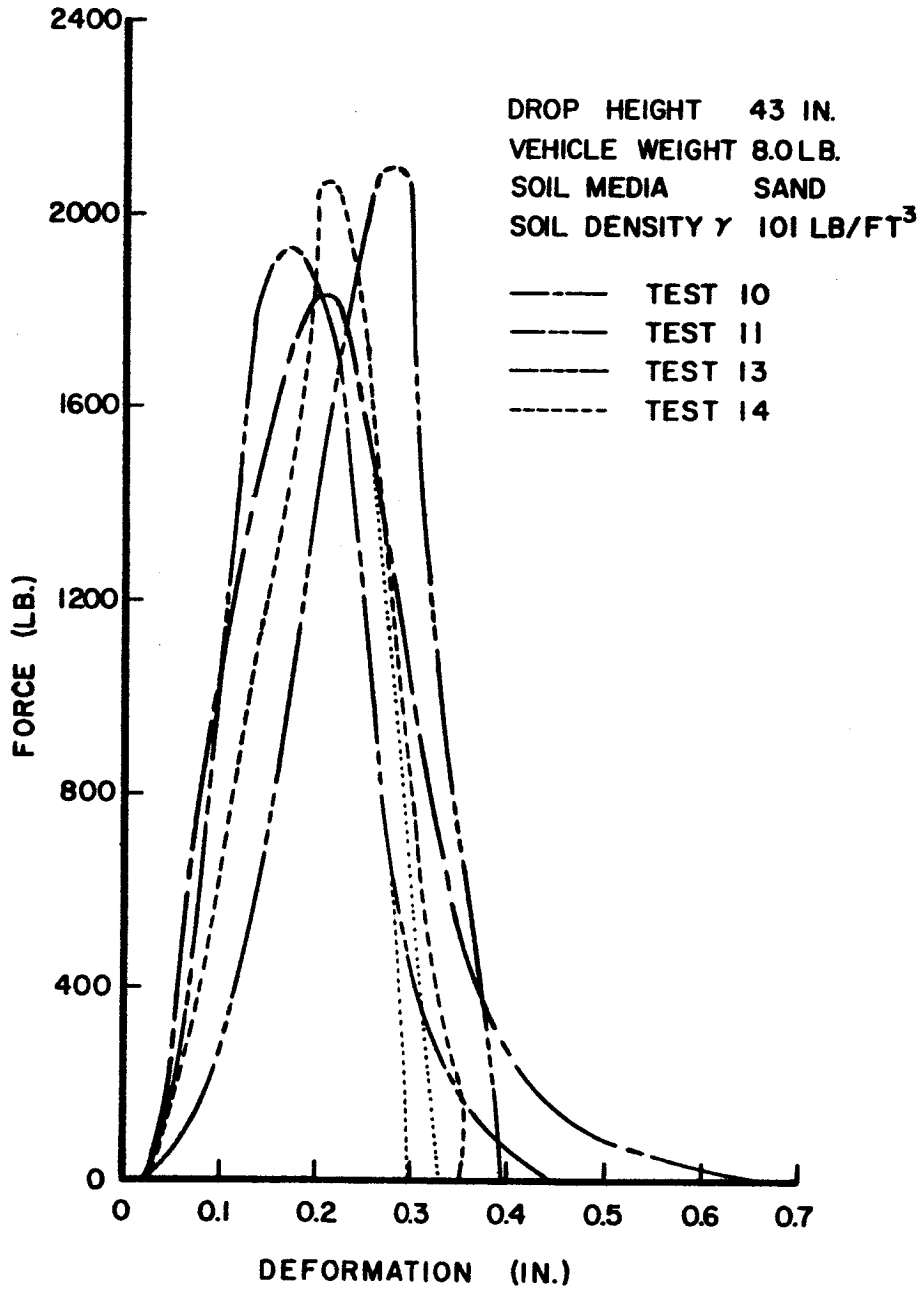

FIG. 25 FORCE-DEFORMATION CURVES
LABORATORY TEST SERIES-10.0 IN. DIA. PLATE

test vehicle as a function of deformation. It can be observed that the force-deformation curves have a characteristic shape. There is an initial deformation before significant force is evidenced, a relatively straight initial portion of the curve, a transition portion in which the deformation continues without appreciable change in force, and a maximum displacement as the vehicle arrives at a rest condition and the force goes to zero. It is interesting to note that the initial deformation before force buildup was 0.02 in. for the plates and 0.03 in. for the spheres. For the cone vehicles, however, this initial deformation approximated 0.37 in. The initial straight line portion of the curve is considered to be of major importance and is arbitrarily defined as the modulus of deformation, E_d. Values for this modulus are established by fitting a straight line to the initial portion of the curve. The intersection of the line establishing the modulus of deformation with a horizontal line through the point of maximum force will determine a corresponding deformation. Knowing the force and deformation, a tangent modulus can be readily computed.

Table 7 provides a summary of the information obtained from the laboratory test series.

6.5 Field Test Series Results

In analyzing the computer data output, it became apparent that in order to portray realistic and meaningful results minor adjustments in the output plots of certain tests would be required. It was reasonable to assume that all drop tests for a test vehicle of one particular configuration should have a common point of impact, or point of zero

TABLE 7

LABORATORY TEST SUMMARY

8.0 lb Test Vehicles

Vehicle Type	Maximum Deformation (in.)	Maximum Force (lb)	Impact Velocity (ft/sec)	Modulus of Deformation (lb/in.)
Sphere	1.4420	768.4	15.19	2272
Sphere	1.5480	575.0	15.19	2265
Sphere	1.5910	549.2	15.19	2287
Sphere	1.6400	565.4	15.19	2260
Cone	4.6040	1260.0	14.83	667
Cone	4.4160	1219.0	14.83	666
Cone	4.7550	1190.0	14.83	665
Cone	4.3780	1288.0	14.83	665
Plate	0.3277	1839.0	15.19	13930
Plate	0.3000	1934.0	15.19	13920
Plate	0.3977	2096.0	15.19	14070
Plate	0.3600	2066.0	15.19	14140

time. That is, for a particular geometry of test vehicle, if all adjustments are constant, the referenced point of impact on the oscilloscope should be a common point for the entire series of tests. This point was established by analyzing all test data pertaining to a particular vehicle sequence at one time. Consideration was given to the oscilloscope records of a particular series, and particularly to the value of the penetration pulse in relation to the computed maximum penetration. Also, all records were examined for the location of the referenced impact point in relation to the computed values.

In almost all instances, the discrepancy consisted of a deformation which was excessive. The reason for this discrepancy can be attributed to a number of factors. Adjustment of the test equipment was difficult to maintain in the field. Weather conditions caused the accelerometer trace and the penetration trace to drift after final adjustment. The speed of the pulse in relation to the width of the trace lines during adjustment contributed some margin of error. For the heavier vehicles, particularly the 64 and 128 lb plates, final adjustment to the zero time condition was extremely difficult. Any delay in initiating the test sequence resulted in a drift of the impact point due to the vehicles stretching the nylon hoist rope. Operator error must also be considered a contributing factor.

The adjustment in the plots was minor as the excessive deformation resulted during the integration of the velocity-time curve. The adjustment of the zero-time point to the correct position eliminated an area under the velocity-time curve which was actually non-existent. The adjustment in the plots in no way effected the acceleration-time record, but only

established a common point of impact.

Typical acceleration-time oscilloscope records are shown in Fig. 26.

Tables 8 through 13 list the results of all drop tests accomplished in the field.

Figure 27 shows a complete plot of the results from Test No. 30 utilizing the 16 lb sphere test vehicle. Space limitations preclude including plots for all tests performed. However, the force-deformation curves for all tests are shown in Figs. 28 through 33. The modulus of deformation, E_d , was computed from the characteristic initial straight-line portion of the curves for each geometric configuration of sphere and plate test vehicles. A summary of values for the field series of impact tests is given in Tables 14 through 19.

The geometric shape of the 60° cone did not change even though the mass and impact velocity varied throughout the testing program. In analyzing the test data, it was necessary to consider the results of all 16 tests at one time. The modulus of deformation was established as for the plates and spheres. However, the straight line through the initial part of the force-deformation curves was established by obtaining a curve fit by least squares techniques on the entire cone series.

A summary of values for the field series of impact tests is given in Tables 14 through 19.

Analysis of the test results indicated that the modulus of deformation for each geometric configuration of sphere and plate test vehicle was a constant value regardless of the change in mass and impact velocity for the test series. Thus, it was concluded that the modulus of deforma-

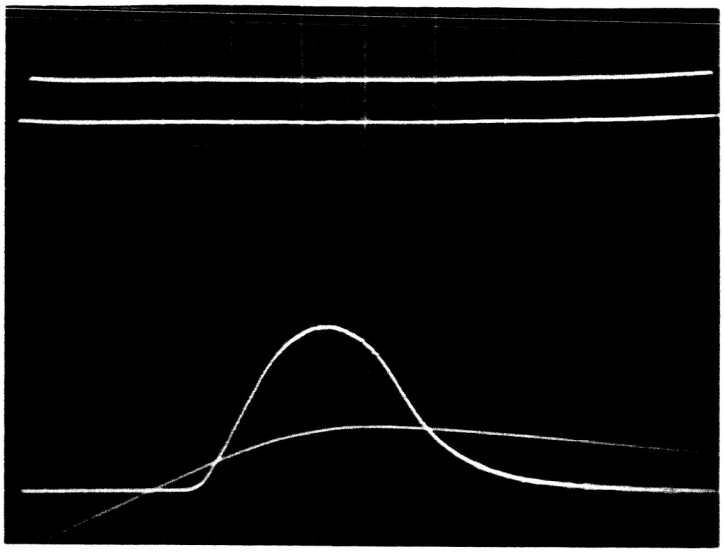

Field Test 30 - 16.0 lb Sphere
Drop Height 6.0 ft Sweep Rate 2 msec/cm
Sensitivity: 0.5 v/cm Penetration Pulse
5 mv/cm Acceleration Pulse

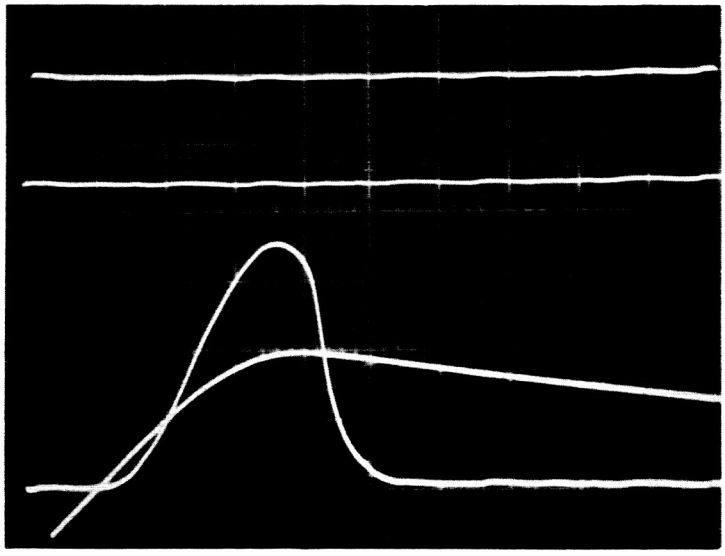

Field Test 23 - 16.0 lb Cone
Drop Height 9.0 ft Sweep Rate 5 msec/cm
Sensitivity: 0.5 v/cm Penetration Pulse
2 mv/cm Acceleration Pulse

Fig. 26 Typical Acceleration-Time Oscilloscope Records

TABLE 8

FIELD TEST SERIES

Sphere Test Vehicle - 8.66 in. Dia.

Test No.	Drop Height (ft)	Vehicle Weight (lb)	Impact Velocity (ft/sec)	Soil Moisture Content (%)	Maximum Acceler-ation (ft/sec^2)	Pulse Duration (ms)	Maximum Force (lb)	Maximum Stress (lb/ft^2)	Maximum Surface Area (ft^2)	Max. Disp. Comp. (in.)	Max. Disp. Meas. (in.)	Final Disp. Comp. (in.)
26	6.0	8.0	19.66	16.19	4,328	11.90	1,075	6,210	0.237	1.084	1.082	1.063
27	9.0	8.0	24.07	18.97	5,808	11.88	1,443	8,000	0.262	1.200	1.190	1.197
28	12.0	8.0	27.80	18.67	7,707	11.58	1,915	9,680	0.282	1.282	1.282	1.292
29	15.0	8.0	31.08	19.69	9,396	9.84	2,334	10,800	0.282	1.289	1.255	1.199
30	6.0	16.0	19.66	19.59	4,273	15.05	2,123	10,240	0.255	1.169	1.075	0.981
31	9.0	16.0	24.07	16.18	4,975	14.22	2,465	11,070	0.302	1.385	1.385	1.204
32	12.0	16.0	27.80	17.95	4,881	14.82	2,425	10,610	0.363	1.660	1.590	1.485
33	15.0	16.0	31.08	18.00	5,325	16.29	2,646	10,540	0.409	1.815	1.600	1.779

TABLE 9

FIELD TEST SERIES

Sphere Test Vehicle - 17.32 in. Dia.

Test No.	Drop Height (ft)	Vehicle Weight (lb)	Impact Velocity (ft/sec)	Soil Moisture Content (%)	Maximum Acceler-ation (ft/sec^2)	Pulse Duration (ms)	Maximum Force (lb)	Maximum Stress (lb/ft^2)	Maximum Surface Area (ft^2)	Max. Disp. Comp. (in.)	Max. Disp. Meas. (in.)	Final Disp. Comp. (in.)
10	6.0	64.0	19.66	17.33	2,468	29.95	4,905	11,200	0.668	1.53	1.50	1.084
11	9.0	64.0	24.07	21.00	3,133	21.80	6,226	15,120	0.782	1.79	1.75	1.648
12	12.0	64.0	27.80	17.23	2,876	27.83	5,716	12,820	1.063	2.43	1.67	2.390
13	15.0	64.0	31.08	15.72	3,429	38.29	6,815	13,180	1.114	2.55	2.235	1.905
14	6.0	128.0	19.66	18.17	1,663	23.72	6,611	15,850	0.914	2.047	1.90	1.875
15	9.0	128.0	24.07	18.40	2,295	37.04	9,122	16,290	1.020	2.335	2.30	1.608
16	12.0	128.0	27.80	19.22	2,389	27.75	9,495	15,770	1.256	2.88	2.40	2.853
17	15.0	128.0	31.08	19.10	2,916	30.82	11,580	18,060	1.291	2.96	2.37	2.515

TABLE 10

FIELD TEST SERIES

CONE TEST VEHICLE - 7.08 in. Dia.

Test No.	Drop Height (ft)	Vehicle Weight (lb)	Impact Velocity (ft/sec)	Soil Moisture Content (%)	Maximum Acceler-ation (ft/sec^2)	Pulse Duration (ms)	Maximum Force (lb)	Maximum Stress (lb/ft^2)	Maximum Surface Area (ft^2)	Max. Disp. Comp. (in.)	Max. Disp. Meas. (in.)	Final Disp. Comp. (in.)
18	6.0	8.0	19.66	19.60	3,243	31.71	805	13,612	0.068	2.159	2.14	1.859
19	9.0	8.0	24.07	18.56	2,875	17.82	714	16,412	0.101	2.606	2.25	2.575
20	12.0	8.0	27.80	17.88	4,572	21.20	1,136	12,642	0.114	2.799	2.73	2.646
21	15.0	8.0	21.08	18.50	4,371	17.90	1,086	6,276	0.145	3.119	3.11	3.077
22	6.0	16.0	19.66	16.46	1,995	21.40	992	17,706	0.120	2.835	2.71	2.805
23	9.0	16.0	24.07	17.48	2,442	27.72	1,213	11,944	0.156	3.292	3.08	5.257
24	12.0	16.0	27.80	18.46	2,634	25.23	1,309	10,114	0.215	3.752	3.74	3.685
25	15.0	16.0	31.08	16.96	4,186	19.77	2,080	13,840	0.201	3.725	3.72	3,670

TABLE 11

FIELD TEST SERIES

CONE TEST VEHICLE - 14.16 in. Dia.

Test No.	Drop Height (ft)	Vehicle Weight (lb)	Impact Velocity (ft/sec)	Soil Moisture Content (%)	Maximum Acceler-ation (ft/sec^2)	Pulse Duration (ms)	Maximum Force (lb)	Maximum Stress (lb/ft^2)	Maximum Surface Area (ft^2)	Max. Disp. Comp. (in.)	Max. Disp. Meas. (in.)	Final Disp. Comp. (in.)
1	6.0	64.0	19.66	15.65	1,388	79.70	2,758	7,496	0.35	4.78	4.61	4.57
2	9.0	64.0	24.07	15.17	1,524	80.95	3,030	7,894	0.44	5.40	5.38	4.94
3	12.0	64.0	27.80	14.05	1,813	83.43	3,603	7,538	0.44	6.05	6.00	5.15
4	14.75	64.0	30.82	14.75	1,976	94.00	3,927	4,322	0.57	6.61	6.51	6.31
6	6.0	128.0	19.66	14.08	893	47.29	3,551	10,588	0.54	6.08	5.95	6.02
7	9.0	128.0	24.07	7.28	1,217	92.27	4,839	11,012	0.69	6.90	6.62	5.84
8	12.0	128.0	27.80	14.28	1,531	98.03	6,086	7,204	0.81	7.34	-	7.00
9	14.75	128.0	30.82	18.20	1,612	94.55	6,410	11,382	0.98	8.11	8.09	7.54

TABLE 12

FIELD TEST SERIES

Plate Test Vehicle - 10.0 in. Dia.

Test No.	Drop Height (ft)	Vehicle Weight (lb)	Impact Velocity (ft/sec)	Soil Moisture Content (%)	Maximum Acceler-ation (ft/sec^2)	Pulse Duration (ms)	Maximum Force (lb)	Maximum Stress (lb/ft^2)	Maximum Surface Area (ft^2)	Max. Disp. Comp. (in.)	Max. Disp. Meas. (in.)	Final Disp. Comp. (in.)
37	6.0	8.0	19.66	16.08	11,050*	9.110	2,747	5,040	0.546	0.4245	0.440	0.4245
38	9.0	8.0	24.07	16.70	9,986*	9.499	2,481	4,550	0.546	0.4611	0.472	0.4611
39	12.0	8.0	27.80	16.68	11,020*	7.191	2,738	5,020	0.546	0.5100	0.545	0.5100
40	15.0	8.0	31.08	15.80	14,080	6.059	3,498	5,130	0.546	0.5625	0.555	0.5625
41	6.0	16.0	19.66	15.37	8,859	16.880	4,402	8,070	0.546	0.4500	0.482	0.3632
42	9.0	16.0	24.07	17.24	11,510	18.170	5,720	10,490	0.546	0.5260	0.648	0.4750
43	12.0	16.0	27.80	13.19	11,320	18.370	5,623	10,300	0.546	0.7384	0.741	0.7384
44	15.0	16.0	31.08	17.45	11,000	11.930	5,465	10,000	0.546	0.8800	0.666	0.8800

*Acceleration exceeded linearity range of accelerometer.

TABLE 13

FIELD TEST SERIES

Plate Test Vehicle - 20.0 in. Dia.

Test No.	Drop Height (ft)	Vehicle Weight (lb)	Impact Velocity (ft/sec)	Soil Moisture Content (%)	Maximum Acceler-ation (ft/sec^2)	Pulse Duration (ms)	Maximum Force (lb)	Maximum Stress (lb/ft^2)	Maximum Surface Area (ft^2)	Max. Disp. Comp. (in.)	Max. Disp. Meas. (in.)	Final Disp. Comp. (in.)
48	6.0	64.0	19.66	21.28	6,786	42.63	13,490	6,180	2.185	0.845	0.411	0.808
49	9.0	64.0	24.07	16.05	8,058	41.91	16,020	7,350	2.185	1.054	-	0.989
50	12.0	64.0	27.80	18.10	11,570	19.29	23,000	10,520	2.185	1.092	0.847	1.092
51	15.0	64.0	31.08	16.96	7,329	12.73	14,570	6,670	2.185	1.810	1.200	1.810
52	6.0	128.0	19.66	13.66	6,476	14.45	25,740	11,800	2.185	0.807	0.751	0.775
53	9.0	128.0	24.07	18.50	6,969	18.78	27,700	12,690	2.185	1.190	1.020	1.170
54	12.0	128.0	27.80	15.13	8,676	18.83	27,250	12,480	2.185	1.517	1.640	1.338
55	15.0	128.0	31.08	16.87	8.172	17.03	32,490	14,870	2.185	1.504	1.360	1.407

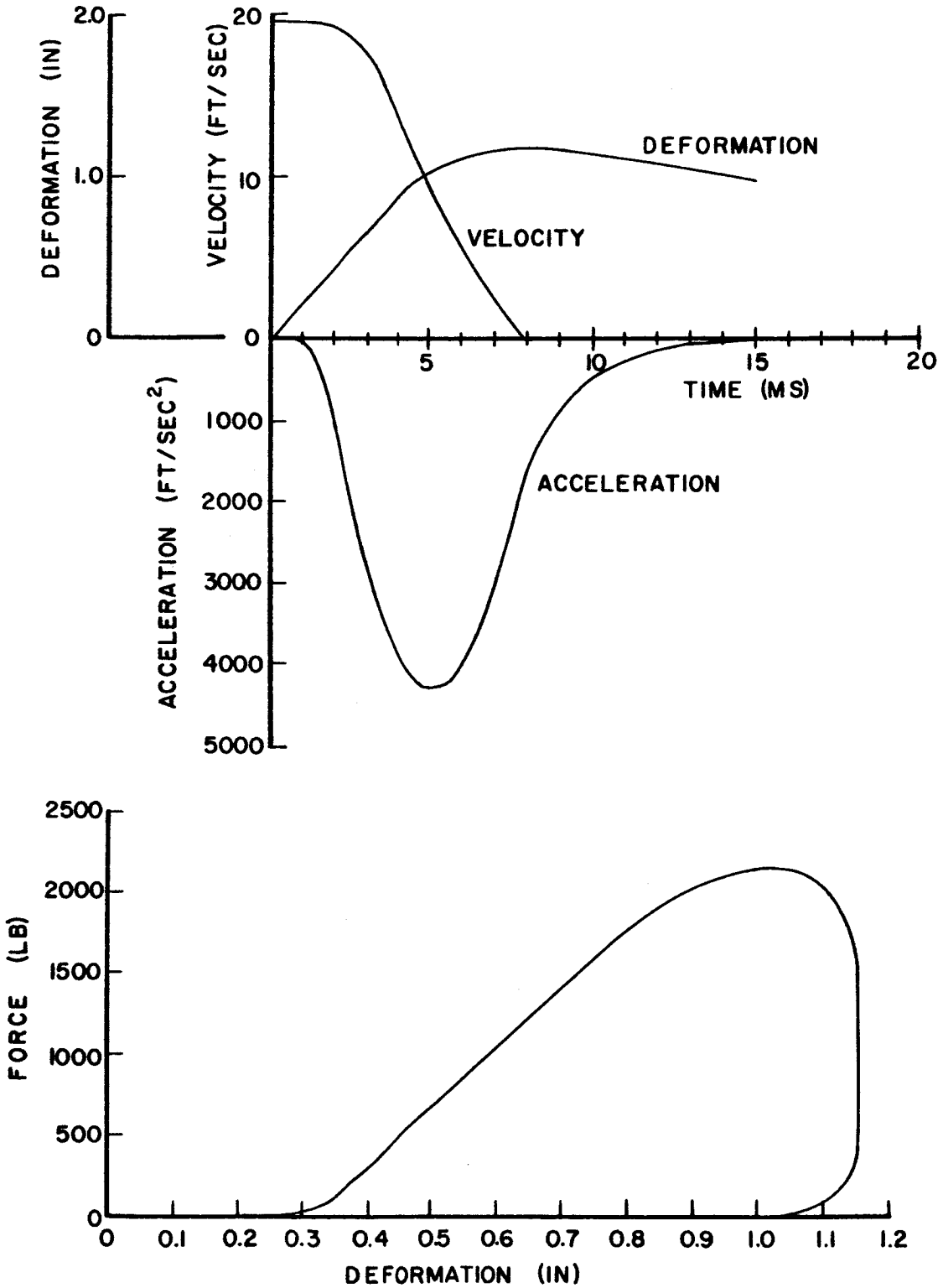

FIG. 27 RESULTS FROM TEST 30 - 16 LB. SPHERE

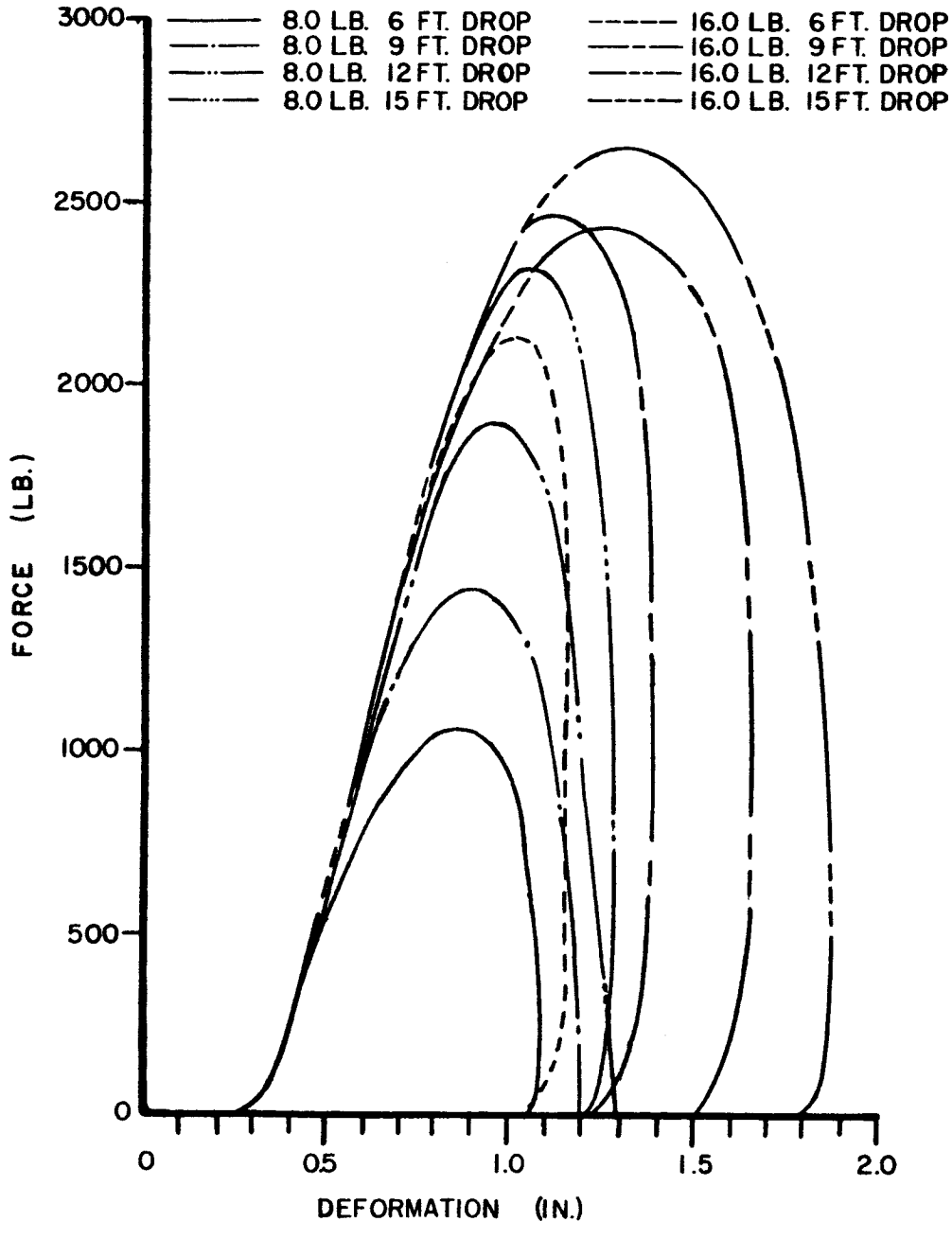

FIG. 28 FORCE-DEFORMATION CURVES
FIELD TEST SERIES – 8.66 IN. DIA. SPHERE

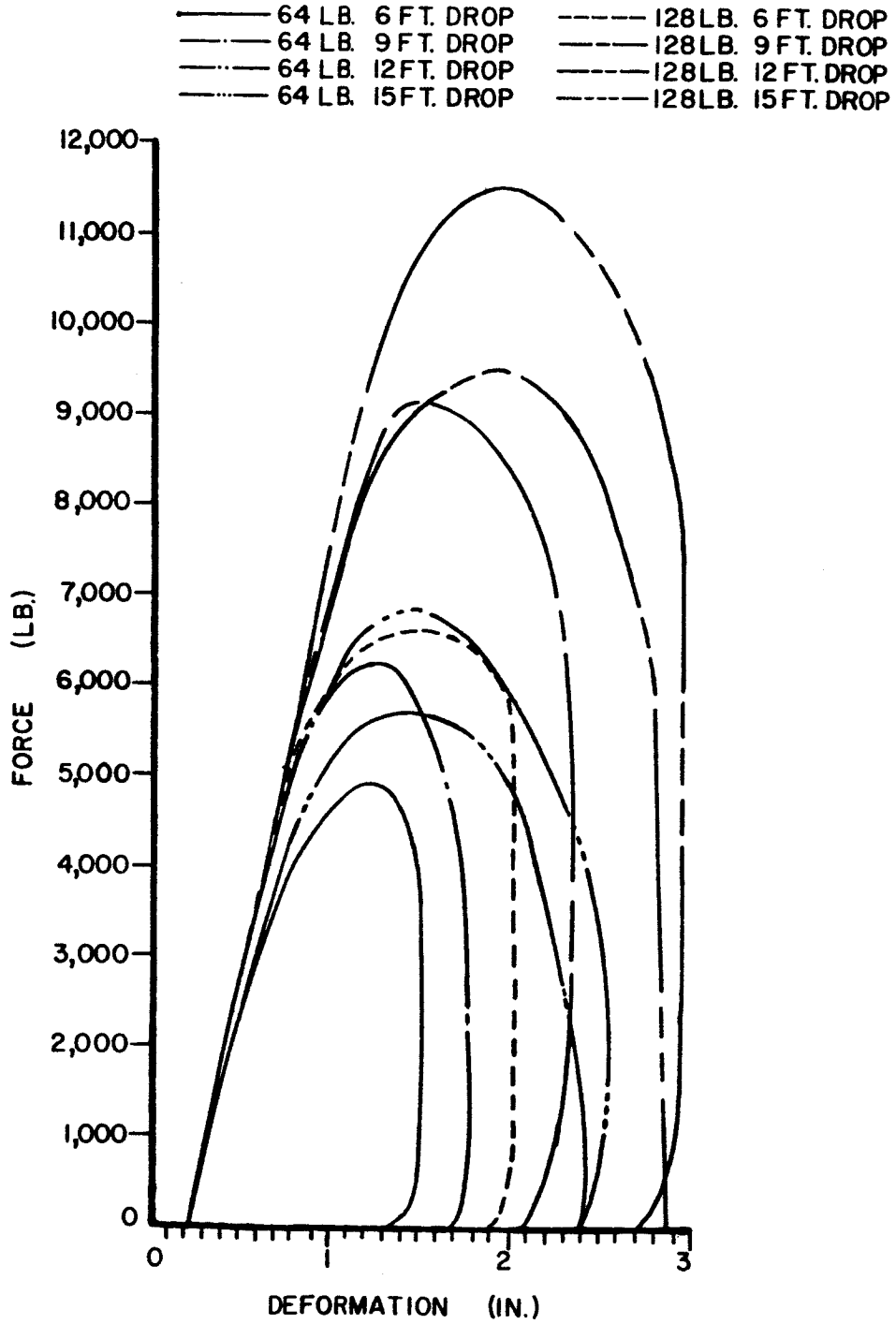

FIG. 29 FORCE-DEFORMATION CURVES
FIELD TEST SERIES - 17.32 IN. DIA. SPHERE

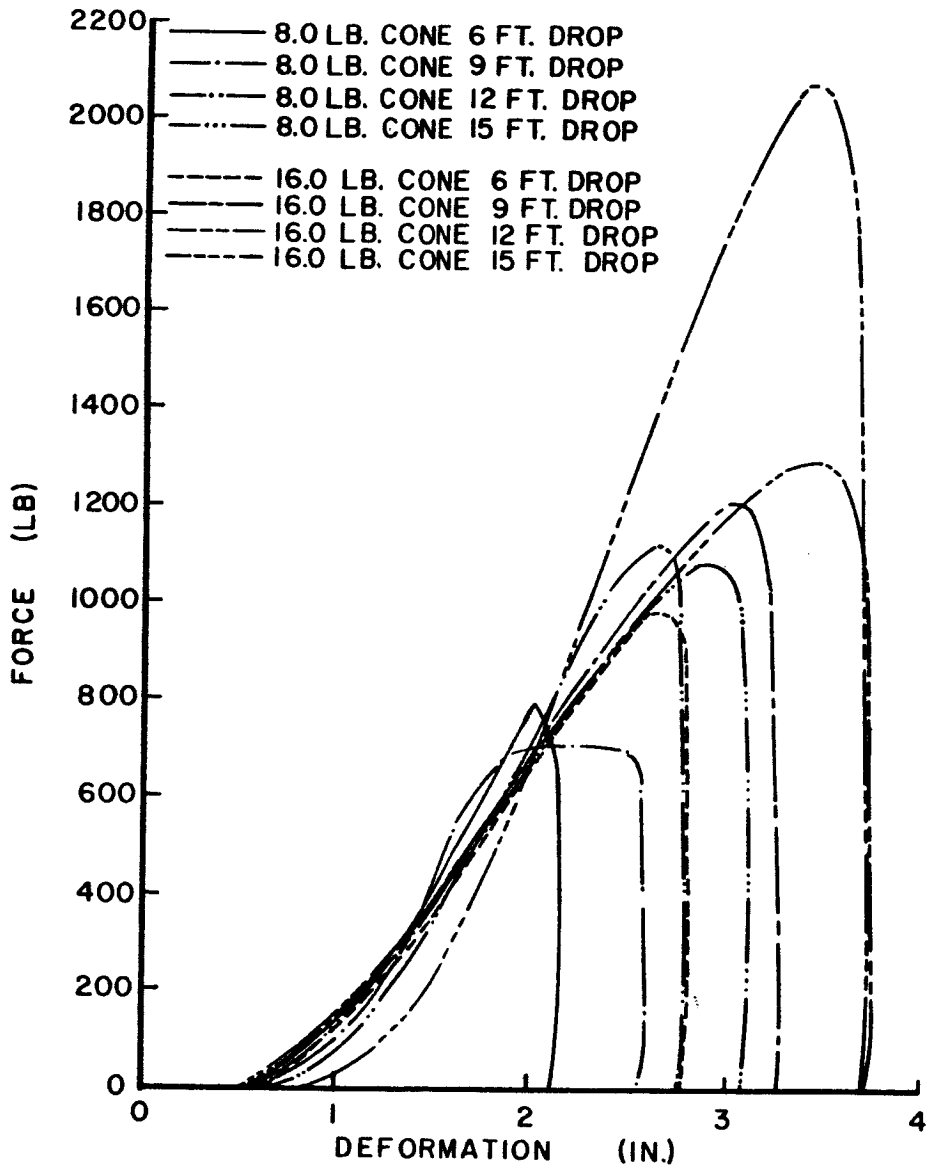

FIG. 30 FORCE–DEFORMATION CURVES
FIELD TEST SERIES – 7.08 IN. DIA. CONE

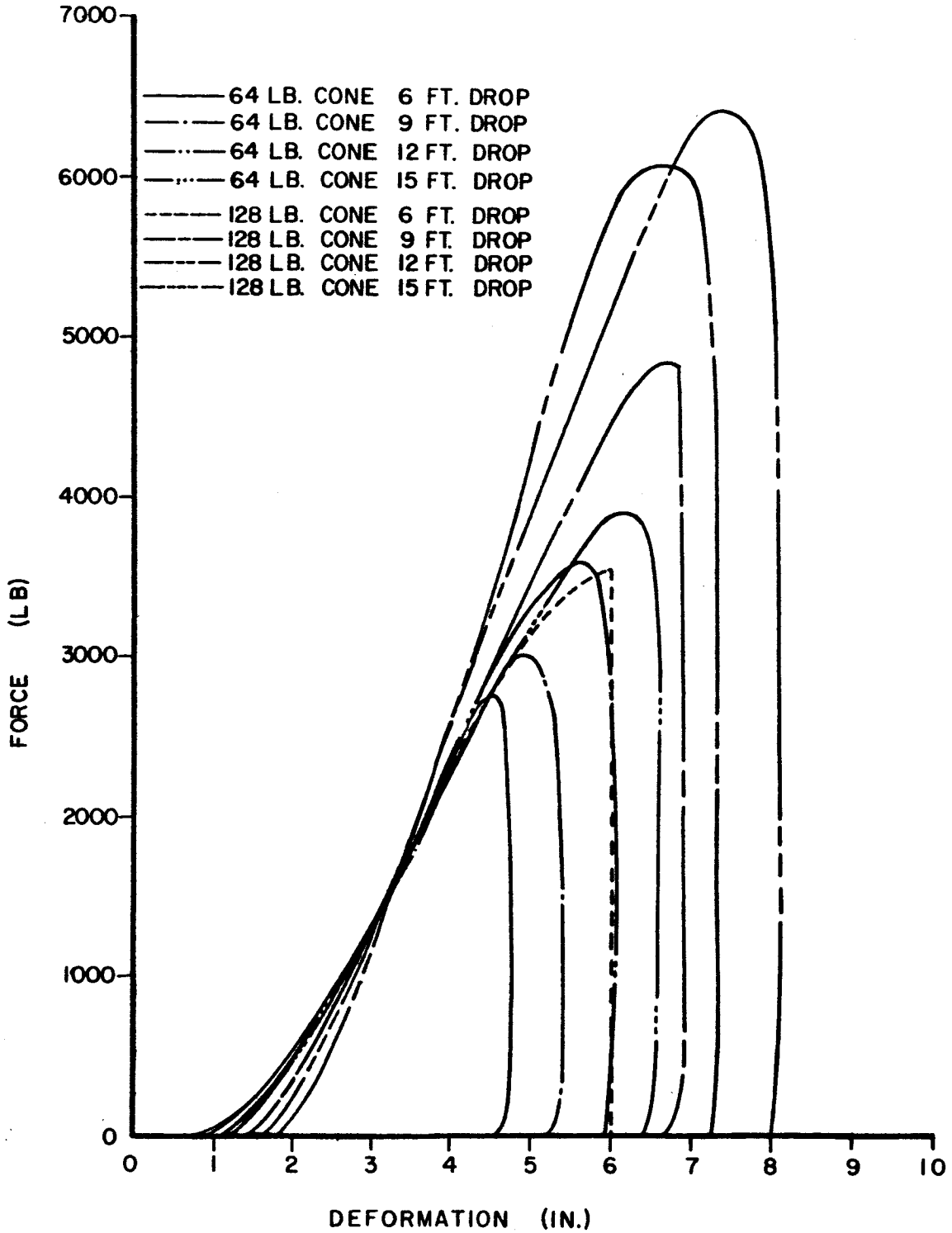

FIG. 31 FORCE-DEFORMATION CURVES
FIELD TEST SERIES - 14.16 IN. DIA. CONE

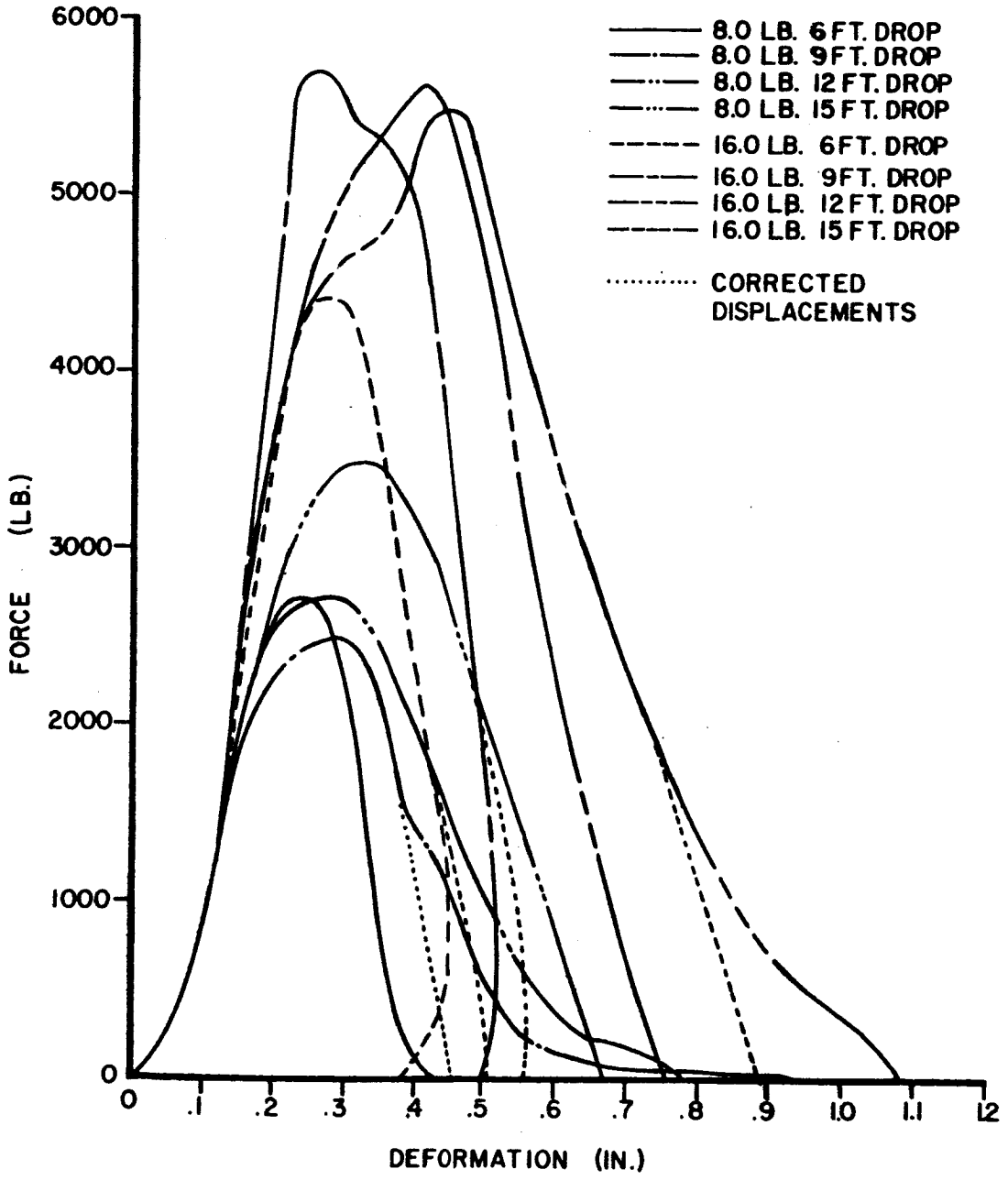

FIG. 32 FORCE–DEFORMATION CURVES
FIELD TEST SERIES – 10.0 IN. DIA. PLATE

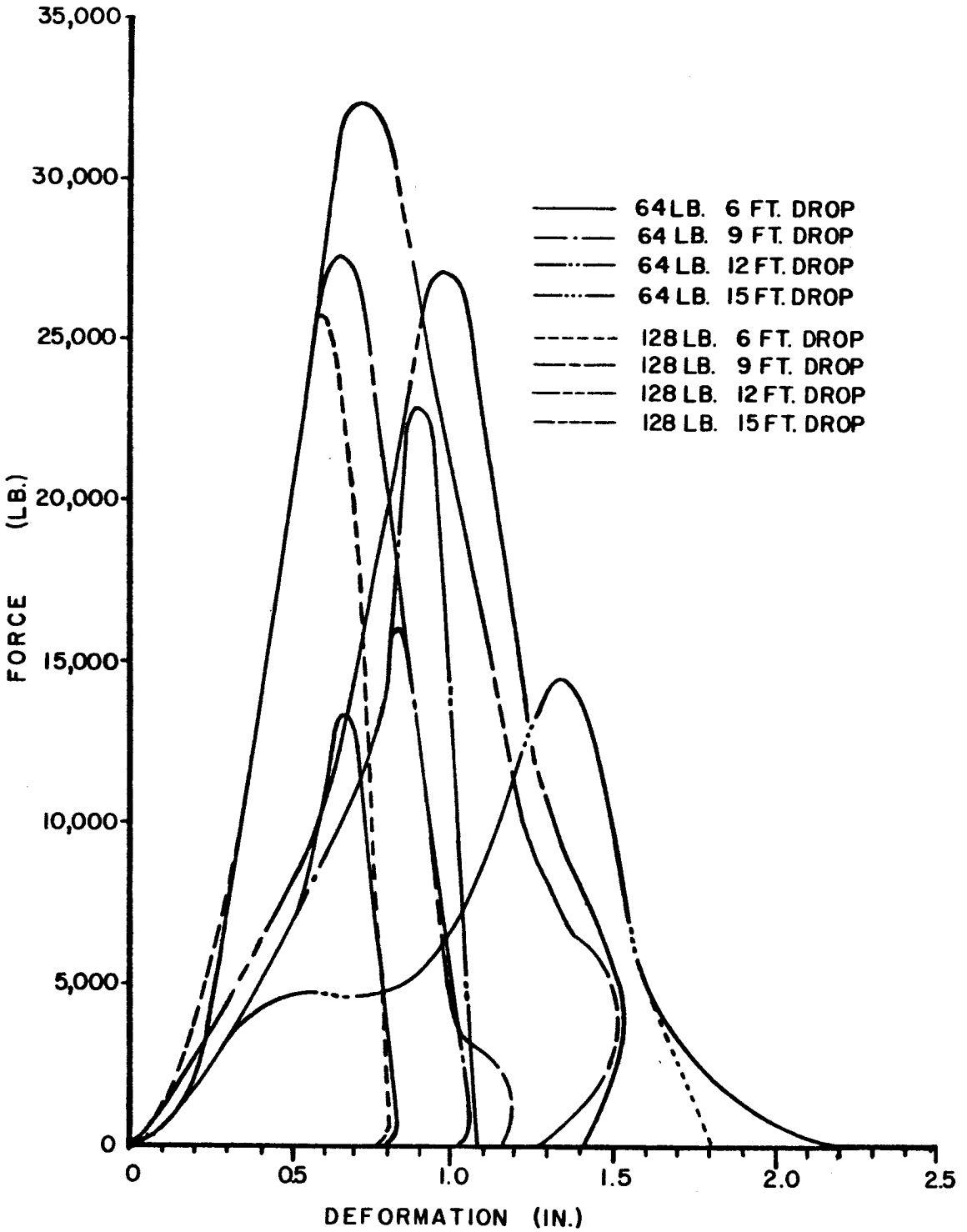

FIG. 33 FORCE—DEFORMATION CURVES
FIELD TEST SERIES – 20.0 IN. DIA. PLATES

TABLE 14

Impact Test Summary - 8.66 in. Dia. Sphere

10.0 in. Spherical Diameter

Vehicle Weight (lb)	Vehicle Mass (Slugs)	Maximum Deformation (in.)	Maximum Force (lb)	Impact Velocity (ft/sec)	Deformation Modulus (lb/in.)
8.0	0.248	1.084	1075	19.66	3708
8.0	0.248	1.200	1443	24.07	3700
8.0	0.248	1.292	1915	27.80	3818
8.0	0.248	1.289	2334	31.08	3825
16.0	0.497	1.169	2123	19.66	3865
16.0	0.497	1.385	2465	24.07	3855
16.0	0.497	1.660	2425	27.80	3820
16.0	0.497	1.875	2646	31.08	3835

TABLE 15

Impact Test Summary - 17.32 in. Dia. Sphere

20.0 in. Spherical Diameter

Vehicle Weight (lb)	Vehicle Mass (Slugs)	Maximum Deformation (in.)	Maximum Force (lb)	Impact Velocity (ft/sec)	Deformation Modulus (lb/in.)
64.0	1.988	1.530	4905	19.66	9440
64.0	1.988	1.790	6226	24.07	9300
64.0	1.988	2.430	5716	27.80	9230
64.0	1.988	2.550	6815	31.08	9470
128.0	3.975	2.047	6611	19.66	9450
128.0	3.975	2.335	9122	24.07	9310
128.0	3.975	2.880	9495	27.80	9400
128.0	3.975	2.960	11,590	31.08	9270

TABLE 16

Impact Test Summary - 7.08 in. Dia. Cone

Vehicle Weight (lb)	Vehicle Mass (Slugs)	Maximum Deformation (in.)	Maximum Force (lb)	Impact Velocity (ft/sec)	Deformation Modulus (lb/in.)
8.0	0.248	2.159	805	19.66	1051
8.0	0.248	2.606	714	24.07	1049
8.0	0.248	2.799	1136	27.80	1051
8.0	0.248	3.119	1086	31.08	1043
16.0	0.497	2.835	991	19.66	1053
16.0	0.497	3.292	1213	24.07	1054
16.0	0.497	3.752	1309	27.80	1054
16.0	0.497	3.725	2080	31.08	1050

TABLE 17

Impact Test Summary - 14.16 in. Dia. Cone

Vehicle Weight (lb)	Vehicle Mass (Slugs)	Maximum Deformation (in.)	Maximum Force (lb)	Impact Velocity (ft/sec)	Deformation Modulus (lb/in.)
64.0	1.988	4.78	2758	19.66	1044
64.0	1.988	5.40	3030	24.07	1048
64.0	1.988	6.05	3603	27.80	1047
64.0	1.988	6.61	3927	30.82	1050
128.0	3.975	6.08	3551	19.66	1047
128.0	3.975	6.90	4839	24.07	1044
128.0	3.975	7.34	6086	27.80	1053
128.0	3.975	8.11	6410	30.82	1048

TABLE 18

Impact Test Summary - 10.00 in. Dia. Plate

Vehicle Weight (lb)	Vehicle Mass (Slugs)	Maximum Deformation (in.)	Maximum Force (lb)	Impact Velocity (ft/sec)	Deformation Modulus (lb/in.)
8.0	0.248	0.4245	2747	19.66	28,950
8.0	0.248	0.4611	2481	24.07	29,200
8.0	0.248	0.5160	2738	27.80	29,150
8.0	0.248	0.5625	3498	31.08	29,900
16.0	0.497	0.4500	4402	19.66	30,350
16.0	0.497	0.5260	5720	24.07	30,100
16.0	0.497	0.7384	5623	27.80	30,000
16.0	0.497	0.8800	5465	31.08	29,900

TABLE 19

Impact Test Summary - 20.00 in. Dia. Plate

Vehicle Weight (lb)	Vehicle Mass (Slugs	Maximum Deformation (in.)	Maximum Force (lb)	Impact Velocity (ft/sec)	Deformation Modulus (lb/in.)
64.0	1.988	0.8454	13,490	19.66	71,000
64.0	1.988	1.0540	16,020	24.07	71,100
64.0	1.988	1.0920	23,000	27.80	71,000
64.0	1.988	1.8100	14,570	31.08	71,700
128.0	3.975	0.8072	25,740	19.66	70,600
128.0	3.975	1.1900	27,700	24.07	70,200
128.0	3.975	1.5170	27,250	27.80	70,900
128.0	3.975	1.5040	32,490	31.08	70,700

tion could be determined by establishing a relationship with the test vehicle geometry.

By plotting the known value of the modulus of deformation for each sphere configuration against the spherical radius of the contact surface, three established points are obtained which lie on a curve whose equation can be determined. A parabolic curve fit was accomplished utilizing least squares techniques to fit a second order polynomial through the known data points. This permitted the derivation of the equation for the modulus of deformation for sphere test vehicles as a function of the spherical radius. This equation is

$$E_{d_s} = 585.2\ R + 35.08\ R^2 = \text{lb/in.} \qquad (7)$$

where R is the spherical radius in in.

The same basic procedure was followed in deriving the modulus of deformation equation for test vehicles with a plate configuration. However, in this derivation, the modulus of deformation was determined as a function of the test vehicle radius. This equation is

$$E_{d_p} = 4{,}787.6\ r + 230.24\ r^2 = \text{lb/in.} \qquad (8)$$

where r is the vehicle radius in in.

Figure 34 shows the curves established for the modulus of deformation as a function of the spherical and vehicle radii.

The modulus of deformation for the cone test vehicles was determined to be a constant, but only considered appropriate for a cone with a 60° vertex angle. This constant is

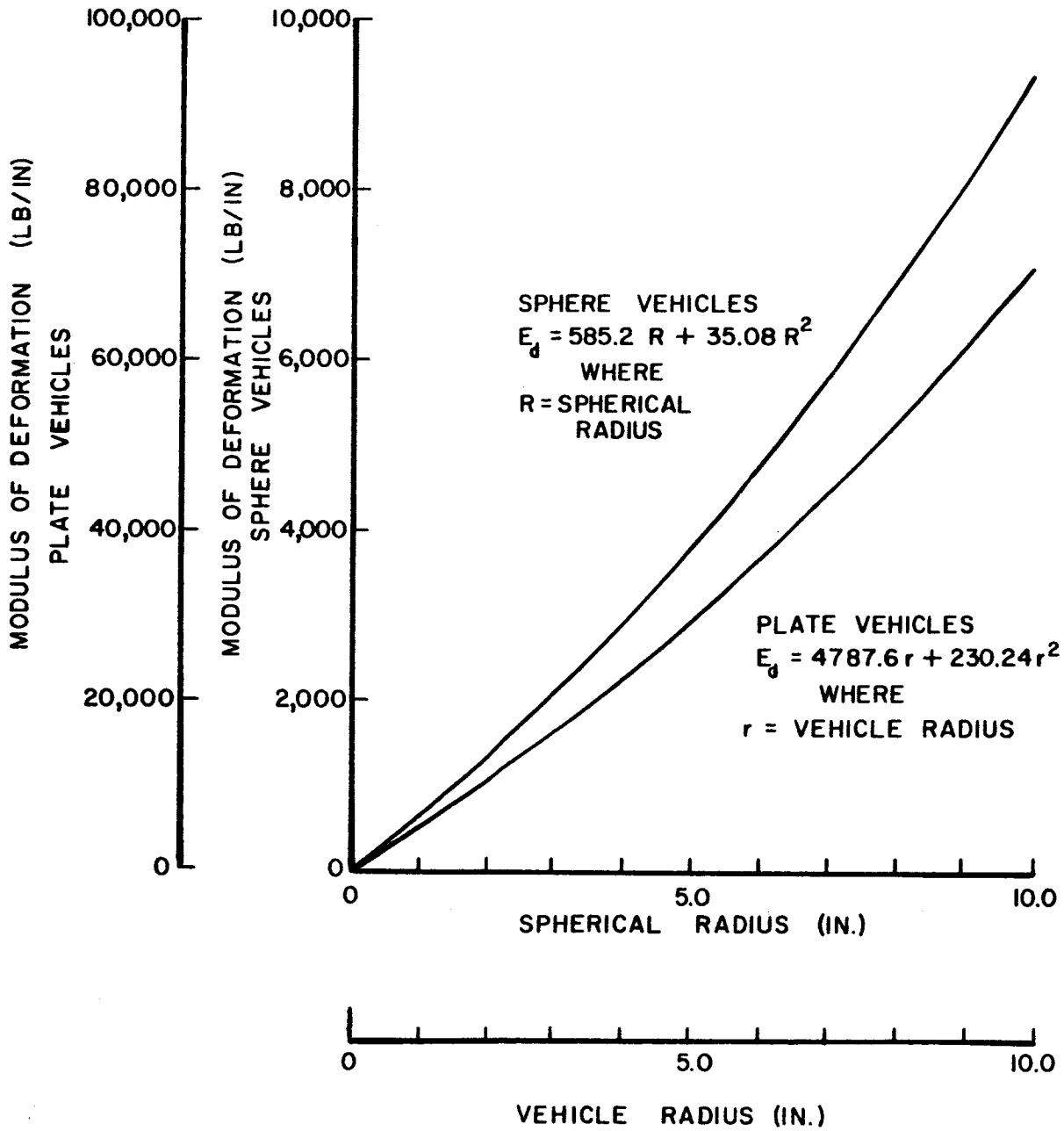

FIG. 34 MODULUS OF DEFORMATION VS. SPHERICAL & VEHICLE RADII

$$E_{dc} = 1{,}049 \text{ lb/in.} \quad (9)$$

In establishing the modulus of deformation as the slope of a straight line through the initial portion of the force-deformation curves, the intercept on the deformation axis gives an initial deformation at zero force. This condition is an approximation which allows part of the force-deformation curve to be defined by two straight lines. The true condition also indicated a certain amount of deformation before the force buildup became significant.

For the 8.0 and 16.0 lb spheres, the deformation intercept was approximately 0.33 in. For the 64.0 and 128.0 lb spheres, this deformation was approximately 0.22 in. This is expected as the true curve is moving closer to the curve axis origin as the contact surface becomes flatter with an increase in the spherical radius.

For the small series of plate vehicles, the initial deformation intercept approximated 0.075 in. For the larger series of plates, the deformation intercept approximated 0.2 in. The actual curves were passing approximately through the axis origin, and the slope of the modulus of deformation rapidly increasing towards a vertical position. This is considered appropriate as the entire surface contact area of the vehicle is impacting the soil at one time.

For the entire cone series of tests, the initial deformation intercept approximated 1.0 in.

From the results of the test program, part of the force-deformation curve can be represented by two straight lines. In Art. 7.5 B, the test results are utilized as a basis for extrapolating to larger size test ve-

hicles. The force-deformation curve is further defined by an expression to determine the upper limit of force for the particular vehicle geometry.

CHAPTER SEVEN

DISCUSSION OF RESULTS

7.1 General

The primary objective of this investigation was to determine the soil response on three geometric shapes during impact loading. As a result of the experimental program, a modulus of deformation was determined for each geometric configuration. This modulus is a function of the impact force and the resulting deformation of the soil system.

Due to the complexities of the entire problem, certain assumptions were made to reduce the unknown parameters. The geometric shapes were considered rigid bodies. The investigation considered only a vertical component of motion with the vehicles striking the soil surface in a normal attitude. The interaction time period was limited from the instant of impact to an at-rest condition, and did not consider the magnitude of plastic deformation and elastic response. The test area was considered as a uniform, homogeneous, and isotropic soil mass to a depth of 15 feet.

Even with the imposed limitations, the interaction relationship between a soil mass and an impacting body comprises unknowns which are indeterminate. From analysis of the test results of this investigation, it was apparent that an extremely complex, intermingled, relationship existed between the modulus of deformation, vehicle mass, impact velocity, vehicle geometry, reactive force exerted by the soil mass, inertial forces, plastic deformation, elastic rebound, and the soil mass properties.

This research program consisted of three major phases, all interrelated and interdependent. The first phase comprised the development of the test vehicles, equipment, instrumentation, and procedures which would allow measurement of the soil response to an impacting vehicle. The second phase consisted of the test area preparation, soil investigation, and the complete testing program. The third phase required determination of the data reduction procedures and analysis of results.

7.2 Equipment and Test Procedure

The equipment and procedures developed during this research investigation performed very well. The testing procedure, though detailed, did provide a sequence to obtain useable data with a minimum amount of operator error. The equipment utilized was reliable, even though problem areas arose in the field which were not apparent in the laboratory. It is worthy of note that the procedure developed provided all appropriate test data on one photographic record of the oscilloscope. This convenience permitted rapid and complete data analysis.

It is believed that the test instrumentation could be refined and become more sophisticated in any follow-on research program. The penetration pulse utilized in this program proved to be an invaluable aid in analyzing the photographic records. However, its actual value was minimal in this investigation compared to its potential capabilities with instrumentation refinements. The oscilloscope utilized had only a single external trigger for both traces. This limited the sweep rate of the penetration pulse to that of the acceleration pulse. By obtaining the capability of triggering each trace individually and at different sweep

rates, it would be possible to utilize the penetration pulse to determine not only the maximum deformation, but also the orders of magnitude of the plastic displacement and elastic rebound.

The number of individual cables required for the instrumentation in this program contributed to operational difficulties during field testing. Considering that only a vertical component of motion was applicable in this investigation, the difficulties will be considerably magnified in follow-on research where the problem is expanded to the two-dimensional or three-dimensional case. Shielded cables were used throughout in this program and kept to a minimum length to minimize pickup of extraneous interference being transmitted to the oscilloscope. Limited cable length necessitated the oscilloscope and control consoles being moved over the terrain with the drop tower for each test position, requiring the oscilloscope to be readjusted and balanced at each test position. It is considered desirable in future work to utilize miniaturized transmitters for each sensor which could broadcast response information directly to the oscilloscopes. This would eliminate the cable interference and permit the oscilloscope to be maintained in a relatively fixed location and in a protected environment.

It is desirable that a more precise procedure be developed to establish the point of contact between the test vehicles and the ground surface. This is particularly true for vehicles with a plate configuration, and becomes more essential for greater sizes of sphere vehicles. Considering the pulse duration of approximately 7 to 9 milliseconds for a plate vehicle, and the resulting small soil deformation, any minimum discrepancy

in adjusting the zero time position on the oscilloscope would be reflected by an error of considerable magnitude after the data reduction process. Possibly, a miniaturized pressure-sensing device could be utilized to fix more precisely the point of contact between the soil surface and the test vehicle.

7.3 Laboratory Test Series

Approximately 100 non-record drop tests were performed in the laboratory in order to formulate and finalize the required instrumentation and testing sequence. This phase of the investigation was necessary to determine the capability of the entire system to provide repeatable results. As is shown on the force-deformation curves for the cones, plates, and spheres tested for record in the laboratory (Reference Figs. 23 and 25) all four tests for each vehicle configuration are remarkably close. It should be noted that on tests 10, 13, and 14 for the plate, the maximum acceleration developed exceeded the linearity range of the 250 g accelerometer. It should also be noted that each test vehicle geometry results in a characteristic force-deformation curve.

For the sphere, a phenomenon occurs near the end of the acceleration-time record (Reference Fig. 22) and which is also evidenced in the force-deformation curves (Reference Fig. 23). This phenomenon is a characteristic small secondary acceleration pulse. It does not occur for any of the other vehicle geometrics and only for the sphere when impacted into a sand medium. At the present time there is no satisfactory explanation for this phenomenon.

The results from the laboratory test series indicate that the test equipment and procedures were capable of providing soil response records with accuracy. The results are remarkable when it is considered that the sand foundation medium was reworked and vibrated to the desired density following each record drop test.

7.4 Field Test Series

The results obtained from the field test series has provided an insight into the complexities of the interaction between a soil system and an impacting mass. The reliability of the test results are considered to be very good for the imposed assumptions and limiting parameters.

The drop test area was assumed to be comprised of a soil which was completely uniform, homogeneous, and isotropic. Even though the soil within the depth of primary significance was the same general classification, it is well known that the index properties, shear strength, angle of internal friction, and cohesion can vary widely within the same general classification. Any or a combination of these properties will vary the reactive force of the soil against the impacting mass. It is significant to note that the average surface moisture content for the entire test area was 17.3%. The range of variance of the surface moisture content for vehicles of a particular configuration was ± 3%. This variation of the surface moisture content did not indicate any pattern of influence on the acceleration-time records. It is believed that the range of moisture contents below the soil surface would be more nearly uniform, as some loss of surface moisture was unavoidable even though the area was protected with plastic covering. Any gross deviation of the force-deformation behavior

occurring within a series of a particular test vehicle configuration is believed to be due to an unconformity in the underlying medium. This could be caused by a rock or a pocket of dense material influencing the acceleration pulse.

A complete explanation of the interaction processes occurring between a soil mass and an impacting body is indeterminate at the present limit of knowledge. Any theoretical relationship between soil properties and soil response to dynamic loading must await development of controlled laboratory procedures for dynamic testing. Terzaghi[6] has indicated in pile driving studies that the dynamic resistance of the earth to rapid penetration has no correlation to the load for static penetration. Procedures are available for analyzing a moving body which strikes a structure and delivers a dynamic force[4]. However, the idealizing assumptions limits their validity when applied to a soil system. These assumptions are:

a. Materials behave elastically, and no dissipation of energy takes place at the point of impact owing to local inelastic deformation.

b. The inertia of a system resisting an impact may be neglected.

c. The deformation of a system is directly proportional to the magnitude of the applied force regardless of whether dynamically or statically applied.

d. At the instant a moving body is stopped, its kinetic energy is completely transformed into internal strain energy. At this instant, the maximum deformation of the resisting system occurs and vibrations commence.

It is evident that the assumptions presented are not appropriate for a soil system which must be considered an elasto-plastic material. By analyzing the force-deformation curves and test data for each test vehicle, it was evident that dissipation of energy occurs, and cohesive, frictional, and inertial forces are in being. Deformations within the soil system are primarily plastic; however, some elastic deformations and rebound are evidenced.

The force-deformation curves obtained from the field test series indicate a characteristic shape for each vehicle configuration. The results obtained are considered to portray the phenomenological processes occurring as the soil system is responding to the impacting force. Some deviation is evidenced in the plate series. Tests for the 8.0 lb plate at drop heights of 6, 9, and 12 ft (Reference Fig. 32) exceeded the linearity range of the 250 g accelerometer. However, the curves maintain the same characteristic shape as the other tests in this series. Certain abnormalities were evidenced in the 64.0 lb plate series (Reference Fig. 33). The abrupt upward break in the initial portion of the curve is indicative that the attitude between the test vehicle and the soil surface was not normal at impact. This is particularly apparent in the drop from 15 ft. The vehicle initially impacted slightly on edge, then rotated with a resulting release of the soil response and finally applied the remaining impact force upon slapping the ground surface. While this action was not discernible from visual observation, it was suspected due to the lateral displacement of the vehicle from its rest position.

The vehicle geometries chosen for this investigation were believed to provide the limiting parameters for spacecraft landing heads. The results of this research indicate that certain analogies exist. For the plate test vehicles, an analogy is presented to a punching shear condition into a soil system. The cone vehicle indicates a lateral displacement of the soil analogous to a passive earth pressure condition. The sphere test vehicle falls into a category between these two extremes. An additional analogy exists between the sphere and plate test vehicles. It is apparent that as the spherical radius of the sphere test vehicle is increased, the contact face becomes flatter and at a limit would present a contact surface to the soil which would approximate a plate. This is indicated in Fig. 34 where the slope of the modulus of deformation curve for the spheres increases at a greater rate than the curve for the plates.

A comparison of the modulus of deformation values readily indicates the effect of vehicle geometry. Table 20 shows a summary of these values.

TABLE 20

MODULUS OF DEFORMATION SUMMARY

	Modulus of Deformation (lb/in.)		
	Plate	Sphere	Cone
8.0 & 16.0 lb Series	29,694	3,803	1,049
64.0 & 128.0 lb Series	70,900	9,360	1,049

A vehicle of cone configuration receives the least reactive thrust for a given displacement and from that consideration is the most appropriate geometry.

However, from a practical viewpoint of spacecraft landing heads, size would limit the usefulness of a cone configuration. The magnitude of the almost instantaneous impact forces would make a plate configuration the least favorable. Therefore, it is believed that future efforts should be devoted to vehicles having a spherical configuration.

7.5 Prediction Methods

The ability to apply the test data towards a prediction of prototype behavior is desirable. Two methods are discussed which are believed appropriate. The discussion is limited to test vehicles having a spherical configuration. The first method is based on the Theory of Similitude for dynamic similarity. The second approach considers extrapolation based on phenomenological behavior.

A. Dynamic Similitude[1,2,3,5,7]

To satisfy the requirements of dynamic similitude, the model-prototype configuration must be constructed and tested to meet the following conditions.

(1) Geometric similarity. Constant ratios must exist between all corresponding lengths of the model and prototype.

(2) Kinematic similarity. Impact velocities, and the sequence and duration of events must be in constant

proportion between model and prototype.

(3) Kinetic similarity. All forces acting on the model must be in relation to the forces acting on the prototype.

Since it is desirable to predict the acceleration-time history of the prototype, the reactive force of the soil, f, on the vehicle mass will be the dependent variable. The independent variables to be considered and their dimensions are defined as follows:

l = A characteristic length, L

R = Spherical radius of vehicle contact surface, L

W = Weight of the test vehicle, F

v_i = Impact velocity, LT^{-1}

g = Gravitational acceleration, LT^{-2}

ρ = Mass density of the soil, FT^2L^{-4}

E = Bulk modulus of the soil, FL^{-2}

η = Viscous property of the soil, FTL^{-2}

c = Cohesion of the soil, FL^{-2}

ϕ = Angle of internal friction of the soil

x = Particle size of the soil, L

t = Time, T.

Since no attempt was made to model the soil properties in this investigation in relation to the sizes of vehicles tested, certain arbitrary assumptions must be made. It is emphasized that the inability to model the soil has resulted in an inherent distortion of the model-prototype relationship. Assumptions relative to certain of the independent variables

should not be construed to negate their importance, but are a result of the existing distortion.

As the field test series was conducted on a soil mass whose average water content approximated 17.3 per cent, it was assumed that no significant change would occur in the viscous properties of the soil within the range of test data. Therefore, this variable was eliminated from consideration.

The ratio of soil grain sizes between model and prototype was assumed not to be significant for the soil classification and the sizes of the test vehicles. Further, the size of the test area would allow the reasonable assumption that the soil mass be considered a continuum.

As the soil was not modeled, the relationship for the angle of internal friction of the soil was automatically satisfied, therefore, it was eliminated from further consideration.

Thus, there remains the equation

$$f = \psi_1 (l, R, W, v_i, g, \rho, E, c, t). \tag{10}$$

There are three dimensions associated with the ten variables of the above equation. By the Buckingham Pi Theorem, these variables will be reduced to seven when placed in nondimensional form. For this analysis, the base variables are established as W, l, and g. Therefore, equation (10) may be rewritten as

$$\left(\frac{f}{W}\right) = \psi_2 \left(\frac{R}{l}, \frac{v_i^2}{gl}, \frac{\rho g l^3}{W}, \frac{El^2}{W}, \frac{cl^2}{W}, \frac{t^2 g}{l}\right). \tag{11}$$

Assuming equation (11) comprises all significant parameters, the following relations define the similitude conditions between the model and prototype. The subscript "m" applies to model, while subscript "p" refers to the prototype.

$$\left(\frac{R}{l}\right)_m = \left(\frac{R}{l}\right)_p. \tag{12}$$

$$\left(\frac{v_i^2}{gl}\right)_m = \left(\frac{v_i^2}{gl}\right)_p. \tag{13}$$

$$\left(\frac{\rho g l^3}{W}\right)_m = \left(\frac{\rho g l^3}{W}\right)_p. \tag{14}$$

$$\left(\frac{El^2}{W}\right)_m = \left(\frac{El^2}{W}\right)_p. \tag{15}$$

$$\left(\frac{cl^2}{W}\right)_m = \left(\frac{cl^2}{W}\right)_p. \tag{16}$$

$$\left(\frac{t^2 g}{l}\right)_m = \left(\frac{t^2 g}{l}\right)_p. \tag{17}$$

Equation (12) defines the geometric similarity requirement between model and prototype. Equation (13) may be rewritten in the case of this investigation where the acceleration of gravity is the same between model and prototype.

$$v_{ip} = v_{im} \sqrt{\frac{l_p}{l_m}} \tag{18}$$

which gives the prototype impact velocity.

Equations (14) through (16) may be rewritten to express the prototype weight as a function of the model weight.

$$W_p = W_m \left(\frac{\rho_p}{\rho_m}\right) \left(\frac{g_p}{g_m}\right) \left(\frac{l_p}{l_m}\right)^3 \tag{19}$$

$$W_p = W_m \left(\frac{l_p}{l_m}\right)^2 \left(\frac{E_p}{E_m}\right) \tag{20}$$

$$W_p = W_m \left(\frac{l_p}{l_m}\right)^2 \left(\frac{c_p}{c_m}\right). \tag{21}$$

Equation (17) may be rewritten as

$$t_p = t_m \sqrt{\frac{l_p}{l_m}}. \tag{22}$$

In equation (19) the gravitational accelerations and the soil mass densities are constants. Thus this equation will reduce to

$$W_p = W_m \left(\frac{l_p}{l_m}\right)^3. \tag{23}$$

The weight of the soil mass, W_s, involved in the interaction motions of the test vehicle at impact may be expressed as

$W_s = \gamma$ volume $= \gamma\, l^3$ where γ is the soil density in lb/ft^3.

By similitude

$$\frac{(W_s)_p}{(W_s)_m} = \frac{\gamma_p l_p^3}{\gamma_m l_m^3}. \tag{24}$$

Assuming that

$$\frac{\gamma_p}{\gamma_m} = 1.$$

it follows that the ratio of the dead load body force of the soil is

$$\frac{(W_s)_p}{(W_s)_m} = \left(\frac{l_p}{l_m}\right)^3. \tag{25}$$

Assuming that the soil resistance force, Q, is a function of the product of the dynamic shear strength, τ_{fd}, and an area A. Further assuming that the dynamic shear strength is equal to the product of the static shear and some strain rate factor, the model-prototype ratio may be written

$$\frac{Q_p}{Q_m} = \frac{(\tau_f)_p}{(\tau_f)_m} \frac{(SRF)_p}{(SRF)_m} \frac{A_p}{A_m} = \frac{(\tau_f)_p}{(\tau_f)_m} \frac{(SRF)_p}{(SRF)_m} \frac{(l_p)^2}{(l_m)^2}. \tag{26}$$

Setting this value equal to the dead load body force

$$\frac{(\tau_f)_p}{(\tau_f)_m} \frac{(SRF)_p}{(SRF)_m} \frac{l_p^2}{l_m^2} = \frac{l_p^3}{l_m^3} \tag{27}$$

or

$$\frac{l_p}{l_m} = \frac{(\tau_f)_p}{(\tau_f)_m} \frac{(SRF)_p}{(SRF)_m}. \tag{28}$$

It is recognized that the loading interval will be longer in the prototype than the model, therefore, the strain rate will be faster in the model than the prototype. However, the time interval is very small. Therefore, the ratio of strain rate factors will approach unity, and will be assumed such. Thus, the soil strength ratios approximate the geometric l_p/l_m ratio. It follows that the bulk modulus ratio and the

cohesion ratio would also approximate the geometric ratio.

From the above discussion it may be assumed that equation (20) may be expressed

$$W_p = W_m \left(\frac{l_p}{l_m}\right)^2 \frac{E_p}{E_m} = W_m \left(\frac{l_p}{l_m}\right)^2 \left(\frac{l_p}{l_m}\right) = W_m \left(\frac{l_p}{l_m}\right)^3 \quad (29)$$

and equation (21) expressed

$$W_p = W_m \left(\frac{l_p}{l_m}\right)^2 \frac{c_p}{c_m} = W_m \left(\frac{l_p}{l_m}\right)^2 \frac{l_p}{l_m} = W_m \left(\frac{l_p}{l_m}\right)^3. \quad (30)$$

It is again emphasized that the relations presented contain a distortion between model and prototype. The inability to model the soil system has resulted in distortion without regard to effect on the dependent variable. Assuming at this point that the distortions are not significant, the acceleration ratio between model and prototype becomes

$$\left(f/W\right)_p = \left(f/W\right)_m . \quad (31)$$

Assuming the 8.0 lb spherical test vehicle to represent the model, the following data are appropriate. (Reference Table 8).

Vehicle weight, W_m	=	8.0	lb.
Spherical radius, R_m	=	5.0	in.
Vehicle diameter, d_m	=	8.66	in.
Drop height, s_m	=	6.0	ft
Impact velocity, v_{im}	=	19.66	ft/sec
Maximum deformation, δ_m	=	1.084	in.
Maximum force, f_m	=	1,075	lb

Assuming the 64.0 lb spherical test vehicle as the prototype, the l_p/l_m ratio will be a factor of two. The following results are compared from the Theory of Similitude and actual test data.

	Similitude	Test Data
Prototype weight, W_p	64.0 lb	64.0 lb
Prototype drop height, s_p	12.0 ft	12.0 ft
Prototype velocity, v_{ip}	27.80 ft/sec	27.80 ft/sec
Maximum deformation, δ_p	2.168 in.	2.43 in.
Maximum force, f_p	8,600.0 lb	5,716.0 lb

Considering the 16.0 lb spherical test vehicle as the model, the following data are applicable. Reference Table 8.

Vehicle weight, W_m	16.0 lb
Spherical radius, R_m	5.0 in.
Vehicle diameter, d_m	8.66 in.
Drop height, s_m	6.0 ft
Impact velocity, v_{im}	19.66 ft/sec
Maximum deformation, δ_m	1.169 in.
Maximum force, f_m	2,123.0 lb.

Considering the 128.0 lb spherical test vehicle as the prototype with the same l_p/l_m ratio of two, the following data are appropriate.

	Similitude	Test Data
Prototype weight, W_p	128.0 lb	128.0 lb
Prototype velocity, v_{ip}	27.80 ft/sec	27.80 ft/sec
Prototype drop height, s_p	12.0 ft	12.0 ft
Maximum deformation, δ_p	2.338 in.	2.88 in.
Maximum force, f_p	17,000.0 lb	9,495.0 lb

As shown by the two examples, the theory of similitude is limited by the necessary assumptions.

The effect of distortion is evident when it is considered that the test vehicles were geometrically similar. Extrapolation towards prototype from the Theory of Similitude must therefore be applied with care. More exacting modeling techniques for the entire vehicle-soil system to more closely approximate the dynamic similarity requirements is essential to reduce the gross error and permit application of this theory with reasonable reliability.

B. Extrapolation by Phenomenological Behavior.

In extrapolation towards prototype size, the maximum force is of primary concern for spacecraft design. It would also be convenient for design purposes to define this force as a function of the vehicle mass, M, and the impact velocity, v_i. As shown on the force-deformation curves for spherical vehicles (Reference Figs. 28 and 29), the magnitude of the maximum force increases with impact velocity and mass for each configuration. The characteristic shapes of these force-deformation curves indicate the maximum reactive force of the soil against the vehicle face occurs prior

to the maximum deformation.

As discussed previously, the modulus of deformation is a constant for each vehicle geometry. The equation defining this relationship (Reference Fig. 34) is

$$E_{d_s} = 585.2\ R + 35.08\ R^2 \quad \text{lb/in.} \tag{32}$$

where R is the spherical radius of the test vehicle.

This equation, which may be extrapolated, defines the slope of the initial portion of the force-deformation curve. However, as the modulus gives the amount of force per in. of deformation, a relation must be established to determine the magnitude of the reactive force in terms of other variables.

Considering the experimental data for maximum force versus the product of the test vehicle mass and impact velocity, an equation has been derived by least squares techniques which will allow extrapolation.

$$f_s = 530 + 114\ (M\ v_i) - 0.214\ (M\ v_i)^2 \tag{33}$$

where f_s is the maximum force for a spherical test vehicle

M is the vehicle mass

v_i is the impact velocity.

The more significant portion of the force-deformation curve may now be approximately defined. The use of Eq. 32 will provide the slope of the initial portion of the force-deformation curve. This line will intercept the deformation axis at approximately 0.02 in. The application of Eq. 33 will provide the upper limit for the force ordinate. Thus, three straight lines will approximately define the initial portion of the force-

deformation curve. From this information, the acceleration values may be determined.

The use of the two equations presented will permit extrapolation towards prototype size. However, it is believed that extrapolation to full prototype size would be beyond the limits or benefits of information obtained in this investigation. It is emphasized that the data obtained was from tests upon a particular classification of soil. Behavior predictions to any other type of soil would not be valid.

The results obtained from this investigation provide much useable information, and an insight into the phenomenological behavior between the test vehicle and an earth mass. The results of a limited number of drop tests utilizing a full or half scale prototype vehicle would provide a valuable adjunct to this research program.

CHAPTER EIGHT

CONCLUSIONS AND RECOMMENDATIONS

8.1 Conclusions

From the results of this investigation the following observations may be made.

1. The experimental procedures developed in the course of this investigation proved to be very reliable and provide useable test data. The following items are considered significant:
   a. The use of accelerometers as primary sensing devices.
   b. The recording of all test information on a photographic record of the oscilloscope.
   c. The use of the second oscilloscope trace to measure the test vehicle penetration.
   d. Providing accelerometer calibration lines on each photographic record for use in the data reduction process.
   e. Digitizing of the accelerometer-time record by use of a suitable device.
   f. Inputing the digitized information directly to the computer on paper tape.
   g. Data reduction computations being accomplished on a digital computer which also provided plots of the output information.
2. Soils similar to that utilized in this testing program exist in many areas. Information developed from this investigation can be applied in performing tests at proposed landing sites

having soil with the same general classification.

3. The characteristic shape of the force-deformation curves is a function of the test vehicle geometry.

4. The slope of the initial straight portion of the force-deformation curves is a function of the vehicle geometry.

5. The force-deformation curves exhibit an increase in deformation without an increase in load.

6. The maximum reactive force of the soil to an impacting vehicle is a function of the mass, impacting velocity, soil properties, and test vehicle geometry.

7. The maximum reactive force of the soil against a vehicle of spherical configuration may be expressed as a function of the impact velocity and vehicle mass as

$$f_s = 530 + 114\ (M\ v_i) - 0.214\ (M\ v_i)^2$$

where M is the vehicle mass and v_i the impact velocity.

8. The modulus of deformation for a sphere test vehicle may be expressed as

$$E_{ds} = 585.2\ R + 35.08\ R^2 \quad lb/in.$$

where R is the spherical radius of the test vehicle in in.

9. The modulus of deformation for a plate test vehicle may be expressed as

$$E_{dp} = 4{,}787.6\ r + 230.24\ r^2 \quad lb/in.$$

where r is the vehicle radius in in.

10. The modulus of deformation for a cone test vehicle may be expressed as a constant

$E_{dc} = 1{,}049$ lb/in.

11. The interaction phenomena occurring from the soil response to an impacting body cannot be explained by existing laboratory techniques for static testing.

12. The use of the Theory of Similitude to predict prototype behavior requires the development of soil modeling techniques which allows dynamic similarity to be obtained between model and prototype.

13. Extrapolation towards prototype size is possible based on phenomenological behavior. The modulus of deformation, or the slope of the initial portion of the force-deformation curve, and the maximum reactive force of the soil against a spherical vehicle of known configuration may be expressed by the following equations:

$$E_{ds} = 585.2\ R + 35.08\ R^2$$

where R is the spherical radius of the test vehicle and

$$f_s = 530 + 114\ (M\ v_i) - 0.214\ (M\ v_i)^2$$

where M is the vehicle mass and v_i the impact velocity.

14. The validity of the investigation is limited to the geometries and sizes of vehicles tested on a particular classification of soil. Extrapolation of results should be limited pending correlation with a full or half scale prototype vehicle.

8.2 Recommendations for Future Research

1. The present program should be expanded to permit prototype testing for correlation of results.
2. Future research should require more sophisticated instrumentation. Recommendations are to utilize sensors with transmitting capability, and recording oscilloscopes with individually controlled traces.
3. An extensive research program is mandatory to develop dynamic laboratory testing procedures if correlation is to be accomplished between soil properties and test vehicle behavior.
4. The range of soil types should be expanded to determine the response to impacting bodies.

APPENDIX A

APPENDIX A

The computer program developed for the data reduction process of this investigation is known as NASA 9. A complete listing of the program is shown beginning on page 135. A flow chart for the program is shown in Fig. 35, beginning on page 143.

Each test to be reduced requires the input of three types of data. The first group contains information which is to be printed or plotted with each test. This includes:

a. The ICELL card which is read at the beginning of the program and which contains the graph headings to be plotted with each test. The ICELL card is read only once.

b. The NPROB card indicates the number of tests which are to be reduced during the run on the computer.

c. The IRUN card contains a heading appearing on each page of the printed output and above the last graph of each individual test.

d. The KIL card contains the test number which is shown on the graphs at the intersection of the coordinate axes. This number is only plotted on the graphs on which a heading does not appear.

e. The NPOINTS card contains the number of data points taken on the Telereader for each test.

The second group of data consists of the test vehicle weight, size, calibration constant of appropriate accelerometer utilized, oscilloscope time scale, and the height of the test drop. The following are the pro-

gram designations for the second data group which is input on the BODYCON card:

a. BODYMAS is the test vehicle weight in lbs.

b. CONTIME is the horizontal time scale of the oscilloscope in milliseconds/centimeter.

c. CONACEL is the calibration constant for the accelerometer utilized in g's.

d. D is the test vehicle diameter in in.

e. H is the height of the test drop in ft.

The third group of data consists of the points taken from the acceleration-time record by means of the Telereader, and which appear on the input paper tape in the following manner. The first two points of the tape are the difference coordinates of the accelerometer calibration traces used to compute the ordinate scale. The third and fourth points are the difference coordinates of the abcissa. The next points are the coordinates of the acceleration-time curve taken at approximately equal intervals thereafter. The total number of points per set minus the first four calibration points establishes the number of data points which is indicated on the NPOINTS card of the first data group.

Figure 36, page 146 shows a schematic representation of the input data procedural sequence.

```
-COOP, CE011159,REESE,I/10/0/34/S/2S,5,1000.
-FTN,L,E.
      PROGRAM NASA9A
      DIMENSION TIMEV(200) TIM(200),ACCEL(200),VELOCIT(200),DIST(200),FORCE
     1(200),FORCE(200),IRUN(10),AREA(200),STRESS(200),IC(200),ITIMEV(200),
     2IACCELV (200),ICELL(50)
C     DEFINITIONS
C     NPROB IS THE NUMBER OF TESTS TO BE REDUCED.
C     NPOINTS = NUMBER OF TELEREADER DATA POINTS.
C     IRUN IS FOR IDENTIFICATION ONLY.  CAN PUT ANY INFORMATION DESIRED.
C     BODYMAS = THE MASS OF THE BODY IN MOTION.
C     FORCE IS THE TOTAL FORCE ON THE MODEL AT AN INSTANT OF TIME.
C     STRESS IS THE UNIT STRESS ON THE MODEL AT AN INSTANT OF TIME.
C     CONTIME = THE CONVERSION FACTOR FOR TIME VALUE FROM TELEREADER.
C     CONACEL = THE CONVERSION FACTOR FOR ACCELERATION FROM THE TELEREADER.
C     VELO = THE INITIAL VELOCITY OF THE BODY IN MOTION.
C     DISTO = THE INITIAL DISPLACEMENT OF THE BODY IN MOTION.
C     TIMEV = THE VALUE OF TIME READ FROM THE TELEREADER.
C     ACCELV = THE VALUE OF ACCELERATION READ FROM THE TELEREADER.
   1 FORMAT (15)
   2 FORMAT (10A8)
   3 FORMAT (//40H                    INPUT DATA           //)
   4 FORMAT (34H          NUMBER OF DATA POINTS = 15   /)
   5 FORMAT (10X,25HMASS OF BODY IN MOTION = ,E10.4,3X,4HSLUG   /)
   6 FORMAT (10X,29HCONVERSION FACTOR FOR TIME = E10.4,3X,8HSEC/MV   /)
```

```
 7 FORMAT (10X,37HCONVERSION FACTOR FOR ACCELERATION = E10.4,3X,14HFT/
  1SEC-SQ-MV    /)
 8 FORMAT (1H1)
 9 FORMAT (10X,19HINITIAL VELOCITY = E10.4,3X,6HFT/SEC /)
10 FORMAT (10X,23HINITIAL DISPLACEMENT = E10.4,3X,2HFT /)
11 FORMAT (40H                  RAW TELEREADER DATA    )
12 FORMAT (42H          TIME (MV)        ACCELERATION (MV)       //)
13 FORMAT (46H                                  OUTPUT DATA     //)
14 FORMAT (83H               TIME      ACCELERATION    VELOCITY
  1DISPLACEMENT        FORCE      )
15 FORMAT (50H           REESE CE-01-1159    PROGRAM NASA 9       //)
16 FORMAT (13X,3HSEC,9X,9HFT/SEC-SQ,8X,6HFT/SEC,11X,2HIN,14X,2HLB //)
17 FORMAT (10X,4(E10.3,5X))
18 FORMAT (13X,4HDIST,11X,4HAREA,9X,7HVELOCIT,9X,6HSTRESS )
19 FORMAT(14X,2HIN,11X,5HSQ-FT,9X,6HFT/SEC,9X,8HLB/SQ-FT /)
20 FORMAT (6E10.4)
21 FORMAT (2(10X,E10.3))
22 FORMAT (10X,5(E10.3,5X))
23 FORMAT (1X, 10A8)
24 FORMAT (X,I4,7X,I4)
25 FORMAT(//26X,5A8)
26 FORMAT(//9H ACCMIN = E10.3,4X,9H FORMIN = E10.3,4X,9H VELMAX = E10
  1.3,4X,9H DISMAX = E10.3,4X,9H TIMMAX = E10.3)
27 FORMAT(A8)
28 FORMAT(8(I4,1X,14,1X))
```

```
      PRINT 8
      PRINT 15
      CALL TIME
      PRINT 8
      READ 2,(ICELL(J),J=I,7)
C     SET BCD CODES FOR PAPER TAPE CHARACTERS  ---------
      CALL CODESET (2)
C     READ NUMBER OF PROBLEMS  -------
      READ 1, NPROB
C     SET ARRAYS EQUAL TO ZERO   --------
      DO 700 IA=1,200$ACCEL(IA)=0.$FORCE(IA)=0.$DIST(IA)=0.
  700 VELOCIT(IA)=0.
C     SET IDFLAG  --------
      IF(KI-NPROB)400,500,400
  400 IDFLAG=1
      GO TO 600
  500 IDFLAG=0
  600 CONTINUE
      READ 2, (IRUN(J), J=1, 10)
      READ 27,KIL
C     READ NUMBER OF DATA POINTS  ----------
      READ 1, NPOINTS
C     READ DATA SET ---------
      READ 20,BODYMAS,CONTIME,CONACEL,D,H
      BODYMAS=BODYMAS/32.2
```

```
      CONTIME=CONTIME/1000.
      D=D/12.
C     SET TELEREADER SCALE FACTORS
C     READ PAPER TAPE CHARACTERS IN BCD IMAGE  -----------
      DO 701,J=1,4
      CALL PAPEREAD (IC(1),IC(3),1,10,IEF)
C     DECODE CHARACTERS
  701 DECODE (23,24,IC(1))ITIMEV(J),IACCELV(J)
      Z=IACCELV(1)-IACCELV(2)
      Y=ITIMEV(3)-ITIMEV(4)
      CONACEL=(CONACEL*32.2)/ABSF(Z)
      CONTIME=CONTIME*10./ABSF(Y)
C     SET INITIAL CONDITIONS  --------
      VELO=SQRTF(64.4*H)
C     READ PAPER TAPE CHARACTERS IN BCD IMAGE  -----------
      DO 777 M-1, NPOINTS
      CALL PAPEREAD(IC(1),IC(3),1,10,IEF)
C     DECODE CHARACTERS  ---------
  777 DECODE(23,24,IC(1))ITIMEV(M),IACCELV(M)
      DO 666 II=1, NPOINTS
      TIMEV(II) = ITIMEV(II)
  666 ACCELV(II) = -IACCELV(II)
C     PRINT INPUT DATA ----------
      PRINT 25, (IRUN(I),I=1,5)
      PRINT 3
```

```
      PRINT 4, NPOINTS
      PRINT 5, BODYMAS
      PRINT 6, CONTIME
      PRINT 7, CONACEL
      PRINT 9, VELO
      PRINT 11
      PRINT 21, (TIMEV(J), ACCELV(J), J=1, NPOINTS)
      PRINT 8
C     SCALE DATA POINTS  ---------
      DO 100 J = 1,NPOINTS
      TIME(J) = TIMEV(J) * CONTIME
  100 ACCEL(J) = ACCELV(J) * CONACEL +32.2
C     COMPUTATION OF VELOCITYS.
C     INTEGRATE ACCELERATION --------
      VELOCIT(1) =VELO
      DO 200 J=2,NPOINTS
  200 VELOCIT (J) = VELOCIT (J-1) + ((ACCEL(J-1)+ACCEL(J))/2.) * (TIM
     1(J)-TIM (J-1)
C     INTEGRATE VELOCITY --------
      DIST(1)=0.
      DO 300 J=2, NPOINTS
  300 DIST(J) = DIST(J-1) +(VELOCIT(J-1))*(TIM (J)-TIM (J-1)) + (ACCEL
     1(J-1)/3.0 + ACCEL(J)/6.0) * (TIM (J) - TIM (J-1))**2
C     COMPUTATION OF FORCE AND STRESS ON THE BODY -
```

```
      FORCE(1)=BODYMAS*ACCEL(1)
      AREA(1)=0.
      STRESS(1)=0
      DO 105 J=2,NPOINTS
      FORCE(J)=BODYMAS*ACCEL(J)
      AREA(J) = 3.1416*D*DIST(J)
      DIST(J)=DIST(J)*12.
  105 STRESS(J)=FORCE(J)/AREA(J )
C     PRINT OUTPUT   ----------
      PRINT 25, (IRUN(I),I=1,5)
      PRINT 13
      PRINT 14
      PRINT 16
      PRINT 22, (TIM (J), ACCEL(J), VELOCIT (J), DIST(J), FORCE(J) ,
     1J=1, NPOINTS
C     SCALE AXES --------
      CALL MINI(ACCEL,ACCMIN)
      CALL MINI(FORCE,FORMIN)
      CALL MAXIE(VELOCIT,VELMAX)
      CALL MAXIE(DIST,DISMAX)
      CALL MAXIE(TIM,TIMMAX)
      PRINT 26, ACCMIN, FORMIN, VELMAX, DISMAX, TIMMAX
      PRINT 8
      PRINT 25, (IRUN(I),I=1,5)
      PRINT 13
```

```
      PRINT 18
      PRINT 19
      PRINT 17, (DIST(J), AREA(J),VELOCIT(J),STRESS(J),J=1, NPOINTS)
      PRINT 8
C     PLOT ROUTINES  ---------
      DISMAX=DISMAX*1.1
      CALL AXES(TIMMAX,6.0,0.5,2.5,DISMAX,6.0,0.5,.002,.1)
      CALL PLOTTITL(KIL,2,0,2,-.375,-.313)
      CALL PLOTTITL(ICELL(1),4,0,2,2.8,-.4)
      CALL PLOTTITL(ICELL(2),12,2,2,2.2,.4)
      CALL PLOT(TIM,DIST,NPOINTS,1)
      CALL AXESTERM(1)
      CALL AXES(TIMMAX,6.0,0.5,2.5,VELMAX,6.0,0.5,.002,1.)
      CALL PLOTTITL(KIL,2,0,2,-.375,-.313)
      CALL PLOTTITL(ICELL(1),4,0,2,2.8,-.4)
      CALL PLOTTITL(ICELL(4),8,2,2,2.8,.4)
      CALL PLOT(TIM,VELOCIT,NPOINTS,2)
      CALL AXESTERM(1)
      CALL AXES(TIMMAX,6.0,0.5,2.5,ACCMIN,0.5,6.0,.002,100.)
      CALL PLOTTITL(KIL,2,0,2,-.375,.173)
      CALL PLOTTITL(ICELL(1),4,0,2,2.8,.4)
      CALL PLOTTITL(ICELL(5),12,2,2,-3.8,.4)
      CALL PLOT(TIM,ACCEL,NPOINTS,3)
      CALL AXESTERM(1)
      CALL AXES(DISMAX,6.0,0.5,2.5,FORMIN,0.5,6.0,.10,10.)
      CALL PLOTTITL(IRUN(1),30,0,3,.8,1.5)
```

```
      CALL PLOTTITL(ICELL(2),12,0,2,2.2,.4)
      CALL PLOTTITL(ICELL(7),5,2,2,-3.4,.4)
      CALL PLOT (DIST,FORCE,NPOINTS,6)
      CALL AXESTERM(IDFLAG)
  999 CONTINUE
      END
```

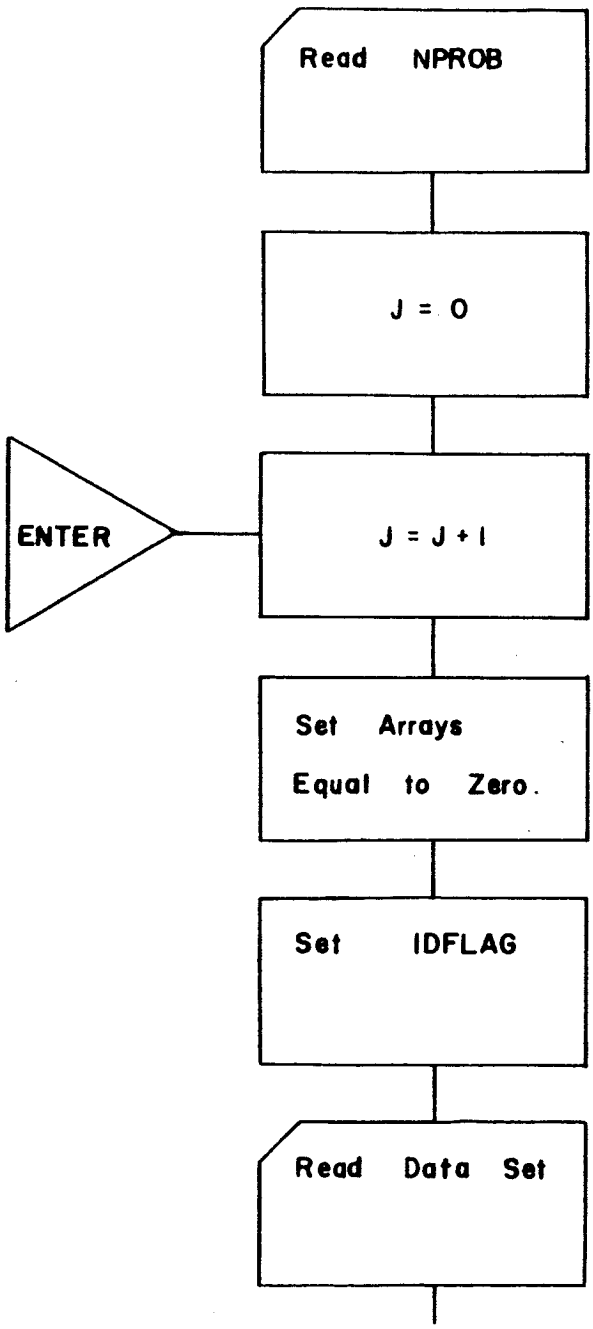

FIG. 35 COMPUTER PROGRAM FLOW DIAGRAM

FIG. 35 CONT'D.

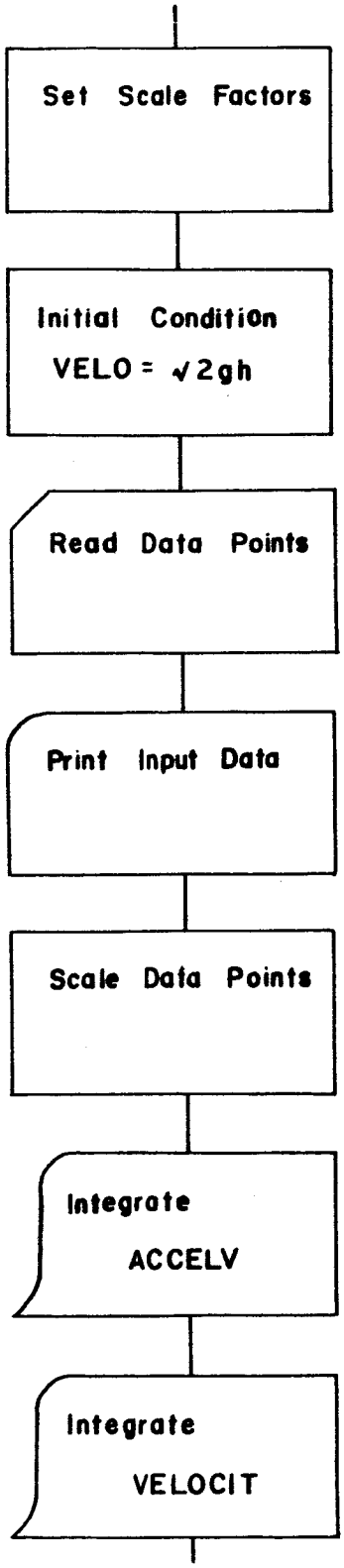
Set Scale Factors
Initial Condition
VELO = √2gh
Read Data Points
Print Input Data
Scale Data Points
Integrate
ACCELV
Integrate
VELOCIT

FIG. 35 CONT'D.

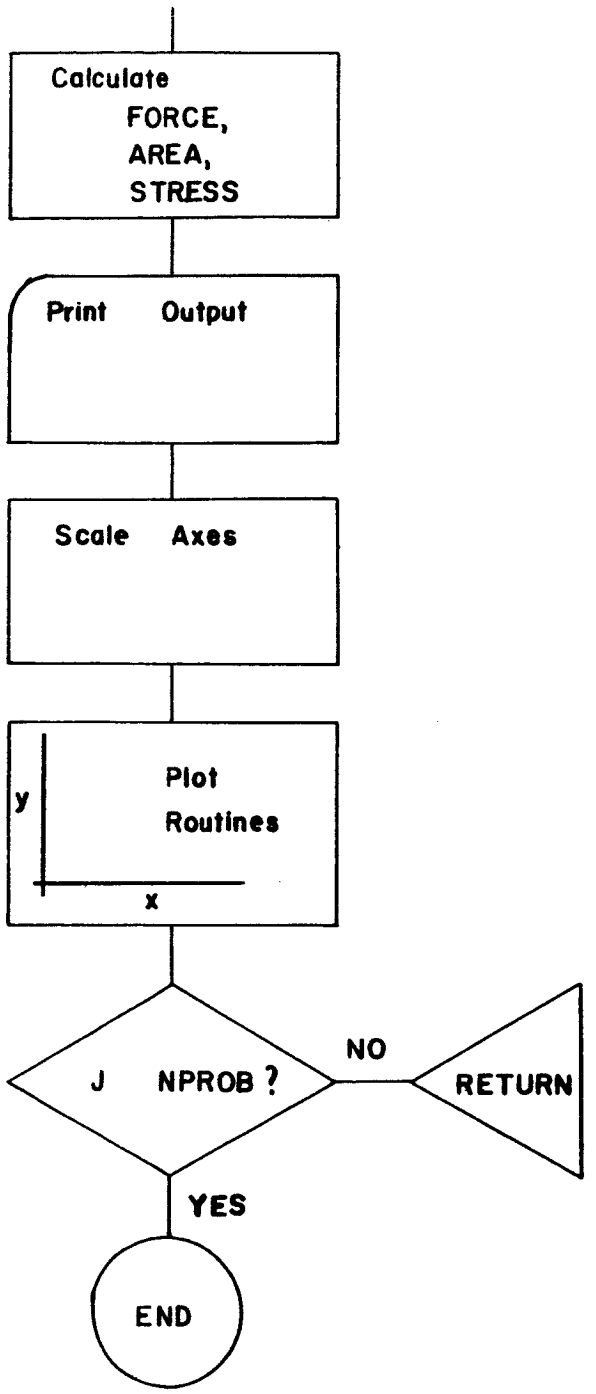
Calculate
FORCE,
AREA,
STRESS
Print Output
Scale Axes
y
Plot
Routines
x
J NPROB ?
NO
RETURN
YES
END

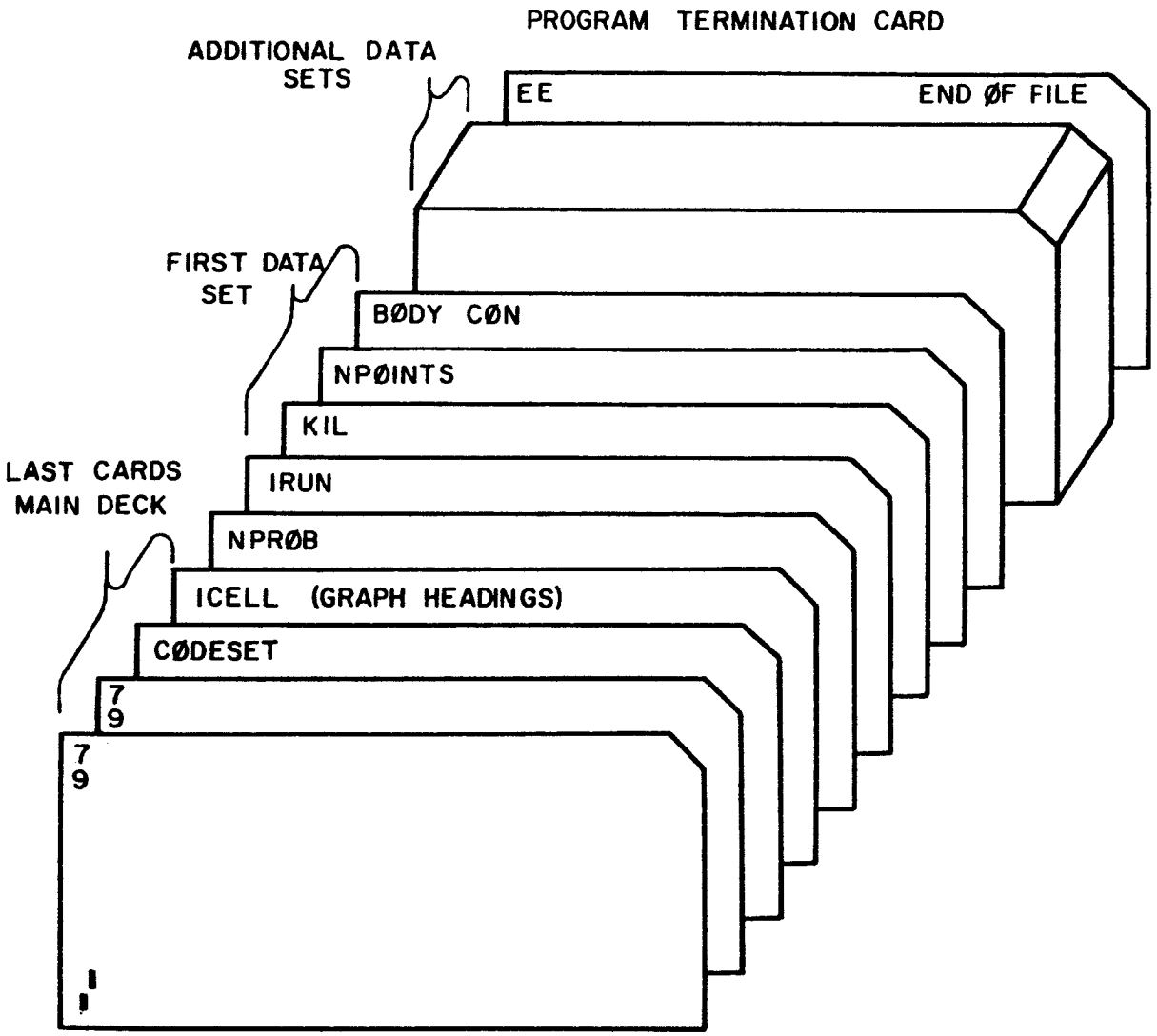

FIG. 36 DATA INPUT SEQUENCE

REFERENCES

1. Bekker, M. G., Theory of Land Locomotion, p. 457, The University of Michigan Press, Ann Arbor, 1956.

2. Huntley, H. E., Dimensional Analysis, p. 43, MacDonald, London, 1952.

3. Nevill, G. E., Jr., Modeling Studies of the Response of Weapon Foundations in Soils. pp. 6-23, Prepared by Southwest Research Institute, San Antonio, Texas, under Contract DA-23-072-ORD-1375 for the Army Material Command, Washington, D. C., June 1963.

4. Popov, E. P., Mechanics of Materials, p. 400, Prentice-Hall, Inc., New York, 1956.

5. Reese, L. C., Dawson, R. F., Coyle, H. M., Baker, W. E., Ghazzaly, O. I., and Smith, R. E., "Investigations of the Effects of Soil Conditions on the Landing of a Manned Spacecraft, Structural Mechanics Research Laboratory, The University of Texas, 1964.

6. Terzaghi, K., Theoretical Soil Mechanics, p. 142, John Wiley and Sons, Inc., New York, 1943.

7. U. S. Army Engineer Waterways Experiment Station, CE, Dynamic Bearing Capacity of Soils, The Application of Similitude to Small-Scale Footing Tests. Technical Report No. 3-599, Report 3, pp. 5-17, Vicksburg, Miss., December, 1964.

8. Iliya, Raja A., and Reese, Lymon C., "Static Load Versus Settlement for Geometric Shapes on Cohesionless Soil," Department of Civil Engineering, The University of Texas, May, 1965. A Report to National Aeronautics and Space Administration, Langley Research Center, Hampton, Virginia.